Volume 7, Number 1, 2007 ISSN 1562-8353

NONLINEAR DYNAMICS AND SYSTEMS THEORY
An International Journal of Research and Surveys

Volume 7 Number 1 2007

CONTENTS

Preface ..... v

Prior-free Inference for Objective Bayesian Analysis and Model Selection ..... 1
*Koki Kyo*

Inverse Determination of Model Parameters of Nonlinear Heat Conduction Problem Using Hybrid Genetic Algorithm ..... 23
*Shouju Li and Yingxi Liu*

Continuous-Time Optimal Portfolio Selection Using Mean-CaR Models ..... 35
*Zhong-Fei Li, Kai W. Ng and Xiao-Tie Deng*

A Simple Nonlinear Adaptive-Fuzzy Passivity-Based Control of Power Systems ..... 51
*H.E. Psillakis and A.T. Alexandridis*

Performance Analysis of Communication Networks Based on Conditional Value-at-Risk ..... 69
*Jun Wu, Wuyi Yue and Shouyang Wang*

Analysis of Network Revenue Management under Uncertainty ..... 85
*Yifan Xu, Shu-Cherng Fang and Youyi Feng*

An Online Learning Algorithm with Adaptive Forgetting Factors for Feedforward Neural Networks in Financial Time Series Forecasting ..... 97
*Lean Yu, Shouyang Wang and Kin Keung Lai*

NONLINEAR DYNAMICS & SYSTEMS THEORY Volume 7, No. 1, 2007

# Nonlinear Dynamics and Systems Theory

## An International Journal of Research and Surveys



 ISSN 1562-8353 Printed in Ukraine
To receive contents and abstracts by e-mail, visit our Website at: **http://www.e-ndst.kiev.ua**

**Academic Periodical Press**

Nonlinear Dynamics and Systems Theory
An International Journal of Research and Surveys





NONLINEAR DYNAMICS AND SYSTEMS THEORY
An International Journal of Research and Surveys

# INSTRUCTIONS FOR CONTRIBUTORS

**(1) General.** The Journal will publish original carefully refereed papers, brief notes and reviews on a wide range of nonlinear dynamics and systems theory problems. Contributions will be considered for publication in ND&ST if they have not been published previously. Before preparing your submission, it is essential that you consult our style guide; please visit our website: http://www.e-ndst.kiev.ua

**(2) Manuscript and Correspondence.** Contributions are welcome from all countries and should be written in English. Two copies of the manuscript, double spaced one column format, and the electronic version by AMSTEX, TEX or LATEX program (on diskette) should be sent directly to

Professor A.A. Martynyuk
Institute of Mechanics,
Nesterov str.3, 03057, MSP 680
Kiev-57, Ukraine
(e-mail: anmart@stability.kiev.ua
e-mail: amartynyuk@voliacable.com)

or to one of the Editors or to a member of the Editorial Board.

The title of the article must include: author(s) name, name of institution, department, address, FAX, and e-mail; an Abstract of 50-100 words should not include any formulas and citations; key words, and AMS subject classifications number(s). The size for regular paper should be 10-14 pages, survey (up to 24 pages), short papers, letter to the editor and book reviews (2-3 pages).

**(3) Tables, Graphs and Illustrations.** All figures must be suitable for reproduction without being retouched or redrawn and must include a title. Line drawings should include all relevant details and should be drawn in black ink on plain white drawing paper. In addition to a hard copy of the artwork, it is necessary to attach a PC diskette with files of the artwork (preferably in PCX format).

**(4) References.** Each entry must be cited in the text by author(s) and number or by number alone. All references should be listed in their alphabetic order. Use please the following style:

Journal: [1] Poincaré, H. Title of the article. *Title of the Journal* **Vol.1**(No.1) (year) pages. [Language].
Book: [2] Liapunov, A.M. *Title of the book.* Name of the Publishers, Town, year.
Proceeding: [3] Bellman, R. Title of the article. In: *Title of the book.* (Eds.). Name of the Publishers, Town, year, pages. [Language].

**(5) Proofs and Reprints.** Proofs sent to authors should be returned to the Editor with corrections within three days after receipt. Acceptance of the paper entitles the author to 10 free reprints.

**(6) Editorial Policy.** Every paper is reviewed by the regional editor, and/or a referee, and it may be returned for revision or rejected if considered unsuitable for publication.

**(7) Copyright Assignment.** When a paper is accepted for publication, author(s) will be requested to sign a form assigning copyright to Informath Publishing Group. Failure to do it promptly may delay the publication.

# NONLINEAR DYNAMICS AND SYSTEMS THEORY

An International Journal of Research and Surveys

Published since 2001

Volume 7 Number 1 2007


## CONTENTS


Preface ..... v

Prior-free Inference for Objective Bayesian Analysis and Model Selection ..... 1
*Koki Kyo*

Inverse Determination of Model Parameters of Nonlinear Heat Conduction Problem Using Hybrid Genetic Algorithm ..... 23
*Shouju Li and Yingxi Liu*

Continuous-Time Optimal Portfolio Selection Using Mean-CaR Models ..... 35
*Zhong-Fei Li, Kai W. Ng and Xiao-Tie Deng*

A Simple Nonlinear Adaptive-Fuzzy Passivity-Based Control of Power Systems ..... 51
*H.E. Psillakis and A.T. Alexandridis*

Performance Analysis of Communication Networks Based on Conditional Value-at-Risk ..... 69
*Jun Wu, Wuyi Yue and Shouyang Wang*

Analysis of Network Revenue Management under Uncertainty ..... 85
*Yifan Xu, Shu-Cherng Fang and Youyi Feng*

An Online Learning Algorithm with Adaptive Forgetting Factors for Feedforward Neural Networks in Financial Time Series Forecasting ..... 97
*Lean Yu, Shouyang Wang and Kin Keung Lai*



*Founded by A.A.Martynyuk in 2001.*
*Registered in Ukraine Number: KB №5267 / 04.07.2001.*

# NONLINEAR DYNAMICS AND SYSTEMS THEORY

An International Journal of Research and Surveys

**Nonlinear Dynamics and Systems Theory** (ISSN 1562-8353 (Print), ISSN 1813-7385 (Online)) is an international journal published under the auspices of the S.P.Timoshenko Institute of Mechanics of National Academy of Sciences of Ukraine and the Laboratory for Industrial and Applied Mathematics (LIAM) at York University (Toronto, Canada). It is aimed at publishing high quality original scientific papers and surveys in area of nonlinear dynamics and systems theory and technical reports on solving practical problems. The scope of the journal is very broad covering:

## SCOPE OF THE JOURNAL

Analysis of uncertain systems • Bifurcations and instability in dynamical behaviors • Celestial mechanics, variable mass processes, rockets • Control of chaotic systems • Controllability, observability, and structural properties • Deterministic and random vibrations • Differential games • Dynamical systems on manifolds • Dynamics of systems of particles • Hamilton and Lagrange equations • Hysteresis • Identification and adaptive control of stochastic systems • Modeling of real phenomena by ODE, FDE and PDE • Nonlinear boundary problems • Nonlinear control systems, guided systems • Nonlinear dynamics in biological systems • Nonlinear fluid dynamics • Nonlinear oscillations and waves • Nonlinear stability in continuum mechanics • Non-smooth dynamical systems with impacts or discontinuities • Numerical methods and simulation • Optimal control and applications • Qualitative analysis of systems with aftereffect • Robustness, sensitivity and disturbance rejection • Soft computing: artificial intelligence, neural networks, fuzzy logic, genetic algorithms, etc. • Stability of discrete systems • Stability of impulsive systems • Stability of large-scale power systems • Stability of linear and nonlinear control systems • Stochastic approximation and optimization • Symmetries and conservation laws

## PUBLICATION AND SUBSCRIPTION INFORMATION

The **Nonlinear Dynamics and Systems Theory** is published four times per year in 2006. Base list subscription price per volume: US$149.00. This price is available only to individuals whose library subscribes to the journal OR who warrant that the Journal is for their own use and provide a home address for mailing. Separate rates apply to academic and corporate/government institutions. Our charge includes postage, packing, handling and airmail delivery of all issues. Mail order and inquires to: Department of Processes Stability, S.P.Timoshenko Institute of Mechanics NAS of Ukraine, Nesterov str.,3, 03057, Kiev-57, MSP 680, Ukraine, Tel: ++38-044-456-6140, Fax: ++38-044-456-0319, E-mail: amartynyuk@voliacable.com, http://www.sciencearea.com.ua; http://www.e-ndst.kiev.ua

## ABSTRACTING AND INDEXING SERVICES

EBSCO Database, Swets Information Services, PASCAL Database, Mathematical Reviews/ MathSciNet, Zentralblatt MATH/Mathematics Abstracts.

# Preface

Many theoretical results and methodologies developed for systems sciences and optimization are now found very useful in dealing with nonlinear dynamics and system theory as well as their high technology applications. These areas of research are interdisciplinary in nature with great potentials for high technology applications. In view of this the Guest Editors had made a call for high quality papers to be submitted to this special issue, where system science and optimization approaches are to be used in dealing with topics in nonlinear dynamics and system theory as well as their high technology applications. This is therefore the theme of this Special Issue:

**System Science and Optimization Approaches to Nonlinear Dynamics and Systems Theory with High Technology Applications (2)**

With this aim in mind, the goal of the special issue is to provide an international forum for scientists, researchers, and practitioners from both academia and industry to present their latest research findings and state-of-the-art solution methods in areas related to the theme of the Special Issue.

Scientists from many countries and regions — Australia, China, Greece, Hong Kong, Japan, India, Saudi Arabia, USA and Vietnam — accepted the invitation of the Guest Editors to submit papers for the Special Issue of the Journal. They all went through a rigorous refereeing process with at least two independent referees for each submitted paper. The number of the submitted papers exceed substantially the size of one issue, and we decided to publish two special issues. Topics included in these papers are modelling, design analysis, simulation, optimization, performance evaluation, intelligent information and technology, nonlinear stochastic systems, and optimal control. Applications involved include communication networks, engineering and management systems, computer and information technology, and knowledge management.

The completion of this volume would not have been possible without the assistance of many of our colleagues. We wish to express our sincere appreciation to all those who helped. We are deeply grateful to our referees who provided prompt and extensive reviews for all submissions. Their constructive comments contributed to the quality of the volume. In particular, we wish to thank Editor-in-Chief, Professor Anatolii A. Martynyuk for his kind cooperation and support. Our special thank also go to Mrs. Lisa Holling for her help during the editing process of this Special Issue. Last but not least, we wish to thank those authors who responded to our call for papers by submitting their papers to be considered for possible publication in this Special Issue.

Wuyi Yue[1] and Kok Lay Teo[2] – Guest Editors

[1]Department of Information Science and Systems Engineering, Konan University, 8-9-1 Okamoto, Higashinada-ku, Kobe 658-8501, Japan. E-mail: yue@konan-u.ac.jp

[2]Department of Mathematics and Statistics, Curtin University of Technology, GPO Box U1987, Perth, Western Australia 6845, Australia. E-mail: K.L.Teo@curtin.edu.au

 

**NONLINEAR DYNAMICS AND SYSTEMS THEORY**

An International Journal of Research and Surveys
Published since 2001

**System Science and Optimization Approaches to Nonlinear Dynamics and Systems Theory with High Technology Applications (1)**

Special Issue

CONTENTS *)

Preface ..... v

Mixed Semidefinite and Second-Order Cone Optimization Approach for the Hankel Matrix Approximation Problem ..... 211
*Mohammed M. Alshahrani and Suliman S. Al-Homidan*

Lagrangian Duality Algorithms for Finding a Global Optimal Solution to Mathematical Programs with Affine Equilibrium Constraints ..... 225
*Pham Ngoc Anh and Le Dung Muu*

Thermal Stresses in a Hexagonal Region With an Elliptic Hole ..... 245
*Sukhwinder Kaur Bhullar*

Duality in Distributed-Parameter Control of Nonconvex and Nonconservative Dynamical Systems with Applications ..... 257
*David Yang Gao*

On a Class of Strongly Nonlinear Impulsive Differential Equation with Time Delay ..... 281
*W. Wei, S.H. Hou and K.L. Teo*

The Matrix-Geometric Solution of the M/$E_k$/1 Queue with Balking and State-Dependent Service ..... 295
*Dequan Yue, Chunyan Li and Wuyi Yue*

*) See *Nonlinear Dynamics and Systems Theory*, Vol. 6, Issue 3, 2006, 211–308.

Nonlinear Dynamics and Systems Theory, **7** (1) (2007) 1–21

# Prior-free Inference for Objective Bayesian Analysis and Model Selection

Koki Kyo *

*School of Agriculture,*
*Obihiro University of Agriculture and Veterinary Medicine,*
*Inada-cho, Obihiro, Hokkaido 080-8555, Japan*

Received: April 18, 2005; Revised: December 25, 2005

**Abstract:** A new approach to Bayesian inference, named the *prior-free inference*, is introduced for developing objective Bayesian analysis based on information-theoretic approach. This new approach is essentially a Bayesian method but it does not depend on a prior distribution for unknown parameters. Thus, this approach not only has the advantages of the Bayesian approach but also can avoid the difficulty, the traditional Bayesian approach encounters due to a lack of prior information. Several examples are illustrated to show the procedure and the performance of the prior-free inference. A new information criterion, named *prior-free information criterion* (PFIC), is introduced as an extension of the procedure of the prior-free inference. Then, minimum PFIC method for model selection is developed based on the use of PFIC. Simulation results show that the minimum PFIC method performs very well.

**Keywords:** *Non-informative priors; prior-free inference; objective Bayesian analysis; model selection; information criterion.*

**Mathematics Subject Classification (2000):** 62B10, 62F15.

## 1 Introduction

A necessary condition of the traditional Bayesian analysis is the use of a prior distribution. As pointed out by Akaike [3], however, in practical applications of Bayesian analysis the available prior information is not usually sufficient to completely specify the prior distribution. For that reason, various procedures of objective Bayesian inference using non-informative or ignorance priors have been developed.

The pioneers in the accomplishment of Bayesian analysis such as Bayes and Laplace developed Bayesian procedure using uniform prior distribution for objectivity [4, 25].

* Corresponding author: x.q.jiang@m2.dion.ne.jp

 

However, sometimes such procedure encounters difficulties because of a lack of invariance under transformation of unknown parameters [15]. Fisher did not accept Bayesian procedure mainly due to the use of uniform prior distribution, he attempted to make statistical inference by proposing the concept of inverse probability and his fiducial approach [12, 13, 14]. Essentially, Fisher's fiducial approach is somewhat in the category of Bayesian, but it is not necessary to suppose a prior distribution. Unfortunately, Fisher's fiducial approach ultimately cannot be achieved as a systematized methodology for statistical inference.

Criticisms of the use of uniform prior distribution caused Jeffreys to develop his ignorance prior distribution [16]. The definition of Jeffreys prior is based on the concept of invariance of the distribution by a transformation of unknown parameters. Lindley applied Shannon entropy to introduce an information-theoretic analysis of the structure of Bayesian modeling [28]. Zellner and Bernardo developed objective Bayesian procedures using the maximal data information prior distribution and the reference prior distribution respectively [33, 34, 7]. These work prompted the work by Akaike on the problem of specifying a prior distribution over a finite number of data distributions [3].

The main concern with objective Bayesian procedures is that they often utilize improper prior distributions, and so do not automatically have desirable Bayesian properties, such as coherency [31]. Also, the use of improper priors may lead to some difficulties of utilizing information-theoretic approach to identification of priors. Thus recent studies of objective Bayesian procedures are mostly about to ensure that such problems do not arise [6, 8].

In this paper, we attempt to contribute to objective Bayesian theory by developing a new approach which is called *prior-free inference*. The remainder of the paper is organized as follows. In Section 2 we explain the procedural and mathematical background and motivation of the present study. In Section 3 we show the procedure of the prior-free inference and related theoretic results. In Section 4 we illustrate the procedure and the performance of the prior-free inference by several examples. In Section 5 we develop a methodology for model selection based on the prior-free inference. Finally, concluding remarks are given in Section 6.

## 2 Settings and motivation

### 2.1 Settings

In the present paper, we attempt to introduce a new approach to Bayesian inference for a vector, $\theta = (\theta_1, \theta_2, \ldots, \theta_k)^{\mathsf{t}}$, of $k$ continuous parameters. Let $X(1:n) = \{X_1, X_2, \ldots, X_n\}$ be a sample of size $n$ with each $X_i$ being univariate continuous random variable, where $n > k$. Generally, suppose we have a statistical model of $X(1:n)$ given $\theta$ that is defined by a joint probability density $f_{X(1:n)}(x(1:n)|\theta)$. Based on $f_{X(1:n)}(x(1:n)|\theta)$ we can obtain a model density of $X_i$ in the conditional density form, $f_{X_i}(x_i|x(1:i-1),\theta)$, given the observations $x(1:i-1) = \{x_1, x_2, \ldots, x_{i-1}\}$ of $X(1:i-1)$ for $i = 1, 2, \ldots, n$. Thus, by defining $f_{X_1}(x_1|x(1:0),\theta) = f_{X_1}(x_1|\theta)$, the model density $f_{X(1:n)}(x(1:n)|\theta)$ can be expressed by

$$f_{X(1:n)}(x(1:n)|\theta) = f_{X_1}(x_1|\theta) f_{X_2}(x_2|x(1:1),\theta) \cdots f_{X_n}(x_n|x(1:n-1),\theta). \quad (1)$$

For the sake of further discussion, we introduce the definition of "support". The concept of support can be found in [26] and [32]. For a density function $u(x)$ of $X$, its

*support* is defined by the set $\boldsymbol{\mathcal{S}}(u) = \{x; u(x) > 0\}$. Further, for a conditional density function $v(x|y)$ of $X$ given $y$, its support is defined by the set $\boldsymbol{\mathcal{S}}(v|y) = \{x : v(x|y) > 0\}$.

In Bayesian approach, the parameter vector $\theta$ can be regarded as a vector of given values of $k$ random variables, say $\Theta = (\Theta_1, \Theta_2, \ldots, \Theta_k)^{\mathsf{t}}$. It is required to set up an initial probability distribution, called the prior distribution, for $\Theta$. Let $\pi(\theta)$ be a prior density, and denote by $f_\Theta(\theta|x(1:k))$ the corresponding posterior density or post data density for $\Theta$ given $x(1:k)$. We have the following relation between the prior density and the post data density:

$$f_\Theta(\theta|x(1:k))h(x(1:k)) = \pi(\theta)f_{X(1:k)}(x(1:k)|\theta), \tag{2}$$

where $h(x(1:k))$ denotes the marginal density of $X(1:k)$.

Let $\boldsymbol{\mathcal{S}}(\pi)$ and $\boldsymbol{\mathcal{S}}(h)$ be the supports of $\pi(\theta)$ and $h(x(1:x))$, respectively. Denote by $\boldsymbol{\mathcal{S}}(f_\Theta|x(1:k))$ the support of $f_\Theta(\theta|x(1:k))$ for $x(1:k) \in \boldsymbol{\mathcal{S}}(h)$, and denote by $\boldsymbol{\mathcal{S}}(f_{X(1:k)}|\theta)$ that of $f_{X(1:k)}(x(1:k)|\theta)$ for $\theta \in \boldsymbol{\mathcal{S}}(\pi)$. For a likelihood oriented inference, it is unnecessary to consider a value of $\theta \in \boldsymbol{\mathcal{S}}(\pi)$ that leads to $f_{X(1:k)}(x(1:k)|\theta) = 0$. So, from equation (2) we can bring the equality $\boldsymbol{\mathcal{S}}(\pi) = \boldsymbol{\mathcal{S}}(f_\Theta|x(1:k))$ for $x(1:k) \in \boldsymbol{\mathcal{S}}(h)$. Similarly, we can also assume that $\boldsymbol{\mathcal{S}}(h) = \boldsymbol{\mathcal{S}}(f_{X(1:k)}|\theta)$ for $\theta \in \boldsymbol{\mathcal{S}}(\pi)$. Suppose that both of the prior density $\pi(\theta)$ and the post data density $f_\Theta(\theta|x(1:k))$ are proper. Then, we can obtain the marginal density of $X(1:k)$ as

$$h(x(1:k)) = \int_{\boldsymbol{\mathcal{S}}(\pi)} f_{X(1:k)}(x(1:k)|\theta)\pi(\theta)d\theta, \tag{3}$$

which is also a proper density. From equation (2), we obtain the post data density by

$$f_\Theta(\theta|x(1:k)) = \frac{f_{X(1:k)}(x(1:k)|\theta)\pi(\theta)}{h(x(1:k))}, \tag{4}$$

which is called Bayes' theorem (see [9]).

Bayes' theorem allows us to continuously update information about $\Theta$ as more observations are obtained. Now, let $f_{X(k+1:n)}(x(k+1:n)|x(1:k),\theta)$ be the model density for $X(k+1:n) = \{X_{k+1}, X_{k+2}, \ldots, X_n\}$ given $x(1:k)$ and $\theta$. Then, we can obtain the post data density for $\Theta$ given $x(1:n)$ as

$$f_\Theta(\theta|x(1:n)) = \frac{f_{X(k+1:n)}(x(k+1:n)|x(1:k),\theta)f_\Theta(\theta|x(1:k))}{g(x(k+1:n)|x(1:k))}, \tag{5}$$

where $g(x(k+1:n)|x(1:k)) = \int_{\boldsymbol{\mathcal{S}}(\pi)} f_{X(k+1:n)}(x(k+1:n)|x(1:k),\theta)f_\Theta(\theta|x(1:k))d\theta$. The expression (5) is precisely of the same form as equation (4) except that $f_\Theta(\theta|x(1:k))$ plays the role of the prior density for the succeeding observations $x(k+1:n)$. Obviously, this process can be repeated times. Thus, Bayes' theorem describes the process of updating the distribution of $\Theta$ as learning from data. As pointed out by Zellner [35], information processing based on Bayes' theorem does not cause loss of information. In this paper, we call $f_\Theta(\theta|x(1:k))$ and $f_\Theta(\theta|x(1:n))$ the initial and the final post data density, respectively.

Bayesian approach gives a basis for inference not only on unknown parameters but also on any unobserved random variable that follows a probability distribution depending on the parameters. In the concrete, for unobserved random variables, say $Y$, that follow the model density $f_Y(y|x(1:n),\theta)$, the predictive density $f_Y(y|x(1:n))$ of $Y$ is given by

$$f_Y(y|x(1:n)) = \int_{\boldsymbol{\mathcal{S}}(\pi)} f_Y(y|x(1:n),\theta)f_\Theta(\theta|x(1:n))d\theta. \tag{6}$$

From the above observations, we can see that the cruxes of the traditional Bayesian analysis are the model density for observed data and the prior density for the parameters. The model density and the prior density are as two inputs for Bayesian information processing [35], but it may be true that the model density should precedes the prior density, because without model density there can be no parameters hence it is not necessary to consider a prior density. In scientific research, setting up hypotheses is the main subject for researchers, the model (or a set of contending models) for observed data may be constructed along with the hypotheses. However, it may be more difficult to have knowledge about the parameters in the constructed model before analyzing the observed data.

### 2.2 Motivation

It can be seen from the discussion in Subsection 2.1 that a feature of the traditional Bayesian approach is the prior-dependency. It leads to a difficulty in applications of Bayesian inference when the prior information is unavailable. This difficulty may be fatal for most situations of scientific research and it is also the main cause of criticism to Bayesian statistics. As pointed out by [11], "The Bayesian methodology, while enjoying good properties (e.g., admissibility and consistency), is peculiar, in that it requires the user to postulate a prior distribution that is basically as complex as the quantities being inferred, if not more so". There are a number of studies on evaluating priors by using model and observed data, e.g., Zellner [33, 34, 36], Bernardo [7], Akaike [2], Jaynes [15], Chuaqui [10], Berger and Bernardo [6], Berger [5], Li and Vitanyi [27]. Such approaches have provided solutions to mitigate the difficulty of the traditional Bayesian analysis.

In order to overcome the difficulty of the traditional Bayesian analysis caused by a lack of prior information, a new approach to objective Bayesian analysis will be introduced in the present paper. The main feature of this approach is that it is free of dependence on a prior distribution. Thus, we call Bayesian inference based on this approach *prior-free inference*. Contrastively, we call Bayesian inference beginning with construction of priors the traditional Bayesian approach. An outline of the prior-free inference is shown in [17] by the name of self-concluding inference, and it was further developed in [18]. Main results on information-theoretic approach to the prior-free inference were given in [19], and an application of the prior-free approach to estimation and identification of regression models was given in [20]. The key idea of the prior-free inference is as follows. The presupposition of the prior-free inference is that we have a model density for the observed data. As the first stage of the procedure, we derive an initial post data density $f_\Theta(\theta|x(1:k))$ of $\Theta$ given $x(1:k)$, from the given model density for $X(1:k)$ directly. Then, in the second stage we apply $f_\Theta(\theta|x(1:k))$ as the prior density for the observations of the remaining sample $X(k+1:n)$ to obtain the final post data density $f_\Theta(\theta|x(1:n))$ by using Bayes' theorem.

The similarity between the prior-free inference approach and the reference priors approach is that both of these two approaches are developed based on an information-theoretic viewpoint. As will be mentioned in Section 3, however, for an improper prior density the Lindley's criterion functional, which lays the foundations of the reference priors approach, cannot be well-defined. Unfortunately, in objective Bayesian analysis the prior is obtained frequently in an improper form. This difficulty is avoided by introducing a new criterion functional which is utilized as the foundations of the prior-free inference approach.

Now, the model selection is always an important problem in statistical analysis. When several contending models are constructed, it is required to evaluate each model and select

one as the best among them. In the present paper, a methodology for model selection is also developed as a natural extension of the prior-free inference.

## 3 Prior-free inference

### 3.1 Definition of inferential functions

First of all, we define a set of probability integral transformations as

$$\varphi_i(x(1:i),\theta) = \int_{-\infty}^{x_i} f_{X_i}(t|x(1:i-1),\theta)dt \tag{7}$$

for $i = 1, 2, \ldots, k$. Obviously, the quantity $\varphi_i(x(1:i),\theta)$ defined by equation (7) is a function of $x(1:k)$ and $\theta$.

In the case that $x(1:k)$ are given, the quantity $\varphi_i(x(1:i),\theta)$ defined by equation (7) becomes a function of $\theta$ only, so we express it as follows:

$$z_i = z_i(\theta) = \varphi_i(x(1:i),\theta)|_{x(1:i)} \quad (i = 1, 2, \ldots, k). \tag{8}$$

Further, when $\theta$ is replaced with $\Theta$, a new vector of random variables, say

$$Z = (Z_1, Z_2, \ldots, Z_k)^{\mathtt{t}} = (z_1(\Theta), z_2(\Theta), \ldots, z_k(\Theta))^{\mathtt{t}}, \tag{9}$$

is defined. The functions defined by equation (9) together with equations (7) and (8) are important for the procedure of the prior-free inference, we call them the *inferential functions*.

Let $f_Z(z|x(1:k)$ be a post data density for $Z$ given $x(1:k)$, and let $\boldsymbol{\mathcal{S}}(f_Z|x(1:k))$ denote its support. The inferential functions can be regarded as a set of transformations from $\boldsymbol{\mathcal{S}}(\pi)$ to $\boldsymbol{\mathcal{S}}(f_Z|x(1:k))$ with

$$J = (\frac{\partial z_i}{\partial \theta_j}) \tag{10}$$

being the Jacobian matrix. When both $x(1:i)$ and $\theta$ are given $z_i$ is the cumulative probability, hence we can see that $\boldsymbol{\mathcal{S}}(f_Z|x(1:k)) \subseteq [0,1] \times [0,1] \times \cdots \times [0,1]$.

For given $x(1:k)$ we call inferential functions *informative* if they satisfy the following conditions:

**(C1)** The partial differential, $\frac{\partial z_i}{\partial \theta_j}$, is a continuous function of $\theta$ at all points of $\boldsymbol{\mathcal{S}}(\pi)$ for $i, j = 1, 2, \ldots, k$.

**(C2)** The Jacobian matrix defined by equation (10) is a nonsingular matrix at all points of $\boldsymbol{\mathcal{S}}(\pi)$.

When inferential functions are informative, they play the role of one-to-one transformations between $\boldsymbol{\mathcal{S}}(\pi)$ and $\boldsymbol{\mathcal{S}}(f_Z|x(1:k))$. Thus, they have a property shown by the following lemma (see Appendix A for proof):

**Lemma 3.1** *If the inferential functions are informative, then the quantity defined by*

$$\lambda = \int_{\boldsymbol{\mathcal{S}}(\pi)} |\det(J)| d\theta \tag{11}$$

*satisfies the inequality* $0 < \lambda \leq 1$, *where* $\det(J)$ *denotes the determinant of the Jacobian matrix defined by equation* (10), *and* $|\det(J)|$ *denotes its absolute value.*

We can classify the informative inferential functions into two types. For the quantity $\lambda$ defined by equation (11), the informative inferential functions are called *fully informative* if $\lambda = 1$, and they are called *partially informative* if $0 < \lambda < 1$. It can be verified that if the inferential functions are fully informative, then $\boldsymbol{\mathcal{S}}(f_Z|x(1:k)) = [0,1] \times [0,1] \times \cdots \times [0,1]$; and if they are partially informative, then $\boldsymbol{\mathcal{S}}(f_Z|x(1:k)) \subset [0,1] \times [0,1] \times \cdots \times [0,1]$. If the inferential functions are informative under $x(1:k)$, then the initial post data density $f_\Theta(\theta|x(1:k))$ for $\Theta$ can be defined in terms of the post data density $f_Z(z|x(1:k))$ for $Z$ by

$$f_\Theta(\theta|x(1:k)) = f_Z(z|x(1:k)) \; |\det(J)|. \tag{12}$$

Thus, we can determine $f_\Theta(\theta|x(1:k))$ through $f_Z(z|x(1:k))$.

### 3.2 Determination of initial post data density

In this subsection, we show how to determine the post data density $f_Z(z|x(1:k))$ for $Z$, or equivalently the initial post data density $f_\Theta(\theta|x(1:k))$ for $\Theta$, by utilizing an information-theoretic approach.

For random variable $Y$, which is possibly multivariate, let $u(y)$ and $v(y)$ be two density functions, the Kullback-Leibler information of $u(y)$ with respect to $v(y)$ is defined by

$$I_K(u;v) = \int \ln\{\frac{u(y)}{v(y)}\}u(y)dy. \tag{13}$$

It is well-known that $I_K(u;v) \geq 0$, and $I_K(u;v) = 0$ if and only if $v(y) = u(y)$ almost everywhere. $I_K(u;v)$ is as a functional of $u(y)$ and $v(y)$ that measures the "distance" between $u(y)$ and $v(y)$ by regarding $v(y)$ as the *reference distribution*. If the reference distribution $v(y)$ is improper and $u(y)$ is proper, then the probability measures defined on $u(y)$ and $v(y)$ cannot be absolutely continuous with respect to one another, hence $I_K(u;v)$ cannot be finite (see [24]). Thus, $I_K(u;v)$ must be infinite as long as $v(y)$ is improper.

Lindley applied the Kullback-Leibler information to Bayesian inference in order to introduce his criterion functional [28]. By the notation, an expression of Lindley's criterion functional is given by

$$F_L(\pi|f_{X(1:k)}) = \int_{\boldsymbol{\mathcal{S}}(h_{X(1:k)})} I_K^C(f_\Theta;\pi|x(1:k))h_{X(1:k)}(x(1:k))dx(1:k), \tag{14}$$

which measures the missing information about $\Theta$ for a given model density. In equation (14),

$$I_K^C(f_\Theta;\pi|x(1:k)) = \int_{\boldsymbol{\mathcal{S}}(\pi)} \ln\{\frac{f_\Theta(\theta|x(1:k))}{\pi(\theta)}\}f_\Theta(\theta|x(1:k))d\theta \tag{15}$$

is the Kullback-Leibler information between $f_\Theta(\theta|x(1:k))$ and $\pi(\theta)$ given $x(1:k) \in \boldsymbol{\mathcal{S}}(h)$. Bernardo [7] developed his reference priors approach that derives a prior density as a solution to maximizing $F_L(\pi|f_{X(1:k)})$. In [7], such solution is regarded as a prior that describes vague initial knowledge about $\theta$.

Obviously, by definition we have

$$F_L(\pi|f_{X(1:k)}) = I_K(s;t), \tag{16}$$

where

$$s(x(1:k),\theta) = f_\Theta(\theta|x(1:k))h(x(1:k)), \tag{17}$$
$$t(x(1:k),\theta) = \pi(\theta)h(x(1:k)). \tag{18}$$

As shown in equations (17) and (18), $s(x(1:k),\theta)$ denotes the joint density for $X(1:k)$ and $\Theta$ under the assumption that $X(1:k)$ and $\Theta$ are correlated, and $t(x(1:k),\theta)$ is that for $X(1:k)$ and $\Theta$ under the assumption that $X(1:k)$ and $\Theta$ are independent of each other. So, Lindley's criterion functional measures the distance between $s(x(1:k),\theta)$ and $t(x(1:k),\theta)$ by regarding $t(x(1:k),\theta)$ as the reference distribution. In the traditional Bayesian approach, if the model density is given, then both of the initial post data density and the marginal density for $X(1:k)$ are as functionals of the prior density, hence both of $s(x(1:k),\theta)$ and $t(x(1:k),\theta)$ are functionals of the prior density $\pi(\theta)$. Therefore, the Lindley's criterion functional $F_L(\pi|f_{X(1:k)})$ is as a functional of the prior density.

A result given in [19] shows that it may be difficult to specify a prior as a solution to maximizing the Lindley's criterion functional. This fact prompts us to introduce another criterion functional for specifying an initial post data density. The newly-introduced criterion functional is defined by

$$F(f_\Theta,\pi|f_{X(1:k)}) = \int_{\boldsymbol{\mathcal{S}}(h_{X(1:k)})} I_K^C(\pi; f_\Theta|x(1:k))h_{X(1:k)}(x(1:k))dx(1:k), \tag{19}$$

where

$$I_K^C(\pi; f_\Theta|x(1:k)) = \int_{\boldsymbol{\mathcal{S}}(\pi)} \ln\{\frac{\pi(\theta)}{f_\Theta(\theta|x(1:k))}\}\pi(\theta)d\theta \tag{20}$$

defines the Kullback-Leibler information between $\pi(\theta)$ and $f_\Theta(\theta|x(1:k))$ given $x(1:k) \in \boldsymbol{\mathcal{S}}(h)$. It is obvious that

$$F(f_\Theta,\pi|f_{X(1:k)}) = I_K(t;s) \tag{21}$$

under the definitions in equations (17) and (18). The criterion functional $F(f_\Theta,\pi|f_{X(1:k)})$ measures the distance between $s(x(1:k),\theta)$ and $t(x(1:k),\theta)$ by regarding $s(x(1:k),\theta)$ as the reference distribution. In the prior-free inference, we consider the criterion functional $F(f_\Theta,\pi|f_{X(1:k)})$ as a functional not only for the prior density but also for the initial post data density because we attempt to determine the initial post data density directly by maximizing $F(f_\Theta,\pi|f_{X(1:k)})$ for a given model density and any fixed prior density.

Perhaps, the intention to specify a prior by maximizing the Lindley's criterion functional is to make inference by using the traditional Bayesian approach with the most vague prior. Contrastively, the intention to obtain an initial post data density by maximizing the newly-introduced criterion functional is that we attempt to make post data inference by using the information contained in $x(1:k)$ to the maximum for a given model density and any fixed prior density that is regarded as a non-informative prior. Obviously, the greater the value of $F(f_\Theta,\pi|f_{X(1:k)})$ the larger the information about $\Theta$ contained in $x(1:k)$. Therefore, in order to obtain an initial post data density that has maximal information contained in $x(1:k)$, we derive the initial post data density directly by maximizing $F(f_\Theta,\pi|f_{X(1:k)})$. As a theoretical finding, we have the following theorem (see Appendix B for proof):

**Theorem 3.1** *Under equation* (4)*, if the inferential functions are informative, then the criterion functional* $F(f_\Theta, \pi | f_{X(1:k)})$ *may have the following two maximizers:*

$$f_\Theta^{(1)}(\theta|x(1:k)) = \frac{1}{\psi}, \tag{22}$$

$$f_\Theta^{(2)}(\theta|x(1:k)) = \frac{1}{\lambda} \, |\det(J)|, \tag{23}$$

*for a given model density of* $X(1:k)$ *and any fixed prior density that is proper, where* $\psi = \int_{\boldsymbol{\mathcal{S}}(\pi)} d\theta$ *is a constant, and* $\lambda$ *is calculated by using equation* (11)*.*

Note that the both of these two maximizers of the criterion functional $F(f_\Theta, \pi | f_{X(1:k)})$ are free of dependence on the prior density.

Now, we have to choose one from the above alternative solutions to maximizing the criterion functional $F(f_\Theta, \pi | f_{X(1:k)})$. We employ here the concept of information. For given $x(1:k)$ the information of the initial post data density $f_\Theta(\theta|x(1:k))$ is defined by

$$I(f_\Theta|x(1:k)) = \int_{\boldsymbol{\mathcal{S}}(\pi)} \ln\{f_\Theta(\theta|x(1:k))\} f_\Theta(\theta|x(1:k)) d\theta. \tag{24}$$

$I(f_\Theta|x(1:k))$ defined by equation (24) can be regarded as the negative conditional entropy of $\Theta$ with respect to $f_\Theta(\theta|x(1:k))$. The greater value of $I(f_\Theta|x(1:k))$ means that we have larger value of information to predict the value of $\Theta$ based on $x(1:k)$. It is desirable to find an initial post data density that maximizes the criterion functional $F(f_\Theta, \pi | f_{X(1:k)})$, and leads to a larger value of $I(f_\Theta|x(1:k))$. The following theorem gives us a strategy of determining the initial post data density (see Appendix C for proof):

**Theorem 3.2** *Under the condition that the initial post data density is proper, we have*

$$I(f_\Theta^{(2)}|x(1:k)) \geq I(f_\Theta^{(1)}|x(1:k)), \tag{25}$$

*where* $I(f_\Theta^{(1)}|x(1:k))$ *and* $I(f_\Theta^{(2)}|x(1:k))$ *denote the values of information* $I(f_\Theta|x(1:k))$ *corresponding to equations* (22) *and* (23)*, respectively.*

Theorem 3.2 together with Theorem 3.1 implies that it is a better strategy to determine the initial post data density by using equation (23).

### 3.3 General procedure

Suppose we have observations $x(1:n)$ for a sample $X(1:n)$ of size $n$, and the model density for $X(1:n)$ is given by equation (1). Assume that we can ensure that the inferential functions are informative under $x(1:k)$ by an appropriate permutation of the observations $x(1:n)$. Based on the results obtained in the previous subsection, we obtain a general procedure for the prior-free inference as follows:

Firstly, we calculate the initial post data density $f_\Theta(\theta|x(1:k))$ by using equation (23) together with equation (11). Then, we utilize $f_\Theta(\theta|x(1:k))$ as the prior density for the remaining observations $x(k+1:n)$, and obtain the final post data density $f_\Theta(\theta|x(1:n))$ by using equation (5). Finally, if it is necessary we compute the predictive density for an unobserved random quantity $Y$ that has the model density $f_Y(y|x(1:n), \theta)$ by using equation (6).

The reason to carry out the prior-free inference by using the two stage constructions of the post data density is as follows: In the stage of determining the initial post density, there may be information loss due to a lack of prior information. The information loss can be minimized by using the proposed procedure. In the stage of calculating the final post density, the information contained in the additional observations $x(k+1:n)$ can be fully employed, because the use of Bayes' theorem. Thus, it is desirable to save the observations for the second stage as many as possible. It should be emphasized that the number $k$ of observations used in the first stage is the minimum requirement for ensuring the inferential functions to be informative.

### 3.4 Comparison between criterion functionals

It can be seen that the newly-introduced criterion functional, defined by equation (19) together with equation (20), lays the foundations of the frior-free inference. To show the necessity for introducing it instead of the Lindley's criterion functional, we compare the properties of these two criterion functionals as follows:

Firstly, as is shown in Theorem 3.1 and Theorem 3.2, the newly-introduced criterion functional is concave with respect to the initial post data density $f_\Theta(\theta|x(1:k))$ for a given model density and any fixed prior density that is proper. It was shown in [19], however, Lindley's criterion functional identically equals zero under some regular conditions. So, it seems to be difficult to specify a prior density by maximizing Lindley's criterion functional.

Secondly, the Bernardo's reference prior approach may lead to improper priors when at least one end point of the support of the prior density is not finite. In such case, a difficulty will arise because the Lindley's criterion functional cannot be well-defined. But this difficulty does not arise in the proposed approach because the maximizer of the newly-introduced criterion functional is free of independence on a prior, so the newly-introduced criterion functional can be defined well on any fixed prior density as long as it is proper.

Finally, as mentioned in Subsection 3.2 both of $s(x(1:k),\theta)$ and $t(x(1:k),\theta)$, defined by equations (17) and (18) respectively, are functionals of the prior density $\pi(\theta)$, so from equation (16) we can see that the Lindley's criterion functional is a more intricate functional of the prior. Thus, its maximization may be complicated. On the other hand, for a given model density and any fixed prior, $t(x(1:k),\theta)$ does not depend on the initial post data density. Thus, from equation (21) it is can be seen that the newly-introduced criterion functional is defined as a functional of the initial post data density with a simple structure, so that it can be easy to be manipulated.

### 3.5 Special procedure for separable models

Let $U(1:n)=\{U_1,U_2,\ldots,U_n\}$ be a sample for a random variable $U$. Suppose $U(1:n)$ follows model density $f_{U(1:n)}(u(1:n)|\theta)$ with $\theta$ being a $k$-dimensional vector of parameters. We consider partition of the sample, $U(1:n)=\{U(1:m),U(m+1:n)\}$, and partition of the parameter vector, $\theta=\{\theta^{(1)},\theta^{(2)}\}$, with the dimension of $\theta^{(1)}$ being $\ell$ $(<k)$ for $\ell \le m < n$ and $k-\ell < n-m$. If the model density for $U(1:n)$ can be expressed by the form

$$f_{U(1:n)}(u(1:n)|\theta)=f_{U(1:m)}(u(1:m)|\theta^{(1)},\theta^{(2)})f_{U(m+1:n)}(u(m+1:n)|\theta^{(2)}), \qquad (26)$$

then we say that the model density $f_{U(1:n)}(u(1:n)|\theta)$ is separable. The feature of the model in equation (26) is that the model density $f_{U(m+1:n)}(u(m+1:n)|\theta^{(2)})$ for $U(m+1:n)$, depends only on $\theta^{(2)}$.

We can obtain the post data density $f_{\Theta^{(2)}}(\theta^{(2)}|u(m+1:n))$ for $\Theta^{(2)}$, given $u(m+1:n)$, and obtain the post data density $f_{\Theta^{(1)}}(\theta^{(1)}|u(1:m),\theta^{(2)})$ for $\Theta^{(1)}$, given $u(1:m)$ and $\theta^{(2)}$ by using the procedure of the prior-free inference separately. Then, the post data density for $\Theta$ can be obtained successively by

$$f_{\Theta}(\theta|u(1:n)) = f_{\Theta^{(1)}}(\theta^{(1)}|u(1:m),\theta^{(2)}) f_{\Theta^{(2)}}(\theta^{(2)}|u(m+1:n)).$$

Further, when the sample $U(1:n)$ for $U$ is obtained from another sample, say $X(1:n)$, for random variable $X$ through a one-to-one transformation

$$U(1:n) = \psi(X(1:n)), \tag{27}$$

the model density of $U(1:n)$ can be derived from that of $X(1:n)$ by

$$f_{U(1:n)}(u(1:n)|\theta) = f_{X(1:n)}(x(1:n)|\theta)|(\frac{\partial u_i}{\partial x_j})|^{-1}, \tag{28}$$

where $(\frac{\partial u_i}{\partial x_j})$ denotes the Jacobian matrix of the transformation (27). If the model density $f_{U(1:n)}(u(1:n)|\theta)$ in equation (28) can be expressed by the separable form expressed by equation (26), then we say the model density for $X(1:n)$ separable.

Sometimes, we can simplify the process of obtaining inferential results through a separated form for a separable model. For illustration we show the following example:

**Example 3.1** Consider $X(1:n)$ as a sample that each $X_i$ is independently distributed with the same normal density

$$f_{X_i}(x_i|\theta) = \frac{1}{\sqrt{2\pi\sigma^2}} \exp\{-\frac{(x_i-\mu)^2}{2\sigma^2}\}, \quad -\infty < x_i < \infty \quad (i = 1, 2, \ldots, n),$$

where $\theta = (\mu, \sigma)^{\mathtt{t}}$ denotes the parameter vector with $\mu$ and $\sigma$ being the mean and the standard deviation. We obtain the values $u(1:n)$ for $U(1:n)$ by using the transformation

$$(u_1, u_2, \ldots, u_n)^{\mathtt{t}} = H(x_1, x_2, \ldots, x_n)^{\mathtt{t}}, \tag{29}$$

where $H$ denotes the Helmert matrix defined by

$$H = \begin{bmatrix} \frac{1}{\sqrt{n}} & \frac{1}{\sqrt{n}} & \cdots & \cdots & \cdots & \frac{1}{\sqrt{n}} \\ \frac{1}{\sqrt{1\times 2}} & -\frac{1}{\sqrt{1\times 2}} & 0 & \cdots & \cdots & 0 \\ \frac{1}{\sqrt{2\times 3}} & \frac{1}{\sqrt{2\times 3}} & -\frac{2}{\sqrt{2\times 3}} & 0 & \cdots & 0 \\ \vdots & \vdots & \vdots & \vdots & \ddots & \vdots \\ \vdots & \vdots & \vdots & \vdots & & 0 \\ \frac{1}{\sqrt{(n-1)n}} & \frac{1}{\sqrt{(n-1)n}} & \cdots & \cdots & \frac{1}{\sqrt{(n-1)n}} & -\frac{n-1}{\sqrt{(n-1)n}} \end{bmatrix}.$$

It can be verified that from the model density of $X(1:n)$, the first part $U(1:1) = U_1$ of the sample $U(1:n)$ follows the model density

$$f_{U(1:1)}(u_1|\mu,\sigma) = \frac{1}{\sqrt{2\pi\sigma^2}} \exp\{-\frac{(u_1-\sqrt{n}\mu)^2}{2\sigma^2}\}, \quad -\infty < u_1 < \infty, \tag{30}$$

and for $i = 2, 3, \ldots, n$, each $U_i$ follows the model density

$$f_{U_i}(u_i|\sigma) = \frac{1}{\sqrt{2\pi\sigma^2}} \exp\{-\frac{u_i^2}{2\sigma^2}\}, \quad -\infty < u_i < \infty$$

independently. That is, $U(2:n)$ depends only on $\sigma$, its model density is given by

$$f_{U(2:n)}(u(2:n)|\sigma) = \frac{1}{(\sqrt{2\pi\sigma^2})^{n-1}} \exp\{-\frac{\sum_{i=2}^{n} u_i^2}{2\sigma^2}\}. \tag{31}$$

So, we can see that $U(1:1)$ and $U(2:n)$ are independent of each other, hence the model density for $U(1:n)$ can be expressed by the separated form

$$f_{U(1:n)}(u(1:n)|\theta) = f_{U(1:1)}(U(1:1)|\mu,\sigma) f_{U(2:n)}(u(2:n)|\sigma).$$

Since the transformation defined by equation (29) is an orthogonal transformation, we have

$$f_{U(1:n)}(u(1:n)|\theta) = f_{X(1:n)}(x(1:n)|\theta).$$

Therefore, the model density for $X(1:n)$ is separable.

## 4 Illustrations

Several examples are given in the present section in order to illustrate the procedure and performance of the prior-free inference.

### 4.1 Examples for single parameter case

In this subsection, we show three examples for the case that the model density is defined on a single parameter. In this case, we put $k = 1$, thus $\theta = \theta_1$, $z = z_1$ and so forth.

**Example 4.1** Let $X(1:n)$ be a sample that each $X_i$ is independently distributed with the same normal density

$$f_{X_i}(x_i|\theta) = \frac{1}{\sqrt{2\pi}} \exp\{-\frac{(x_i-\theta)^2}{2}\}, \quad -\infty < x_i < \infty \quad (i = 1, 2, \ldots, n),$$

where $\theta \in (-\infty, \infty)$ is the mean as an unknown parameter. Given $x_1$, the inferential function is defined by

$$z = \varphi(x_1, \theta)|_{x_1} = \int_{-\infty}^{x_1} \frac{1}{\sqrt{2\pi}} \exp\{-\frac{(t-\theta)^2}{2}\} dt. \tag{32}$$

For a given value of $\theta \in (-\infty, \infty)$, $v = t - \theta \to -\infty$ as $t \to -\infty$. Thus, we have

$$z = \int_{-\infty}^{x_1-\theta} \frac{1}{\sqrt{2\pi}} \exp\{-\frac{v^2}{2}\} dv.$$

Hence,

$$\begin{aligned} \frac{\partial z}{\partial \theta} &= -\frac{1}{\sqrt{2\pi}} \exp\{-\frac{(\theta - x_1)^2}{2}\}, \\ \lambda &= \int_{-\infty}^{\infty} |\frac{\partial z}{\partial \theta}| d\theta = \int_{-\infty}^{\infty} \frac{1}{\sqrt{2\pi}} \exp\{-\frac{(\theta - x_1)^2}{2}\} d\theta = 1. \end{aligned}$$

It shows that the inferential function defined by equation (32) is fully informative. Therefore, from equations (23) and (11) we obtain the initial post data density for $\Theta$ as

$$f_\Theta(\theta|x_1) = \frac{1}{\sqrt{2\pi}} \exp\{-\frac{(\theta - x_1)^2}{2}\}, \quad -\infty < \theta < \infty.$$

Moreover, from equation (5) the final post data density for $\Theta$ is given by

$$f_\Theta(\theta|x(1:n)) = \sqrt{\frac{n}{2\pi}} \exp\{-\frac{n\ (\theta - \bar{x})^2}{2}\},$$

where $\bar{x} = \frac{1}{n}\sum_{i=1}^{n} x_i$ is the sample mean.

Incidentally, for an unobserved random variable $Y$ which follows the normal density

$$f_Y(y|\theta) = \frac{1}{\sqrt{2\pi}} \exp\{-\frac{(y - \theta)^2}{2}\}, \quad -\infty < y < \infty,$$

we obtain the predictive density as

$$\begin{aligned} f_Y(y|x(1:n)) &= \int_{-\infty}^{\infty} f_Y(y|\theta) f_\Theta(\theta|x(1:n)) d\theta \\ &= \sqrt{\frac{n}{2\pi(n+1)}} \exp\{-\frac{n(y - \bar{x})^2}{2(n+1)}\}, \quad -\infty < y < \infty. \end{aligned}$$

It shows that $Y \sim \mathrm{N}(\bar{x}, \sqrt{\frac{n+1}{n}})$ for given $x(1:n)$.

**Example 4.2** Let $X(1:n)$ be a sample, and suppose each $X_i$ is independently distributed with the same normal density

$$f_{X_i}(x_i|\theta) = \frac{1}{\sqrt{2\pi\theta^2}} \exp\{-\frac{x_i^2}{2\theta^2}\}, \quad -\infty < x_i < \infty \quad (i = 1, 2, \ldots, n),$$

where $\theta$ denotes the standard deviation as an unknown parameter. Assume that $x_1 \neq 0$, we define the inferential function as

$$z = \varphi(x_1, \theta)|_{x_1} = \int_{-\infty}^{x_1} \frac{1}{\sqrt{2\pi\theta^2}} \exp\{-\frac{t^2}{2\theta^2}\} dt. \tag{33}$$

For a given value of $\theta \in (0, \infty)$, $\frac{t}{\theta} \to -\infty$ as $t \to -\infty$. So, we have

$$\frac{\partial z}{\partial \theta} = -\frac{|x_1|}{\sqrt{2\pi}\theta^2} \exp\{-\frac{x_1^2}{2\theta^2}\}.$$

Hence,

$$\lambda = \int_0^\infty |\frac{\partial z}{\partial \theta}| d\theta = \int_0^\infty \frac{|x_1|}{\sqrt{2\pi}\theta^2} \exp\{-\frac{x_1^2}{2\theta^2}\} d\theta = \frac{1}{2}.$$

It shows that the inferential function defined by equation (33) is partially informative. From equations (23) and (11) we obtain the initial post data density of $\Theta$ as

$$f_\Theta(\theta|x_1) = \sqrt{\frac{2}{\pi}} \frac{|x_1|}{\theta^2} \exp\{-\frac{x_1^2}{2\theta^2}\}, \quad 0 < \theta < \infty.$$

Further, from equation (5) the final post data density for $\Theta$ is obtained as

$$f_\Theta(\theta|x(1:n)) = \frac{(\sum_{i=1}^n x_i^2)^{n/2}}{2^{(n-2)/2}\Gamma(n/2)} \frac{1}{\theta^{n+1}} \ \exp\{-\frac{\sum_{i=1}^n x_i^2}{2\theta^2}\}.$$

For an unobserved random variable $Y$ which follows the normal density

$$f_Y(y|\theta) = \frac{1}{\sqrt{2\pi\theta^2}} \exp\{-\frac{y^2}{2\theta^2}\}, \quad -\infty < y < \infty,$$

we obtain the predictive density as

$$\begin{aligned} f_Y(y|x(1:n)) &= \int_{-\infty}^{\infty} f_Y(y|\theta) f_\Theta(\theta|x(1:n)) d\theta \\ &= \frac{4}{\sqrt{\pi}} \frac{\Gamma((n+1)/2)}{\Gamma(n/2)} \left( \frac{\sum_{i=1}^n x_i^2}{\sum_{i=1}^n x_i^2 + y^2} \right)^{n/2}, \quad -\infty < y < \infty. \end{aligned}$$

**Example 4.3** Assume that $X(1:n)$ is a sample which each $X_i$ is independently distributed with the same uniform density

$$f_{X_i}(x_i|\theta) = \frac{1}{\theta}, \quad 0 \le x_i < \theta \quad (i = 1, 2, \ldots, n),$$

where $\theta \in (0, \infty)$ denotes the upper limit which is regarded as an unknown parameter. Given $x_1$, the inferential function is defined by

$$z = \varphi(x_1, \theta)|_{x_1} = \int_0^{x_1} f_X(t|\theta) dt = \int_0^{x_1} \frac{1}{\theta} \, dt = \frac{x_1}{\theta}, \quad \theta \in (x_1, \infty). \tag{34}$$

Then, we have

$$\frac{\partial z}{\partial \theta} = -\frac{x_1}{\theta^2},$$

hence,

$$\lambda = \int_{x_1}^{\infty} |\frac{\partial z}{\partial \theta}| d\theta = \int_{x_1}^{\infty} \frac{x_1}{\theta^2} d\theta = 1.$$

Thus, the inferential function defined by equation (34) is fully informative. Further, from equations (23) and (11) we obtain the initial post data density as

$$f_\Theta(\theta|x_1) = \frac{x_1}{\theta^2}, \quad \theta \in (x_1, \infty).$$

Moreover, from equation (5) the final post data density of $\Theta$ is given by

$$f_\Theta(\theta|x(1,n)) = \frac{n x_{max}^n}{\theta^{n+1}}, \quad \theta \in [x_{max}, \infty),$$

where $x_{max} = \max\{x_1, x_2, \ldots, x_n\}$.

For an unobserved random variable $Y$ which follows the uniform density

$$f_Y(y|\theta) = \frac{1}{\theta}, \quad 0 \le y < \theta,$$

we obtain the predictive density as follows:

$$\begin{aligned} f_Y(y|x(1:n)) &= \int_{x_{max}}^{\infty} f_Y(y|\theta) f_\Theta(\theta|x(1:n))d\theta = \int_{x_{max}}^{\infty} \frac{n x_{max}^n}{\theta^{n+2}} d\theta \\ &= \frac{n}{(n+1)x_{max}}, \quad 0 \le y < \frac{n+1}{n} x_{max}. \end{aligned}$$

It can be seen that the above results in Examples 4.1 and 4.2 agree with the results obtained by using Jeffreys priors. Example 4.3 is very simple and the result can be easily obtained by using the proposed approach. However, it may be difficult when some traditional Bayesian approaches are applied because the model density is not defined by an explicit function of the parameter.

### 4.2 Example for multivariate parameter case

In the following example, we continue Example 3.1 and show how to utilize the procedure of prior-free inference to obtain the post data density for the parameter vector $\theta = (\mu, \sigma)^{\mathsf{t}}$.

**Example 4.4** From the model density of $U(1:1)$ expressed by equation (30), we obtain the post data density for $\mu$, given $u_1$ and $\sigma$, as

$$f_\mu(\mu|u_1, \sigma) = \sqrt{\frac{n}{2\pi\sigma^2}} \exp\{-\frac{(\sqrt{n}\mu - u_1)^2}{2\sigma^2}\}, \quad -\infty < \mu < \infty.$$

The results in Example 4.1 imply that given $u_1$ and $\sigma$, $\mu \sim \mathrm{N}(\frac{u_1}{\sqrt{n}}, \frac{\sigma^2}{n})$. Moreover, from the model density of $U(2:n)$ expressed by equation (31), we obtain the post data density for $\sigma$, given $u(2:n)$, as

$$f_\sigma(\sigma|u(2:n)) = \frac{(\sum_{i=2}^n u_i^2)^{(n-1)/2}}{2^{(n-3)/2}\Gamma((n-1)/2)} \frac{1}{\sigma^n} \exp\{-\frac{\sum_{i=2}^n u_i^2}{2\sigma^2}\},$$

by applying the results in Example 4.3. Thus, the post data density of $\theta = (\mu, \sigma)^{\mathsf{t}}$ is given by

$$\begin{aligned} f_\Theta(\theta|u(1:n)) &= f_\mu(\mu|u(1:1), \sigma) f_\sigma(\sigma|u(2:n)) \\ &= \frac{n^{1/2}(\sum_{i=2}^n u_i^2)^{(n-1)/2}}{2^{(n-2)/2}\pi^{1/2}\Gamma((n-1)/2)} \frac{1}{\sigma^{n+1}} \exp\{-\frac{\sum_{i=2}^n u_i^2 + (\sqrt{n}\mu - u_1)^2}{2\sigma^2}\}. \end{aligned}$$

Since $U(1:n)$ is obtained from $X(1:n)$ by equation (29) which is an one-to-one transformation, the post data density given $x(1:n)$ is the same as that given $u(1:n)$, i.e., $f_\Theta(\theta|x(1:n)) = f_\Theta(\theta|u(1:n))$. Finally, for an unobserved random variable $Y$ which follows the normal density

$$f_Y(y|\theta) = \frac{1}{\sqrt{2\pi\sigma^2}} \exp\{-\frac{(y-\mu)^2}{2\sigma^2}\}, \quad -\infty < y < \infty,$$

we obtain the predictive density of $Y$ based on $x(1:n)$ as

$$f_Y(y|x(1:n)) = c \left( \frac{(n+1)\sum_{i=2}^n u_i^2}{(n+1)\sum_{i=2}^n u_i^2 + (\sqrt{n}y - u_1)^2} \right)^{n/2},$$

where $c = (\frac{n}{(n+1)\pi\sum_{i=2}^n u_i^2})^{1/2} \frac{\Gamma(n/2)}{\Gamma((n-1)/2)}$.

It can be verified that the results in Example 4.4 agree with the results obtained by using Jeffreys priors. It should be noted that our procedure is well systematized and the procedure using Jeffreys priors is somewhat ad hoc.

## 5 Methodology for model selection

When a number of contending models are constructed, we have to select one as the best among them. Recently, many information criteria are introduced for statistical model selection (for example, see [23]). A well-known and widely applied information criterion is Akaike information criterion, AIC (see [1, 21, 29]). The definition of AIC is really simple but it can be applied only to the case that each contending model density is defined by a specific function. For a case that the likelihood can not be defined, Konishi and Kitagawa developed generalized information criterion, GIC [22]. In this section, we introduce a new information criterion by extending the procedure of the prior-free inference.

### 5.1 Prior-free information criterion

Consider here $X(1:n)$ as a random simple that each $X_i$ follows the same model density $f_X(x_i|\theta)$ with $\theta$ being a $k$-dimensional parameter vector. Let $\widetilde{X}$ be a set of $m$ values in $X(1:n)$ for $k \leq m < n$. The model density for $\widetilde{X}$ can be defined based on the model density $f_X$, then the post data density $f_\Theta(\theta|\widetilde{x})$, that is regarded as a functional of $f_X$ for given $\widetilde{x}$, can be obtained by using the procedure of the prior-free inference. For an unobserved random quantity, $Y$, which follows the model density $f_X(y|\theta)$, the predictive density is given by

$$p(y|\widetilde{x}) = \int f_X(y|\theta) f_\Theta(\theta|\widetilde{x}) d\theta.$$

We attempt to evaluate the model density $f_X$ through evaluating the predictive density $p(y|\widetilde{x})$ because $p(y|\widetilde{x})$ can also be regarded as a functional of $f_X$.

Let $g_X(y)$ and $g_{\widetilde{X}}(\widetilde{x})$ denote the true densities of $Y$ and $\widetilde{X}$, respectively. For given $\widetilde{x}$, the Kullback-Leibler information between $g_X(y)$ and $p(y|\widetilde{x})$ is as

$$I_K^C(g_X; p|\widetilde{x}) = \int \ln\{\frac{g_X(y)}{p(y|\widetilde{x})}\} g_X(y) dy.$$

Then, the expectation of $I_K^C(g_X; p|\widetilde{x})$ with respect to $g_{\widetilde{X}}(\widetilde{x})$ is given by

$$\mathrm{E}\{I_K^C(g_X; p|\widetilde{x})\} = \int I_K^C(g_X; p|\widetilde{x}) g_{\widetilde{X}}(\widetilde{x}) d\widetilde{x} = c + EIP,$$

where $c = \int \ln\{g_X(y)\} g_X(y) dy$ is a quantity that does not depend on $p(y|\widetilde{x})$, and $EIP$ is the expected information for prediction defined by

$$EIP = -\int \ln\{p(y|\widetilde{x})\} g_X(y) g_{\widetilde{X}}(\widetilde{x}) dy d\widetilde{x}. \tag{35}$$

It is advisable to obtain a predictive density leading to a smaller value of $\mathrm{E}\{I_K^C(g_X; p|\widetilde{x})\}$, or equivalently a smaller value of $EIP$.

In order to estimate the value of $EIP$ in equation (35), we draw a random sample (called the re-sample) of size $m$ from $X(1:n)$ without replacement in once re-sampling

and repeat such re-sampling $N$ times. Let $\widetilde{X}^{(i)} = \{X_1^{(i)}, X_2^{(i)}, \ldots, X_m^{(i)}\}$ be the $i$-th re-sample, and let $\{X_{m+1}^{(i)}, X_{m+2}^{(i)}, \ldots, X_n^{(i)}\}$ be the elements of $X(1:n)$ except $\widetilde{X}^{(i)}$. From the law of large numbers, an estimate for twice $EIP$, which is called prior-free information criterion (PFIC), is obtained as

$$PFIC = -\frac{2}{N(n-m)} \sum_{i=1}^{N} \sum_{j=m+1}^{n} \ln\{p(x_j^{(i)}|\widetilde{x}^{(i)})\}, \tag{36}$$

where $\widetilde{x}^{(i)}$ and $x_j^{(i)}$ denote the observations for $\widetilde{X}^{(i)}$ and $X_j^{(i)}$, respectively. Obviously, $PFIC$ defined by equation (36) is as a functional of the model density $f_X$. Thus, we can use PFIC as a criterion for evaluating the model density for $X(1:n)$. It can be seen that a model is better than the others if it leads to a smaller value of PFIC. Such rule of model selection is called minimum PFIC method.

Note that we only give here a formula of PFIC for a random sample. The formula of PFIC may depend on a sample scheme, but the basic consideration may be eternal.

### 5.2 Selection of regression models

Consider a linear regression model as

$$x_j^{(i)} = \sum_{\ell=1}^{L} w_{j\ell}^{(i)} \beta_\ell + e_j^{(i)} \quad (j = 1, 2, \ldots, m), \tag{37}$$

for the observations $\widetilde{x}^{(i)} = \{x_1^{(i)}, x_2^{(i)}, \ldots, x_m^{(i)}\}$ of the $i$-th re-sample $\widetilde{X}^{(i)}$ with $m \geq L+1$. Here, $w_{j\ell}^{(i)}$ is a given regressor, $\beta_\ell$ is an unknown regression coefficient, $e_j^{(i)}$ is an error term. As the usual case, we assume that the error terms are uncorrelated normal random variables distributed with zero mean and unknown variance $\sigma^2$. Redefining by $\widetilde{x}^{(i)} = (x_1^{(i)}, x_2^{(i)}, \ldots, x_m^{(i)})^{\mathtt{t}}$ a vector of the observations for $i$th re-sample, the regression model (37) can be expressed as

$$\widetilde{x}^{(i)} = W^{(i)}\beta + \varepsilon^{(i)}, \tag{38}$$

where $W^{(i)}$ is an $m \times L$ matrix with rank $L$, $\beta = (\beta_1, \beta_2, \cdots, \beta_L)^{\mathtt{t}}$ is a vector of the regression coefficients, $\varepsilon^{(i)} = (e_1^{(i)}, e_2^{(i)}, \ldots, e_m^{(i)})^{\mathtt{t}}$ is an random vector distributed with $\mathrm{N}(0, \sigma^2 I_m)$.

In order to simplify the procedure, we find an orthogonal matrix $H^{(i)} = ((H_1^{(i)})^{\mathtt{t}}|(H_2^{(i)})^{\mathtt{t}})^{\mathtt{t}}$ to reduce the regression model (38) into a separated form:

$$\begin{aligned} H_1^{(i)}\widetilde{x}^{(i)} &= R^{(i)}\beta + H_1^{(i)}\varepsilon^{(i)}, \\ H_2^{(i)}\widetilde{x}^{(i)} &= H_2^{(i)}\varepsilon^{(i)}, \end{aligned}$$

where $R^{(i)}$ is an $L \times L$ right-trigonometric matrix. Thus, from the properties of orthogonal matrix, we have $H^{(i)}\varepsilon^{(i)} \sim \mathrm{N}(0, \sigma^2 I_m)$, and we can see also that $H_1^{(i)}\varepsilon^{(i)} \sim \mathrm{N}(0, \sigma^2 I_L)$ and $H_2^{(i)}\varepsilon^{(i)} \sim \mathrm{N}(0, \sigma^2 I_{m-L})$ are independent of each other.

By using the procedure of the prior-free inference, we obtain the post data density for $\beta$ given $\widetilde{x}^{(i)}$ and $\sigma$ as follows:

$$f_\beta(\beta|\sigma, \widetilde{x}^{(i)}) = (\frac{1}{\sqrt{2\pi\sigma^2}})^L |\det(R^{(i)})| \exp\{-\frac{a_i(\beta)}{2\sigma^2}\},$$

and the post data density for $\sigma$ given $\widetilde{x}^{(i)}$ is

$$f_\sigma(\sigma|\widetilde{x}^{(i)}) = \frac{(b_i)^{(m-L)/2}}{2^{(m-L-2)/2}\Gamma((m-L)/2)\sigma^{m-L+1}} \exp\{-\frac{b_i}{2\sigma^2}\}.$$

Moreover, for $j = m+1, m+2, \ldots, n$, the predictive distribution density of $X_j^{(i)}$ is given by

$$\begin{aligned} p(x_j^{(i)}|\widetilde{x}^{(i)}) &= (\frac{d_{ij}}{\pi b_i})^{1/2}\frac{\Gamma((m-L+1)/2)}{\Gamma((m-L)/2)} \\ &\quad \times(1+\frac{d_{ij}(x_j^{(i)}-c_{ij})^2}{b_i})^{-(m-L+1)/2} \end{aligned} \tag{39}$$

In the above equations, $a_i(\beta)$, $b_i$, $c_{ij}$, and $d_{ij}$ are defined, respectively, as the follows:

$$\begin{aligned} a_i(\beta) &= (R^{(i)}\beta - H_1^{(i)}\widetilde{x}^{(i)})^{\mathtt{t}}(R^{(i)}\beta - H_1^{(i)}\widetilde{x}^{(i)}), \\ b_i &= (H_2^{(i)}\widetilde{x}^{(i)})^{\mathtt{t}}H_2^{(i)}\widetilde{x}^{(i)}, \\ c_{ij} &= (w_j^{(i)})^{\mathtt{t}}(R^{(i)})^{-1}H_1^{(i)}\widetilde{x}^{(i)}, \\ d_{ij} &= (1+(w_j^{(i)})^{\mathtt{t}}((R^{(i)})^{\mathtt{t}}(R^{(i)}))^{-1}w_j^{(i)})^{-1}, \end{aligned}$$

where $w_j^{(i)} = (w_{j1}^{(i)}, \ldots, w_{jL}^{(i)})^{\mathtt{t}}$ is the vector of the regressors corresponding to $\widetilde{x}^{(i)}$. Thus, PFIC for the model can be obtained by using equations (36) and (39).

### 5.3 Simulation study

In order to examine the performance of the minimum PFIC method, we carried out a simulation study. The data used here are generated by using the polynomial of degree three:

$$x_t = -10 + 0.2t - 0.09t^2 + 0.002t^3 + r_t, \quad (t = 1, 2, \ldots, n), \tag{40}$$

which can be regarded as the true distribution, where $r_t$ is generated by using the standard normal random numbers. We fit the polynomial regression model

$$x_t = \sum_{\ell=0}^{L} t^\ell \beta_\ell + e_t, \quad (t = 1, 2, \ldots, n)$$

to the data generated by equation (40), where $L$ denotes the degree of the model, and $e_t$ is a random error term. The probability distribution for the error terms in this model is the same as that in the model (37).

Here, we compare our minimum PFIC method with other methods such as the minimum AIC method (see [21] and [29]) and the minimum BIC method (see [30]). The values of PFIC, AIC and BIC are calculated respectively for $L = 0, 1, \ldots, 5$. Then, we can estimate the model degrees of by using the minimum PFIC, AIC and BIC methods. Such experiment was repeated 1000 times with the size of re-sample being $m = 6$ and the times of re-sampling for each experiment being $N = 1000$.

Table 5.1 and Table 5.2 show the frequencies of the model degrees determined by using each method for $n = 30$ and $n = 60$, respectively. As shown in the tables, the model degrees determined by using the minimum PFIC method agree with the true model degree perfectly but the others are not. The result shows that the performance of minimum PFIC method is obviously better than that of the others, and it can be seen that the minimum PFIC method works well even for a small sample.

**Table 5.1:** Frequencies of estimated model degree ($n = 30$).

| model order | 0 | 1 | 2 | 3 | 4 | 5 |
|---|---|---|---|---|---|---|
| PFIC | 0 | 0 | 0 | 1000 | 0 | 0 |
| AIC | 0 | 0 | 0 | 725 | 166 | 109 |
| BIC | 0 | 0 | 0 | 880 | 86 | 34 |

**Table 5.2:** Frequencies of estimated model degree ($n = 60$).

| model order | 0 | 1 | 2 | 3 | 4 | 5 |
|---|---|---|---|---|---|---|
| PFIC | 0 | 0 | 0 | 1000 | 0 | 0 |
| AIC | 0 | 0 | 0 | 752 | 142 | 106 |
| BIC | 0 | 0 | 0 | 934 | 46 | 20 |

## 6 Concluding remarks

A new procedure of statistical inference, named by the prior-free inference, was introduced for developing objective Bayesian analysis based on an information-theoretic approach. The feature of this new approach is that it is essentially a Bayesian method but it may be free of dependence on a prior distribution for unknown parameters. Thus, this approach does not only have the advantages of the Bayesian approach but also can avoid the difficulty of the traditional Bayesian approach encounters due to a lack of prior information. A methodology, named by the minimum PFIC method, for model selection was also developed by utilizing a newly-introduced information criterion, PFIC, based on the extension of the procedure for prior-free inference. The result of simulation study shown that the performance of minimum PFIC method is very good.

An important problem is the relation between our prior-free inference and Fisher's fiducial approach. It can be verified that for models with a single parameter that has a sufficient statistic, these two approaches can lead to the same result, otherwise our prior-free inference is better than Fisher's fiducial approach. Further, it is well-known that Fisher's fiducial approach maybe difficult for multivariate parameter cases.

Nowadays many objective Bayesian approaches use Jeffreys priors. Sometimes, the procedure of the prior-free inference and that using Jeffreys priors may lead to a same result. However, it can be seen that the procedure of prior-free inference is well systematized and the procedure using Jeffreys is somewhat ad hoc. Moreover, a number of objections can be made to the Bayesian procedure using Jeffreys priors, the most important of which is that it depends on the values of the observed data. Such objection is reasonable, perhaps, because the prior distribution should only represent the information prior to the observed data, it can not be influenced by the data. Sometimes, the Bayesian procedure using Jeffreys priors will violate the likelihood principle, and it is difficult to apply the procedure to multivariate parameter cases. Also, there are diffi-

culties in Bernardo's reference priors approach using the Lindley's criterion functional. Such difficulties can be overcome by the use of the procedure of prior-free inference.

## References


[1] Akaike, H. A new look at the statistical model identification. *IEEE Trans. Automat. Control* **AC19** (1974) 716–723.

[2] Akaike, H. Likelihood and the Bayes procedure. In: *Bayesian Statistics*. (Bernardo, J.M., DeGroot, M.H., Lindley, D.V., Smith, A.F.M., eds.) University Press, Valencia, 1980, 143–166.

[3] Akaike, H. On minimum information prior distributions. *Ann. Inst. Statist. Math.* **35** (1983) 139–149.

[4] Bayes, T. An essay towards solving a problem in the doctrine of chances. *Philos. Trans. Roy. Soc.* **53** (1763) 370–418.

[5] Berger, J.O. An overview of robust Bayesian analysis. *Test* **3** (1994) 5–124.

[6] Berger, J.O., Bernardo, J.M. On the development of reference priors (with discussion). In: *Bayesian Statistics 4*. (Bernardo, J.M., Berger, J.O., Dawid, A.P., Smith, A.F.M., eds). Oxford University Press, Oxford, 1992, 35–60.

[7] Bernardo, J.M. Reference posterior distributions for Bayesian inference (with discussion). *J. Roy. Statist. Soc.* **B41** (1979) 113–147.

[8] Bernardo, J.M. Nested hypothesis testing: the Bayesian reference criterion (with discussion). In: *Bayesian Statistics 6*. (Bernardo, J.M., Berger, J.O., Dawid, A.P., Smith, A.F.M., eds). Oxford University Press, Oxford, 1999, 101–130.

[9] Box, G.E.P., Tiao, G.C. *Bayesian Inference in Statistical Analysis*. Addison-Wesley, Massachusetts, 1973.

[10] Chuaqui, R. *Truth, Possibility and Probability: New Logical Foundations of Probability and Statistical inference*. North-Holland, Amsterdam, 1991.

[11] Fine, T.L. Foundations of probability (update). In: *Encyclopedia of Statistical Sciences, Up. Vol. 3* (Kotz, S., ed.). John Wiley and Sons, New York, 1999, 246–254.

[12] Fisher, R.A. Inverse probability. *Proc. Camb. Phil. Soc.* **26** (1930) 528–535.

[13] Fisher, R.A. The concepts of inverse probability and fiducial probability referring to unknown parameters. *Proc. Roy. Soc.* **A139** (1933) 343–348.

[14] Fisher, R.A. The fiducial argument in statistical inference. *Ann. Eugenics* **6** (1935) 391–398.

[15] Jaynes, E.T. *Papers on Probability, Statistics and Statistical Physics* (Rosenkrantz, R.D., ed.). Kluwer, Dordrecht, 1983.

[16] Jeffreys, H. An invariant form for the prior probability in estimation problems. *Proc. Roy. Soc.* **A186** (1946) 453–461.

[17] Jiang, X.Q. A general procedure of statistical inference based on information theory, In: *Statistical Physics* (Tokuyama, M., Stanley, H.E., eds.). American Institute of Physics, Melville, 2000, 642–644.

[18] Jiang, X.Q. A new approach to objective Bayesian analysis. *The Journal of Asahikawa University* No.53 (2002) 1–25.

[19] Jiang, X.Q. Prior-free Bayesian inference based on information-theoretic approach. *The Journal of Asahikawa University* No. 57·58 (2004) 1–17.

[20] Jiang, X.Q. Estimation and identification of regression models via prior-free Bayesian inference. In: *Bayesian Inference and Maximum Entropy Methods in Science and Engineering* (Fischer, R., Preuss, R., Toussaint, U., eds). American Institute of Physics, Melville, 2004, 501–508.

[21] Kitagawa, G., Gersch, W. *Smoothness Prior Analysis of Time Series*. Springer-Verlag, New York, 1996.

[22] Konishi, S., Kitagawa, G. Generalized information criterion in model selection. *Biometrika* **83** (1996) 875–890.

[23] Konishi, S., Kitagawa, G. *Information Criteria*. Asakura Syoten, Tokyo, 2004. [in Japanese]

[24] Kullback, S. *Information Theory and Statistics*. John Wiley and Sons, New York, 1959.

[25] Laplace, P.S. *Théorie Analytique des Probabilités*. Courcier, Paris, 1812.

[26] Lehmann, E.L., Casellab, G. *Theory of Point Estimation* (2-nd edn). Springer-Verlag, New York, 1998.

[27] Li, M., Vitanyi, P. *An Introduction to Kolmogorov Complexity and Its Applications*. Springer-Verlag, New York, 1997.

[28] Lindley, D.V. On a measure of the information provided by an experiment. *Ann. Math. Statist.* **27** (1956) 986–1005.

[29] Sakamoto, Y., Ishiguro, M., Kitagawa, G. *Akaike Information Criterion*. KTK Scientific Publishers, Tokyo, 1986.

[30] Schwarz, G. Estimation the dimension of a model. *Ann. Statist.* **6** (1978) 461–464.

[31] Stone, M. Strong inconsistency from uniform priors (with discussion). *J. Amer. Statist. Assoc.* **71** (1976) 114–125.

[32] Zacks, S. *The Theory of Statistical Inference*. John Wiley and Sons, New York, 1971.

[33] Zellner, A. *An Introduction to Bayesian Inference in Econometrics*. John-Wiley and Sons, New York, 1971.

[34] Zellner, A. Maximal data information prior distributions, In: *New Developments in the Applications of Bayesian Methods* (Aykac, A., Brumat, C., eds). North-Holland, Amsterdam, 1977, 211–232.

[35] Zellner, A. Optimal information processing and Bayes's theorem (with discussion). *Amer. Statist.* **42** (1988) 278–294.

[36] Zellner, A. Bayesian methods and entropy in economics and econometrics. In: *Maximum Entropy and Bayesian Methods*. (Grandy, W.T., Schick, L.H., eds). Kluwer Academic Publishers, Dordrecht, 1991, 17–31.

## Appendix A: proof of Lemma 3.1

Under the conditions C1 and C2, we have $\lambda = \int_{\boldsymbol{\mathcal{S}}(f_{Z|x(1:k)})} dz$ from equations (10) and (11). Thus, the proof is completed from the fact that $\boldsymbol{\mathcal{S}}(f_Z|x(1:k)) \subseteq [0,1] \times [0,1] \times \cdots \times [0,1]$.

## Appendix B: proof of Theorem 3.1

From equation (20), we have

$$I_K^C(\pi; f_\Theta|x(1:k)) = \int_{\boldsymbol{\mathcal{S}}(\pi)} \ln\{\frac{\pi(\theta)}{f_\Theta(\theta|x(1:k))}\}\frac{\pi(\theta)}{f_\Theta(\theta|x(1:k))} f_\Theta(\theta|x(1:k))d\theta.$$

By applying equation (4), the above equation can be rewritten as

$$I_K^C(\pi; f_\Theta|x(1:k)) = \int_{\boldsymbol{\mathcal{S}}(\pi)} \ln\{\phi(x(1:k),\theta)\}\phi(x(1:k),\theta) f_\Theta(\theta|x(1:k))d\theta, \tag{41}$$

where

$$\phi(x(1:k),\theta) = \frac{h(x(1:k))}{f_{X(1:k)}(x(1:k)|\theta)}.$$

For a given model density $f_{X(1:k)}(x(1:k)|\theta)$, if $\pi(\theta)$ is fixed in a proper density, then the marginal density $h(x(1:k))$ is fixed by equation (3). Hence, the function $\phi(x(1:k),\theta)$ in equation (41) cannot be changed through $f_\Theta(\theta|x(1:k))$. Thus, we have to maximize $I_K^C(\pi; f_\Theta|x(1:k))$ with respect to $f_\Theta(\theta|x(1:k))$. It is well-known that a solution to maximizing $I_K^C(\pi; f_\Theta|x(1:k))$ can be obtained when we put

$$f_\Theta^{(1)}(\theta|x(1:k)) = c_1 \tag{42}$$

with $c_1 = 1/\psi$ being a constant. Thus, the solution given by equation (22) is obtained.

On the other hand, by applying equation (12) to equation (41), we have

$$\begin{aligned} I_K^C(\pi; f_\Theta|x(1:k)) &= \int_{\boldsymbol{\mathcal{S}}(\pi)} \ln\{\phi(x(1:k),\theta)\}\phi(x(1:k),\theta) f_Z(z|x(1:k))|\det(J)|d\theta \\ &= \int_{\boldsymbol{\mathcal{S}}(f_Z|x(1:k))} \ln\{\phi(x(1:k),\theta)\}\phi(x(1:k),\theta) f_Z(z|x(1:k))dz. \end{aligned}$$

It is obvious that $I_K^C(\pi; f_\Theta|x(1:k))$ can also be maximized when we put $f_Z(z|x(1:k)) = c_2$ or equivalently

$$f_\Theta^{(2)}(\theta|x(1:k)) = c_2\ |\det(J)| \tag{43}$$

from equation (12) with $c_2 = 1/\lambda$ being a constant. Then, the solution given by equation (23) is obtained from equation (43). Moreover, from equation (19), we can see that $F(f_\Theta, \pi|f_{X(1:k)})$ is maximized as long as $I_K^C(\pi; f_\Theta|x(1:k))$ is maximized. Thus, Theorem 3.1 is proved.

## Appendix C: proof of Theorem 3.2

If the value of $\psi = \int_{\boldsymbol{\mathcal{S}}(\pi)} d\theta$ is finite, then the value of $I(f_\Theta|x(1:k))$ is given by

$$I(f_\Theta^{(1)}|x(1:k)) = \ln\{c_1\}, \tag{44}$$

for the solution given by equation (42). On the other hand, the value of $I(f_\Theta|x(1:k))$ is as

$$\begin{aligned} I(f_\Theta^{(2)}|x(1:k)) &= c_2 \int_{\boldsymbol{\mathcal{S}}(\pi)} \ln\{c_2|\det(J)|\}|\det(J)|d\theta \\ &= c_2 \int_{\boldsymbol{\mathcal{S}}(f_Z|x(1:k))} \ln\{c_2|\det(J)|\}dz \end{aligned} \tag{45}$$

for the solution given by equation (23). It is obvious that

$$I(f_\Theta^{(2)}|x(1:k)) - I(f_\Theta^{(1)}|x(1:k)) = c_2 \int_{\boldsymbol{\mathcal{S}}(\pi)} \ln\{\frac{c_2|\det(J)|}{c_1}\}|\det(J)|d\theta > 0.$$

from equations (44) and (45).

Further, if the value of $\psi = \int_{\boldsymbol{\mathcal{S}}(\pi)} d\theta$ is infinite, then $I(f_\Theta^{(1)}|x(1:k)) = -\infty$ as $c_1 \to 0$ under the assumption that $f_\Theta(\theta|x(1:k))$ is proper. On the other hand, from the conditions C1 and C2, equations (11) and (45), we can see that $I(f_\Theta^{(2)}|x(1:k))$ must be finite. Thus, we have $I(f_\Theta^{(2)}|x(1:k)) - I(f_\Theta^{(1)}|x(1:k)) = \infty$. So, Theorem 3.2 is proved.

Nonlinear Dynamics and Systems Theory, **7** (1) (2007) 23–34

INFORMATH Publishing Group

# Inverse Determination of Model Parameters of Nonlinear Heat Conduction Problem Using Hybrid Genetic Algorithm

Shouju Li and Yingxi Liu

*State Key Laboratory of Structural Analysis of Industrial Equipment, Dalian University of Technology, Dalian 116023, China*

Received: June 17, 2005; Revised: October 16, 2006

**Abstract:** A new interpretation is proposed to solve the inverse heat conduction problem using hybrid genetic algorithm. In order to identify parameters of non-linear heat transfer efficiently and in a robust manner, the hybrid genetic algorithm, which combines genetic algorithm with simulated annealing and the elitist strategy, is presented for the identification of the material thermal parameters. The procedure is based on the minimization of an objective function which accounts for experimental data and the calculated response of the mathematical model. The performances of the proposed optimization algorithm were investigated with simulating data, and the effectiveness was consequently confirmed.

**Keywords:** *Inverse heat conduction problem; evolutionary algorithm; objective function; optimization algorithm; measurement noise.*

**Mathematics Subject Classification (2000):** 65N21.

## 1 Introduction

The accurate knowledge of the heat transfer coefficients is of importance in many engineering applications, including the cooling of continuously cast slabs and of electronic chips. In order to determine the heat transfer coefficients of materials, some identification methods have been developed for solving the problem [1]. For example, the sensitivity coefficient method was developed to solve multidimensional inverse heat conduction problems. The sensitivity coefficients are used directly to estimate the responses of the system considered under unit loading conditions. The finite-element discretization procedure is applied to evaluate the total response under all loading conditions. The conjugate gradient method is a powerful minimization technique, which can be applied

 

to parameter and function estimations, as well as to linear and nonlinear inverse problems [2]. The conjugate gradient method with a suitable stopping criterion belongs to the class of iterative regularization techniques, where the number of iterations of the estimation procedure is determined so that stable solutions are obtained for the inverse problem [3]. The method consists in choosing a suitable direction of descent and a search step size along this direction at each of iteration for the minimization of the objective function.

The direct heat problem is concerned with the determination of the temperature field when the heat transfer coefficient, as well as the physical properties, initial condition and other quantities appearing in the boundary condition are known. Direct heat transfer problems can be mathematically classified as well-posed. The solution of a well-posed problem is required to satisfy the conditions of existence, uniqueness, and stability with respect to the input data. The inverse heat transfer problem is usually ill-posed. An ill-posed problem is characterized by the non-uniqueness and instability of solution. The regularization technique has been employed to overcome the ill-posedness of inverse heat transfer problems. Several such techniques have been introduced in the literature [4]. Most of the literature, however, uses a gradient-based optimization method and the solution often vibrates or diverges, depending upon the initial search point, since the model and the measurement errors can make the objective function complex [5]. There are numerous nonlinear optimization algorithms that could be employed in this problem. However, many nonlinear optimization techniques suffer from at least one of the tow shortcomings: either they are overly computationally intensive, or they tend to get trapped in local optima. One of the approaches used to overcome this problem is to use a robust optimization method and computational intelligences have been most successfully used to find the parameter set in a stable manner [6]. Genetic algorithm is effective nonlinear optimization techniques. It is based on the general approach apparent in nature by which species of organisms adapt, change, and improve. It is different from traditional optimization techniques in several ways. The genetic algorithm has been widely used in the identification, short-term load forecasting, the design optimization, dynamic channel assignment, the parameter identification of inelastic constitutive models [7, 8, 9, 10].The main purpose of the paper is to present a procedure for determining the thermal parameters in a robust manner.

## 2 Direct Problems for Heat Transfer

The partial differential equation governing the steady-state temperature distribution in a two-dimensional region described by the Cartesian coordinates, $x$ and$y$, takes the form

$$\frac{\partial}{\partial x}(k_x\frac{\partial T}{\partial x})+\frac{\partial}{\partial y}(k_y\frac{\partial T}{\partial y})=0, \tag{1}$$

where $T$ is the temperature, and $k_x$ and $k_y$ are the thermal conductivities in the $x$ and $y$ directions, respectively. The physical parameters, $k_x$ and $k_y$, can be treated to be temperature dependent. The following three kinds of boundary conditions occur in the direct heat transfer problems, prescribed temperature (Dirichlet type), prescribed heat flux (Neumann type), and prescribed heat transfer coefficient (mixed or Robin type).

$$\begin{aligned} &T(x,y)=T_0, \qquad (x,y)\in\Omega_1,\\ &k_x(\partial T/\partial x)n_x+k_y(\partial T/\partial y)n_y=q_0, \quad (x,y)\in\Omega_2,\\ &k_x(\partial T/\partial x)n_x+k_y(\partial T/\partial y)n_y=h(T_a-T), \quad (x,y)\in\Omega_3, \end{aligned} \tag{2}$$

where $T_0$ represents the value on the surface or boundary $\Omega_1$, $q_0$ is a heat flux vector on subsurface$\Omega_2$, $h$ is the convective heat transfer coefficient on subsurface $\Omega_3$, $n_x$ and $n_y$ are the direction cosines of the outward drawn normal to the boundary, $T_a$ is the surrounding temperature.

## 3 Inverse Problem for Heat Transfer and solution Approach with Hybrid Genetic Algorithm

### 3.1 Definition of inverse problem for parameter identification

For the inverse problem, the heat transfer coefficient is regarded as unknown. The parameter identification problem can be formulated to find the model parameters by adjusting identified parameter vector $\boldsymbol{m}$ until the measured data match the corresponding data computed from the parameter set in a least-squares fashion. The objective function is defined as follows [3]

$$J(m) = [h_m - h_c(m)]^T w[h_m - h_c(m)], \tag{3}$$

where $h_m$ is the measured temperature vector; $h_c$ is the computing temperature vector, which is related to the identified parameter vector $\boldsymbol{m}$, $\boldsymbol{w}$ is weighting matrix in order to take into account the different observed equipments for the temperature measurements. This objective function clearly depends on the measured data and the parameters of model. The objective function can become complex, such as non-convex, or even multi-modal if errors contained in the model equation or /and errors in the measurement data are large.

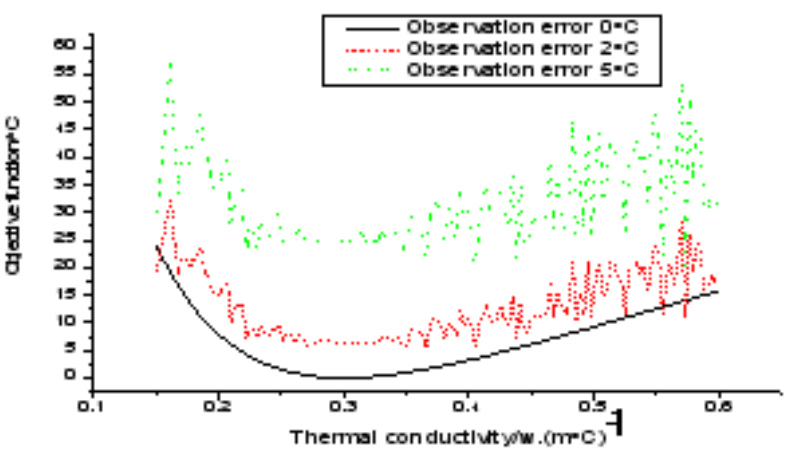


**Figure 3.1:** Objective functions of the different measurement errors.

When taking account of measurement errors, the objective function will have many local minima for the inverse heat conduction problem, as shown in Figure 3.1. When random measurement error is 2 ° C, the objective function has 35 local minima. When

random measurement error is 5 ° C, the objective function has 38 local minima. In such a case, the solution may vibrate or diverge when conventional gradient-based optimization methods are used, which gives rise to the necessary for a robust optimization method such that a stable convergence is always achieved. The solution of the inverse problem consists in obtaining a minimum of an objective function which is defined taking into account the mathematical structure of the material model and asset of experimental data. This generally results in a non-linear programming constrained problem of the form [2]:

$$\min\{J(m,h_m)\ ,\quad m\in R^{\ P},h_m\in R^M;g^j<0\},\tag{4}$$

where $\boldsymbol{m}$ belongs to the space of admissible parameters $R^P$, $h_m$ belongs to the space $R^M$, $g^j$ are inequality constraints, which define the feasible domain

$$D=\{m\in R^P,g^j<0\}.\tag{5}$$

The constraints can represent physical links between the primary physical variables and the model parameters, information concerning the values of parameters and conditions to guarantee that all mathematical functions involved can be defined and calculated. In the optimization process, the difference between the experimental result and the theoretical prediction is measured by a norm value $J$ here referred to as the Euclidean norm. The Euclidean norms of the tests form an objective function $J(m)$ which then gives a scalar measure of the error between the experimental observations and the model predictions. From mathematical point of view, the optimization problem involves the minimization of the objective function [4]:

$$J(m)\rightarrow\min.\tag{6}$$

The bound constraints:

$$m_l<m<m_u,\tag{7}$$

where $m_l$ and $m_u$ are, respectively, the lower and upper bounds of $m$. Traditional mathematical optimization methods that have been used include dynamic programming, conjugate-gradient, random search, and simplex optimization.

### 3.2 Continuous Evolutionary Algorithm and Its Improvements

Genetic algorithm (GA) is a search method based on Darwin's theory of evolution and survival of the fittest [11]. Based on the concept of genetics, GA simulates the evolutionary process numerically. Genetic algorithms strongly differ in conception from other search methods, including traditional optimization methods and other stochastic search methods. The basic difference is that while other methods always process single points in the search space, genetic algorithms maintain a population of potential solutions. Genetic algorithms constitute a class of search methods especially suited for solving complex optimization problems. Search algorithms in general consist of systematically walking through the search space of possible solutions until an acceptable solution is found. Genetic algorithms transpose the notions of natural evolution to the world of computers, and imitate natural evolution. They were initially introduced by John Holland for explaining the adaptive processes of natural systems and for creating new artificial systems that work on similar bases [12]. In Nature new organisms adapted to their environment develop through evolution. Genetic algorithms evolve solutions to the given problem in a similar way. The main contents of genetic algorithm include the evaluation of fitting function, selection operation, crossover operation, mutation and elitist strategy.

The probability of survival of any individual is determined by its fitness: through evolution the fitter individuals overtake the less fit ones. In order to evolve good solutions, the fitness assigned to a solution must directly reflect its 'goodness', i.e. the fitness function must indicate how well a solution fulfills the requirements of the given problem. The evaluation of the fitness can be conducted with a linear scaling, where the fitness of each individual is calculated as the worst individual of the population subtracted from its objective function value. Fitness assignment can be performed in several different ways: We define a fitness function and incorporate it in the genetic algorithm. When evaluating any individual, this fitness function is computed for the individual.

$$f_j = \max\{J_j / j = 1, 2, , , S\} - J_j, \tag{8}$$

where $f_j$ is the fitting function of $j$-th individual; $S$ is the population size; $J_j$ is the objective function of $j$-th individual. Selection, also called reproduction, is simply the copying of quality solution in proportion to their effectiveness. Here, since the goal is to minimize the objective function, several copies of candidate solutions with small objective functions are made; solutions with large objective functions tend not to be replicated. The intrinsic principle of the genetic algorithm is Darwin's natural selection principle. Selection is the impetus of the genetic algorithm, by which, the superior individual are selected into the next generation while the inferior ones are washout. A part of the new population can be created by simply copying without change selected individuals from the present population.

One of the most commonly used is the roulette wheel selection, where individuals are extracted in probability following a Monte Carlo procedure. The extraction probability of each individual is proportional to its fitness as a ratio to the average fitness of all the individuals. In the selection process, the reproduction probabilities of individuals are given by their relative fitness:

$$pro_j = f_j / \sum_{j=1}^{s} f_j, \tag{9}$$

where $pro_j$ is the reproduction probability of the $j$-th individual.

Recombination, also called crossover, is a process by which information contained in two candidate solutions is combined. In the recombination, each individual is first paired with an individual at random. New individuals are generally created as offspring of two parents (as such, crossover being a binary operator). One or more so-called crossover points are selected (usually at random) within the chromosome of each parent, at the same place in each. The parts delimited by the crossover points are then interchanged between the parents. The individuals resulting in this way are the offspring. Beyond one point and multiple point crossover there exist more sophisticated crossover types. Let a pair of present individuals be given by $[m_\alpha^t, m_\beta^t]$. a new pair $[m_\alpha^{t+1}, m_\beta^{t+1}]$ is then created in terms of a phenomenological recombination formula[8]:

$$m_\alpha^{t+1} = (1-\mu)\, m_\alpha^t + \mu \cdot m_\beta^t, \tag{10}$$

$$m_\beta^{t+1} = (1-\mu)\, m_\beta^t + \mu \cdot m_\alpha^t, \tag{11}$$

where $\mu$ is a random number changing from 0 to 1.

A new individual is created by making modifications to one selected individual. The modifications can consist of changing one or more values in the representation or in adding/deleting parts of the representation. In genetic algorithms mutation is a source

of variability, and is applied in addition to crossover and reproduction. Mutation is a process by which vectors resulting from selection and recombination are perturbed. The mutation is conducted with only a small probability by definition. An individual, after this mutation $m_i^{t+1}$, is described as

$$m_i^{t+1} = rand\{m_l, m_u\}, \tag{12}$$

where $rand\{.\}$ represents the random selection from the reasonable solution domains. At different stages of evolution, one may use different mutation operators. At the beginning mutation operators resulting in bigger jumps in the search space might be preferred. Later on, when the solution is close by, a mutation operator leading to slighter shifts in the search space could be favored. However, the above mutation operation is a random one with no clear aim.

Simulated annealing is another important algorithm which is powerful in optimization and high-order problems [13]. It uses random processes to help guide the form of its search for minimal energy states. In an annealing process a melt, initially at high temperature and disordered, is slowly cooled so that the system at any time is approximately in thermodynamic equilibrium. As cooling proceeds, the system becomes more ordered and approaches a "frozen" ground state at $T$=0. The paper provides a mutation method based on the simulating annealing algorithm, which makes the average fitness of the population tend to be optimized. Firstly, we define a neighborhood structure, then select a new solution in the neighborhood structure of the intermediate solution, that is to say, getting a new solution by cause a disturb on the old one [14]

$$m_{new} = m_{old} + \Delta m, \tag{13}$$

where $m_{new}$ and $m_{old}$ represents a new solution and an old solution, respectively; $\Delta m$is a random disturb. Then, reject or accept the new solution according the Metropolis rule, the probability of accepting the new generated solution is expressed as the follows [15]:

$$p_{new} = \left\{ \begin{array}{cc} 1 & J_{old} \geq J_{new} \\ \exp[-\Delta J/T_k] & J_{old} < J_{new} \end{array} \right\}, \tag{14}$$

where $J_{new}$ and $J_{old}$ are the objective functions of the new solution and the old solution; $p_{new}$ is the probability of accepting the new generated solution; $\Delta J$is the increasement of the objective function, $\Delta J = J_{new} - J_{old}$, $T_k$ is the annealing temperature, which tends to be drooped during the evolutional process. The probability of rejecting the new solution is:

$$P_{old} = 1 - p_{new}, \tag{15}$$

where $p_{old}$ is the probability of rejecting the new solution. One feature that is currently missing in this selection procedure is that it does not guarantee the best individual always survives into the next generation, particularly when many individuals have fitness close to that of the best individual. The elitist strategy, where the best individual is always survived into the next generation on behalf of the worst individual, can compensate for some disadvantages of missing the best individual in selection operation or mutation operation. With the elitist strategy, the best individual always moves in a descent direction, thereby a stable convergence is obtained. The gradient search algorithm adopted in genetic algorithm is the most popular quasi-Newton method with the BFGS algorithm. The individual after the recombination is formulated as follows [8]

$$m_{new} = \left\{ \begin{array}{ll} -A^{-1}\nabla f(m_{old}) & if \quad f(m_{new}) > f(m_{old}) \\ m_{old} & otherwise \end{array} \right\}, \tag{16}$$

where $A$ is a well-known positive-define matrix used on behalf Hessian matrix. The main steps for parameter identification using genetic algorithm are shown in follows:

Step 1: Choose the size of population, the crossover probability, mutation probability, and stopping criterion.

Step 2: Determine the identified parameter domains according to prior information

Step 3: Randomly generate an initial population of candidate solutions.

Step 4: Define a fitness function to measure the performance of an individual in the problem domain.

Step 5: Compute model responses with given model parameters by using Newton iteration method.

Step 6: Calculate the fitness of each individual based on observed dada and model responses computed by Newton iteration method.

Step 7: Execute recombination operation by using continuous floating codes.

Step 8: Create new individuals by mutation operation based on simulated annealing.

Step 9: Execute select operation according to the roulette wheel selection.

Step 10: Perform elitist strategy in order to keep current best individual from missing and accelerate convergence speed of inverse problem.

Step 11: Replace the initial(parent) population with the new (offspring) population.

Step 12: Execute stopping criterion. If stopping criterion can not be reached, then, go to Step 5; otherwise, the inversion computation stops and best solution is recorded as the solution of the inverse problem.

## 4 Numerical Examples for Identification of Model Parameters in Heat Transfer

In order to demonstrate the accuracy of the proposed algorithm with nonlinear problem, a heat transfer problem with nonlinear material properties is considered in this example. An annular cylinder is subjected to a constant prescribed heat flux, $q_0$, on the outer surface, and a temperature $T_0$, prescribed on the inner surface, and shown in Figure 4.1.

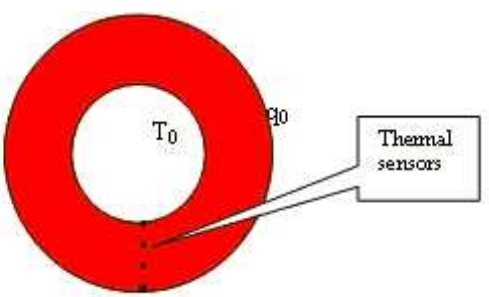


**Figure 4.1:** An annular cylinder and sensor locations.

The governing equation of heat transfer can be expressed as

$$\frac{1}{r}\frac{d}{dr}\left[k\left(T\right)r\frac{dT}{dr}\right]=0, \tag{17}$$

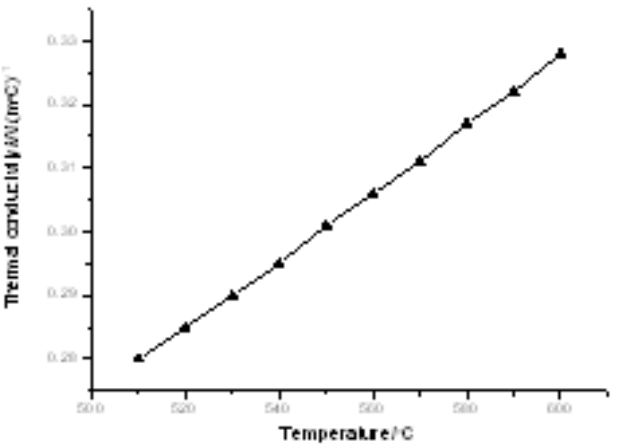


**Figure 4.2:** Change of thermal conductivity versus temperatures.

where $k(T)$ is a quadratic function of temperature; $r$ is radial coordinate. And $k$ can be expressed as follows

$$k\left(T\right) = k_0 + k_1 T + k_2 T^2, \tag{18}$$

where $k_0$, $k_1$, and $k_2$ are unknown material thermal parameters. The thermal conductivity is depended on the temperatures as shown in Figure 4.2. The change of thermal conductivity versus temperatures is shown in Figure 4.2.

The analytical solution of Equation (17) can be expressed as follows:

$$k_0\left(T - T_0\right) + k_1\left(T - T_0\right) + k_2\left(T - T_0\right)^2 = q_0 R_0 \ln\left(r/R_i\right), \tag{19}$$

where $R_i$ is the inner radius, $R_i$ =1.0 m; $R_o$ is the outer radius of the annular cylinder, $R_o$ =2.0 m; $q_0$ is a constant prescribed heat flux, $q_o$=10 W/m$^2$. The above algebraic equation can be solved numerically by using Newton iteration algorithm. Suppose the material thermal parameters are known, the simulated measured temperature values are shown in Figure 4.3.

Contrasting with the direct analysis, the inverse heat transfer analysis is ill-conditioned; the latter predicts the surface temperature or heat flux across the surface using temperature measured at certain discrete points inside the domain considered. Figure 4.4 is the objective function value versus number of iterations for the optimal individual. Figure 4.4 shows that the hybrid genetic algorithm can make searching more accurate and faster near global minima on the error surface.

Table 4.1 shows the comparison of the identified thermal conductivity by using different inverse methods without measurement errors. Identified values (A) and (B) shown in Table 4.1 represent for the identified thermal conductivity by using hybrid genetic algorithm and classical genetic algorithm, respectively. The hybrid genetic algorithm has higher identification precision than classical genetic algorithm.

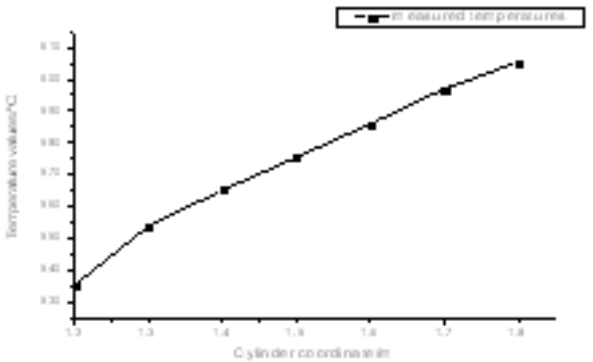

**Figure 4.3:** Simulated measurement temperatures in sensor.

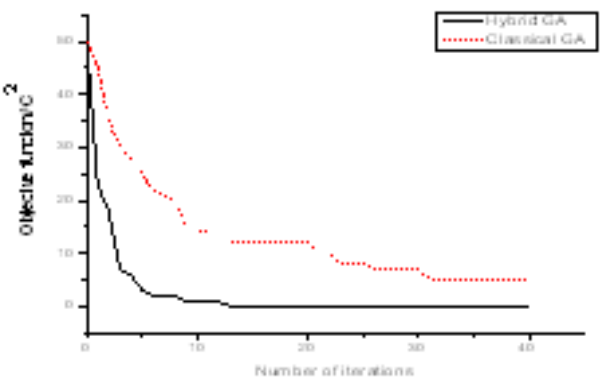

**Figure 4.4:** Objective function value versus number of iterations for the optimal individual.

| Parameters | $k_0/W\cdot(m\,^\circ C)^{-1}$ | $k_1/10^{-3}$ $*Wm\cdot(m\,^\circ C)^{-2}$ | $k_2/10^{-6}$ $*Wm^2\cdot(m\,^\circ C)^{-3}$ |
|---|---|---|---|
| Theoretical values | 0.100 | 0.198 | 0.303 |
| Identified values(A) | 0.101 | 0.199 | 0.302 |
| Identified values(B) | 0.112 | 0.203 | 0.305 |

**Table 4.1:** Comparison of the identified thermal conductivity by using different inverse methods without measurement errors.

Often a small measurement error can dramatically change the boundary values predicted. The temperature measurement errors can come from many sources and can be caused by calibration errors, presence of the sensor, conduction and convection losses of the sensor, or signal analysis. Also, these can be further determined by errors from measurements of time, sensor location, or dimension of the domain considered. Several studies simulated measurement noise numerically by superimposing a random noise with zero mean and a specified variance on measured data. The proportional error, in which the uncertainty for each measured data is proportional to its own value, is used to study the influence of measurement noise on the identified thermal conductivity. These measurements were generated from the solution of the direct problem. The measurements containing random errors were obtained by adding an error term to the errorless measurements resulting from the solution of the direct problem; that is:

$$T_m = T_{exa} + \xi\sigma, \tag{20}$$

where $T_{exa}$ are the errorless measurements; $\xi$ is a random variable with normal distribution, zero mean, and unitary standard deviation; $\sigma$ is the standard deviation of the measurement errors, which is supposed constant; and $T_m$ are the measurements containing random errors. Three different levels of measurement errors are considered here. Table 4.2 shows the influences of measurement noises on the identified thermal conductivity.

| Parameters | $k_0$/W·(m $^\circ$C)$^{-1}$ | $k_1/10^{-3}$ ∗Wm·(m $^\circ$C)$^{-2}$ | $k_2/10^{-6}$ ∗Wm$^2$·(m $^\circ$C)$^{-3}$ |
|---|---|---|---|
| Theoretical values | 0.100 | 0.198 | 0.303 |
| Identified values(C) | 0.103 | 0.202 | 0.310 |
| Identified values(D) | 0.107 | 0.195 | 0.322 |
| Identified values(E) | 0.984 | 0.210 | 0.298 |

**Table 4.2:** Influences of measurement noises on the identified thermal conductivity.

Identified values (C), (D) and (E) shown in Table 4.2 represent for the identified thermal conductivity when the measurement error of temperature is 1.0 $^\circ$C, 2.0 $^\circ$C and 5.0 $^\circ$C, respectively. The proposed scheme accurately identifies the thermal conductivity of nonlinear heat conduction problem for a large random error. As the random error becomes larger, detailed information on the thermal parameters is lost slightly, and the identification precision decreases.

## 5 Conclusion

The proposed identification scheme is based on the minimization of the least-squared errors between measured and calculated temperatures at observation points. The evolutionary algorithm is employed to overcome numerical difficulties caused by the ill-posedness of inverse problems. The validity and effectiveness of the proposed method are demonstrated by the examples. In order to demonstrate the stability of proposed method to measurement errors, the Monte-Carlo simulation is performed of various amplitudes of random errors in the example. And numerical computational results show

the insensitivity of the proposed algorithm to measurement errors. Simulated temperature measurements of several sensors located inside the material were utilized for the estimation of the spatial variations of the heat transfer coefficient. Different cases are examined here, involving different numbers of sensors, levels of measurement error. It is shown that the proposed method converges very fast in a robust manner, and is not only simple and flexible, but also versatile and accurate. With considering measurement errors for 5%, the inversion method can identify the thermal conductivity within 1%, as compared with theoretical values.

## Acknowledgements

This research is funded by the National Natural Science Foundation of China (No. 10472025).

## References

[1] Tseng, A. A. Direct sensitivity coefficient method for solving two-dimensional inverse heat conduction problems by finite-element scheme. *Numerical Heat Transfer* **27**(2) (1995) 291–307.

[2] Marcelo, J. Comparison of different versions of the conjugate gradient method of function estimation. *Numerical Heat Transfer* **36**(2) (1999) 229–249.

[3] Lee, H. S. A new spatial regularization scheme for the identification of the geometric shape of an inclusion in a finite body. *Int. J. for Numerical Methods in Engineering* **46**(7) (1999) 973–992.

[4] Tervola, P. A method to determine the thermal conductivity from measured temperature profiles. *Int. J. Heat Mass Transfer* **32**(8) (1989) 1425–1431.

[5] Lin, J Y. Numerical estimation of thermal conductivity from boundary temperature measurements. *Numerical Heat Transfer* **32**(2) (1997) 187–203.

[6] Garcia, S. Use of genetic algorithms in thermal property estimation: simultaneous estimation of thermal properties. *Numerical Heat Transfer* **33**(2) (1998) 149–168.

[7] Yue, W. Y., Miyazaki, K., and Deng, X. T. Optimal channel assignment in wireless communication networks with distance and frequency interferences. *Computer Communications* **27**(16) (2004) 1661–1669.

[8] Furukawa, T. An automated system for simulation and parameter identification of inelastic constitute models. *Comput. Methods Appl. Mech. Eng.* **191**(6) (2002) 2235–2260.

[9] Coats, L. Evolutionary algorithms approach to the solution of mixed integer non-linear programming problems. *Computers and Chemical Engineering* **25**(2-3) (2001) 257–266.

[10] Sahab, M. G. A hybrid genetic algorithm for reinforced concrete flat slab buildings. *Computers and Structures* **83**(8-9) (2005) 551–559.

[11] Kustrin, K. Basic Concepts of artificial neural network (ANN) modeling and its application in pharmaceutical research. *J. of Pharmaceutical and Biomedical Analysis* **22**(5) (2000) 717–727.

[12] Abbass, H. A. An evolutionary artificial neural networks approach for breast cancer diagnosis. *Artificial Intelligence in Medicine* **25**(3) (2002) 265–281.

[13] Alkhanmis, T. M. Simulated annealing for discrete optimization with estimation. *European Journal of Operational Research* **116**(3) (1999) 530–544.

[14] Jeong, I. K. Adaptive simulated annealing genetic algorithm for system identification. *Engineering Applications of Artificial Intelligence* **9**(5) (1996) 523–532.

[15] Chen, T. Y. Efficiency improvement of simulated annealing in optimal structural designs. *Advances in Engineering Software* **33**(7–10) (2002) 675–680.

Nonlinear Dynamics and Systems Theory, **7** (1) (2007) 35–49

# Continuous-Time Optimal Portfolio Selection Using Mean-CaR Models

Zhong-Fei Li [1*], Kai W. Ng [2] and Xiao-Tie Deng [3]

[1] *Department of Risk Management and Insurance, Lingnan (University) College, Sun Yat-Sen University, Guangzhou 510275, People's Republic of China*
[2] *Department of Statistics and Actuarial Science, The University of Hong Kong, Pokfulam Road, Hong Kong*
[3] *Department of Computer Science, City University of Hong Kong, Kowloon, Hong Kong*

Received: July 18, 2005; Revised: October 22, 2006

**Abstract:** This paper studies continuous-time optimal portfolio selection under the setting of Black-Scholes financial markets and constant re-balanced portfolio (CRP) investment strategies. Three mean-CaR models are formulated, which minimize the risk measured by capital-at-risk (CaR) under the constraint that the expected terminal wealth is not lower than a pre-assigned level. These models are converted into bi-level optimization problems by virtue of a decomposition of the feasible solution set and, as a result, explicit optimal strategies and efficient frontiers are obtained in closed-form. A comparison of the three mean-CaR models and a numerical example illustrating the results are presented. Some economic implications of the results are also examined.

**Keywords:** *Continuous-time portfolio selection; Capital-at-Risk (CaR); Black-Scholes financial markets; constant-rebalanced portfolios (CRP); mean-CaR models.*

**Mathematics Subject Classification (2000):** 91B28, 91B62, 90B50, 90C90, 49M37.

* Corresponding author: lnslzf@zsu.edu.cn

 

## 1 Introduction

The pioneering work of Markowitz [13] introduced the mean-variance framework for portfolio selection and risk management. The mean-variance approach has become the foundation of modern finance theory and inspired a substantial number of extensions and applications in literature. From a theoretical point of view, there are two challenges. The first is the extension of the classical single-period mean-variance analysis to a multi-period or continuous-time mean-variance analysis. There is a considerable volume of literature on dynamic asset allocation. The main focus, however, is on maximizing some time-additive utility of terminal wealth and/or consumption (see, e.g., Merton [15, 16], Samuelson [18] and Smith [20]). At the same time, enormous difficulties in solving dynamic mean-variance problems were reported (see, e.g., Chen, Jen and Zionts [4]). Consequently, Markowitz's mean-variance formulation has not been fully exploited in dynamic cases for quite a long time since the dynamic mean-variance problems were set in a very general approach, by Schweizer [19] among others. Up to recently, the dynamic mean-variance problems have been solved analytically by Li and Ng [12] and Zhou and Li [21], respectively, in a discrete-time and a continuous-time frameworks.

The second challenge lies on appropriate measures of risk. The classical risk measure is the variance, as used in the mean-variance approach. However, the variance as a measure of risk has the drawback that it penalizes equally both upside and downside movement in the portfolio value. Realizing this, Markowitz [14] proposed semivariance as an alternative that measures risk as deviations below the mean only. Unfortunately he did not resolve the difficulties of the mean-semivariance framework caused by the non-differentiability in the setup. Consequently, other alternatives have been suggested, such as downside risk (see, e.g., Fishburn [5] and Harlow [9]), coherence risk (see, e.g., Artzner *et al.* [1]), the limited expected loss (see, e.g., Basak and Shapiro [2]), and so on. Among them, value-at-risk (VaR) (see, e.g., Jorior [11]) is the most prominent risk measure and has become an industry benchmark, which has been accepted by the regulators and banks in more than 100 countries around the world for controlling market risk.

Recently, Emmer, Klüppelberg and Korn [6, 7] developed the classic mean-variance method along the two clues mentioned above. In continuous-time financial markets with a Black-Scholes setting, they proposed a VaR-based related risk concepts known as capital-at-risk (CaR), which includes mainly three kinds of measures. Under constant rebalanced portfolio (CRP) investment strategies, they formulated two mean-CaR portfolio optimization models using the first two kinds of CaR as a replacement of the variance in a continuous-time mean-variance portfolio selection model, and derived analytically the optimal solutions for their models and the mean-variance model. Their solutions, however, involve a parameter that is a solution of a nonlinear algebra equation. In this sense, their solutions are not close-form. A possible reason for this is that they maximize the expected terminal wealth under the constraint that the CaR or the variance of the terminal wealth is not higher than a prescribed level.

In this paper, we reformulate the continuous-time mean-CaR portfolio selection models so as to minimize the risk measured by CaR under the constraint that the expected terminal wealth is not lower than a pre-assigned level. We aim at explicit expressions for optimal solutions and efficient frontiers in closed-form. We solve the mean-CaR model associated with the third kind of CaR and compare the three mean-CaR models. In addition to closed-form solutions, our approach has the advantage of easily comparing the

optimal strategies to different mean-CaR models and the convenience of solving different mean-CaR models as they have the same set of feasible portfolios and hence can use the same decomposition of the feasible set. It is believed that the approach can be applied to some other continuous-time portfolio selection problems.

## 2 The financial market and CaR

Consider a standard Black-Scholes type financial market in which $n+1$ assets (or securities) are traded continuously in the horizon $[0,T]$ and indexed by $i = 0, 1, \ldots, n$. One of the assets, say $i = 0$, is the riskless bond whose price process $P_0(t)$ evolves according to the following (deterministic) ordinary differential equation

$$dP_0(t) = P_0(t)rdt \quad \text{for} \quad t \in [0,T],$$

where $r$ is the rate of interest and is assumed to be constant. The other $n$ assets are risky stocks whose price processes $P_1(t), \ldots, P_n(t)$ follow the following stochastic differential equations

$$dP_i(t) = P_i(t)\left(b_i dt + \sum_{j=1}^{n} \sigma_{ij} dB_j(t)\right) \quad \text{for} \quad t \in [0,T], \quad i = 1, \ldots, n,$$

where $b = (b_1, \ldots, b_n)'$ is the vector of stock-appreciation rate, $\sigma = (\sigma_{ij})_{n\times n}$ is the matrix of stock-volatilities and $B(t) = (B_1(t), \ldots, B_n(t))'$ is a standard $n$-dimensional Brownian motion. Here $b$ and $\sigma$ are assumed to be constant in time. As usual, we further assume that $\sigma$ is invertible and that $b_i \geq r$ for each $i$.

Let $\pi_i(t)$ be the fraction of the wealth $W^\pi(t)$ invested in asset $i$ at time $t$. Let $\pi(t) = (\pi_1(t), \ldots, \pi_n(t))' \in \mathbb{R}^n$. Then $\pi_0(t) = 1 - \pi(t)'\mathbf{1}$, where $\mathbf{1} = (1, \ldots, 1)'$ is the vector whose components are all units. The portfolio process $\pi(t)$ is called a portfolio strategy.

Throughout the paper, we assume that transaction costs and consumption are not considered and that portfolio strategy $\pi(t)$ is self-financing. Thus

$$dW^\pi(t) = W^\pi(t)\left\{((1 - \pi(t)'\mathbf{1})r + \pi(t)'b)dt + \pi(t)'\sigma dB(t)\right\}$$

with $W^\pi(0) = w > 0$ being the initial wealth of an investor.

In what follows, we restrict ourselves to constant-rebalanced portfolio (CRP) strategies. A CRP strategy is an investment strategy which keeps a fixed fraction of the wealth in each of the underlying stocks from time to time. Therefore, a CRP strategy employs the same investment vector $\pi(t) = \pi = (\pi_1, \ldots, \pi_n)'$ at each $t$ in the planning horizon $[0,T]$. Such an investment strategy does not imply that there is no trading, since at each time instant $t$ the investment proportions are rebalanced back to the vector $\pi$. See an example in Helmbold *et al.* [10] for the power of CRP investment strategies.

Standard Itô integral and the fact that $E[e^{sB_j(t)}] = e^{ts^2/2}$, where $E$ is the expectation operator, yield the following explicit formulae for the wealth process $W^\pi(t)$ for all $t \in [0,T]$ (see, e.g., [6]).

$$W^\pi(t) = w\exp((\pi'(b - r\mathbf{1}) + r - \|\pi'\sigma\|^2/2)t + \pi'\sigma B(t)), \tag{2.1}$$

$$E[W^\pi(t)] = w\exp((\pi'(b - r\mathbf{1}) + r)t), \tag{2.2}$$

$$Var[W^\pi(t)] = w^2\exp(2(\pi'(b - r\mathbf{1}) + r)t)(\exp(\|\pi'\sigma\|^2 t) - 1), \tag{2.3}$$

where $\|\cdot\|$ denotes the Euclidean norm in $\mathbb{R}^n$ and $Var$ is the variance operator.

Associated with a real number $\alpha \in (0,1)$, initial wealth $w$, time horizon $T$ and portfolio $\pi$, we denote by $\rho_0(\alpha,\pi,w,T)$ the $\alpha$-quantile of the terminal wealth $W^\pi(T)$, that is, it is implicitly defined by

$$P(W^\pi(T) \le \rho_0(\alpha,\pi,w,T)) = \alpha, \tag{2.4}$$

where $P(\cdot)$ is the probability. Using the notation $\rho_0$, the expected shortfall or more precisely the conditional tail expectation of $W^\pi(T)$ is defined as

$$\rho_1(\alpha,\pi,w,T) = E[W^\pi(T)|W^\pi(T) \le \rho_0(\alpha,\pi,w,T)]. \tag{2.5}$$

Furthermore, the conditional tail semi-standard derivation of $W^\pi(T)$ is defined as

$$\rho_2(\alpha,\pi,w,T) = \sqrt{E[(W^\pi(T))^2|W^\pi(T) \le \rho_0(\alpha,\pi,w,T)]}. \tag{2.6}$$

Using the risk measures $\rho_k(\alpha,\pi,w,T)$, $k=0,1,2$, Emmer, Klüppelberg and Korn [7] defined the Capital-at-Risk with respect to $\rho_k(\alpha,\pi,w,T)$ as its difference to the terminal wealth of the pure bond strategy.

**Definition 2.1 (Capital-at-Risk)** *The* Capital-at-Risk (CaR) *of a CRP investment strategy $\pi$ with respect to $\rho_k$ ($k=0,1,2$) with initial wealth $w$ and time horizon $T$ is the difference between the terminal wealth of the pure bond strategy and the risk measure $\rho_k$, i.e.,*

$$CaR_k(\pi) := w\exp(rT) - \rho_k(\alpha,\pi,w,T). \tag{2.7}$$

Let $z_\alpha$ be the $\alpha$-quantile of the standard normal distribution and $\Phi$ the distribution function of a standard normal random variable.

Since $\pi'\sigma B(T)/(\|\pi'\sigma\|\sqrt{T})$ is a standard normal random variable, by using (2.1) and (2.4)–(2.7), we can express explicitly the risk measures $\rho_k, k=0,1,2$ as (see [7])

$$\rho_0(\alpha,\pi,w,T) = w\exp\left(\left(\pi'(b-r\mathbf{1})+r-\|\pi'\sigma\|^2/2\right)T + z_\alpha\|\pi'\sigma\|\sqrt{T}\right), \tag{2.8}$$

$$\rho_1(\alpha,\pi,w,T) = w\exp\left((\pi'(b-r\mathbf{1})+r)T\right)\frac{\Phi(z_\alpha-\|\pi'\sigma\|\sqrt{T})}{\alpha}, \tag{2.9}$$

$$\rho_2(\alpha,\pi,w,T) = w\exp\left((\pi'(b-r\mathbf{1})+r+\|\pi'\sigma\|^2/2)T\right)\sqrt{\frac{\Phi(z_\alpha-2\|\pi'\sigma\|\sqrt{T})}{\alpha}}. \tag{2.10}$$

Consequently, closed-form expressions of $CaR_k(\pi)$ for $k=0,1,2$ can be given.

To avoid discussions of some subcases, throughout this paper we make the following assumption.

**Assumption 2.1** *The parameter $\alpha$ satisfies $\alpha < 0.5$ and hence $z_\alpha < 0$.*

Denote by $\varphi$ the density function of a standard normal random variable.

**Lemma 2.1** *Let $x > 0$. Then*

$$\left(\frac{1}{x}-\frac{1}{x^3}\right)\varphi(x) < \Phi(-x) < \frac{\varphi(x)}{x}.$$

***Proof*** See Gänssler and Stute [8]. □

## 3 Mean-CaR portfolio selection

Emmer, Klüppelberg and Korn [6] solved the portfolio optimization problem that maximizes the expected terminal wealth under a given level of $CaR_0$, i.e.,

$$\max_{\pi\in\mathbb{R}^n} E[W^\pi(T)] \quad \text{subject to} \quad CaR_0(\pi) \le C. \tag{3.1}$$

Emmer, Klüppelberg and Korn [7] solved the portfolio optimization problem that maximizes the expected terminal wealth under a given level of $CaR_1$, i.e.,

$$\max_{\pi\in\mathbb{R}^n} E[W^\pi(T)] \quad \text{subject to} \quad CaR_1(\pi) \le C. \tag{3.2}$$

The two models are analogues of the Markowitz's mean-variance model that maximizes the expected terminal wealth under a given level of the variance of the terminal wealth. In this paper, we solve the portfolio optimization problem associated with $CaR_2$. However, our model is to minimize $CaR_2$ of the terminal wealth under a given level of the expected terminal wealth. This is an analogue of the Markowitz's mean-variance model that minimizes the variance of the terminal wealth under a given level of the expected terminal wealth. As an application of our method, we also solve the portfolio optimization models that minimizes respectively $CaR_0$ and $CaR_1$ under a given level of the expected terminal wealth. We refer the three portfolio optimization models as mean-CaR models.

### 3.1 Mean-$CaR_2$ portfolio selection

Consider the following mean-CaR model associated with $CaR_2$:

$$\min_{\pi\in\mathbb{R}^n} CaR_2(\pi) \quad \text{subject to} \quad E[W^\pi(T)] \ge C, \tag{3.3}$$

where $C > 0$ is a predetermined level of the expected terminal wealth $E[W^\pi(T)]$. Since the pure bond policy (i.e., the one that invests all of the wealth in the bond for the entire investment period) yields a deterministic terminal wealth of $w\exp(rT)$, throughout this paper we assume that the expected wealth level $C$ satisfies the following lower bound condition:

$$C \ge w\exp(rT). \tag{3.4}$$

Obviously, this is a reasonable assumption, for the solution of problem (3.3) under $C < w\exp(rT)$ is foolish for rational investors.

In the following we derive analytically the best CRP investment strategy; i.e., the optimal solution to problem (3.3). As a by-product, we also obtain a closed-form expression for the efficient frontier of the mean-CaR model.

Let $\theta := \|\sigma^{-1}(b - r\mathbf{1})\|$ and denote $a^+ = \max\{a, 0\}$ for a real number $a$.

**Theorem 3.1** *Assume that $b \ne r\mathbf{1}$. Assume furthermore that $C$ satisfies*

$$C \ge w\exp(rT + (\theta\sqrt{T} + z_\alpha)^+\theta\sqrt{T}). \tag{3.5}$$

*Then the unique optimal policy of the mean-CaR model (3.3) is*

$$\pi^* = (\varepsilon^*/\theta)\,(\sigma\sigma')^{-1}(b - r\mathbf{1}), \tag{3.6}$$

*where*

$$\varepsilon^* = (\ln(C/w) - rT)\,/(\theta T). \tag{3.7}$$

*The corresponding expected terminal wealth is* $E[W^{\pi^*}(T)] = C$ *and Capital-at-Risk is*

$$CaR_2(\pi^*) = w\exp(rT) - C\sqrt{\exp\left(\varepsilon^{*2}T\right)\Phi(z_\alpha - 2\varepsilon^*\sqrt{T})/\alpha}. \tag{3.8}$$

***Proof*** With the help of expressions (2.2) and (2.10) and the definition of $CaR_2$, problem (3.3) cab be equivalently written as

$$\begin{cases} \max & w\exp\left((\pi'(b - r\mathbf{1}) + r + \|\pi'\sigma\|^2/2)T\right)\sqrt{\Phi(z_\alpha - 2\|\pi'\sigma\|\sqrt{T})/\alpha} \\ \text{s.t.} & w\exp\left((\pi'(b - r\mathbf{1}) + r)T\right) \geq C. \end{cases} \tag{3.9}$$

The feasible set of the problem is

$$\Pi = \left\{\pi : (b - r\mathbf{1})'\pi T \geq \ln(C/w) - rT\right\}.$$

Given $\varepsilon > 0$, the intersection of $\Pi$ and the ellipsoid $\|\pi'\sigma\| = \varepsilon$ is

$$\Pi(\varepsilon) = \left\{\pi : \|\pi'\sigma\| = \varepsilon, \quad (b - r\mathbf{1})'\pi T \geq \ln(C/w) - rT\right\}.$$

The hyperplane $(b - r\mathbf{1})'\pi T = \ln\frac{C}{w} - rT$ is tangent to the ellipsoid $\|\pi'\sigma\| = \varepsilon$ if and only if $\varepsilon\theta T = \ln(C/w) - rT$, that is $\varepsilon = \varepsilon^* := \left(\ln(C/w) - rT\right)/(\theta T) > 0$. Consequently $\Pi(\varepsilon) = \emptyset$ if $\varepsilon < \varepsilon^*$ and hence $\Pi = \bigcup_{\varepsilon \geq \varepsilon^*} \Pi(\varepsilon)$. Thus problem (3.9) is equivalent to the following bilevel optimization problem

$$\max_{\varepsilon \geq \varepsilon^*} \max_{\pi \in \Pi(\varepsilon)} w\exp\left((\pi'(b - r\mathbf{1}) + r + \varepsilon^2/2)T\right)\sqrt{\Phi(z_\alpha - 2\varepsilon\sqrt{T})/\alpha}. \tag{3.10}$$

For each fixed $\varepsilon \geq \varepsilon^*$, we solve the inner-level optimization problem

$$\max_{\pi \in \Pi(\varepsilon)} \quad w\exp\left((\pi'(b - r\mathbf{1}) + r + \varepsilon^2/2)T\right)\sqrt{\Phi(z_\alpha - 2\varepsilon\sqrt{T})/\alpha}$$

or equivalently

$$\max_{\pi \in \Pi(\varepsilon)} (b - r\mathbf{1})'\pi. \tag{3.11}$$

The unique optimal solution is the tangent point

$$\pi^*_\varepsilon = (\varepsilon/\theta)(\sigma\sigma')^{-1}(b - r\mathbf{1})$$

of the hyperplane that parallels $(b - r\mathbf{1})'\pi T = \ln\frac{C}{w} - rT$ to the ellipsoid $\|\pi'\sigma\| = \varepsilon$, with maximum $(b - r\mathbf{1})'\pi^*_\varepsilon = \varepsilon\theta$. Therefore, we obtain the solution of problem (3.10) by solving the problem

$$\max_{\varepsilon \geq \varepsilon^*} \quad w\exp\left((\varepsilon\theta + r + \varepsilon^2/2)T\right)\sqrt{\Phi(z_\alpha - 2\varepsilon\sqrt{T})/\alpha}. \tag{3.12}$$

Consider the functions $h$ on $[0, +\infty)$ defined by

$$h(\varepsilon) = 2\varepsilon\theta T + \varepsilon^2 T + \ln\left(\Phi(z_\alpha - 2\varepsilon\sqrt{T})\right).$$

Noting $1-\Phi(x)=\Phi(-x)$ and $\varphi(-x)=\varphi(x)$, setting $x=2\varepsilon\sqrt{T}-z_\alpha$ in the second inequality in Lemma 2.1 yields $\varphi(z_\alpha-2\varepsilon\sqrt{T})>\Phi(z_\alpha-2\varepsilon\sqrt{T})(2\varepsilon\sqrt{T}-z_\alpha)$. Thus

$$\begin{aligned} h'(\varepsilon) &= 2\theta T+2\varepsilon T+\frac{(-2\sqrt{T})\varphi(z_\alpha-2\varepsilon\sqrt{T})}{\Phi(z_\alpha-2\varepsilon\sqrt{T})} < 2\sqrt{T}\left[\theta\sqrt{T}+\varepsilon\sqrt{T}-(2\varepsilon\sqrt{T}-z_\alpha)\right] \\ &= 2\sqrt{T}(\theta\sqrt{T}+z_\alpha-\varepsilon\sqrt{T}). \end{aligned}$$

If $\theta\sqrt{T}+z_\alpha\le 0$, then obviously $h'(\varepsilon)<0$ for $\varepsilon\ge 0$. If $\theta\sqrt{T}+z_\alpha>0$, then condition (3.5) implies that $\varepsilon^*\ge(\theta\sqrt{T}+z_\alpha)/\sqrt{T}$ and hence $h'(\varepsilon)<0$ for $\varepsilon\ge\varepsilon^*$. Thus, function $h$ is strictly decreasing when $\varepsilon\ge\varepsilon^*$. Consequently, problem (3.12)'s objective function, equal to $\exp\left((h(\varepsilon)+2rT-\ln\alpha)/2\right)$, is strictly decreasing when $\varepsilon\ge\varepsilon^*$. Therefore, the optimal solution of problem (3.12) is the unique $\varepsilon^*$. This completes the proof. □

As an immediate consequence, the analytic result in Theorem 3.1 provides an explicit relation between the optimal Capital-at-Risk and the expected terminal wealth. Letting $\xi:=E[W^{\pi^*}(T)]$, we have

$$CaR_2(\xi)=we^{rT}-\xi\sqrt{\frac{1}{\alpha}\exp\left(\frac{\left(\ln\frac{\xi}{w}-rT\right)^2}{\theta^2T}\right)\Phi\left(z_\alpha-\frac{2\left(\ln\frac{\xi}{w}-rT\right)}{\theta\sqrt{T}}\right)} \tag{3.13}$$

for $\xi\ge w\exp(rT+(\theta\sqrt{T}+z_\alpha)^+\theta\sqrt{T})$. The above relationship is known as the *efficient frontier* of the mean-CaR model associated with $CaR_2$ in mean-CaR space.

### 3.2 Mean-$CaR_1$ portfolio selection

Consider the following mean-CaR model associated with $CaR_1$:

$$\min_{\pi\in\mathbb{R}^n} CaR_1(\pi) \quad \text{subject to} \quad E[W^\pi(T)]\ge C, \tag{3.14}$$

where $C$, as in model (3.3), is again the predetermined level of the expected terminal wealth $E[W^\pi(T)]$ and satisfies condition (3.4).

Using a quite similar derivation as that in the proof of Theorem 3.1, we can also obtain a closed-form solution for problem (3.14), which is summarized by the following theorem stated without proof.

**Theorem 3.2** *Assume that $b\ne r\mathbf{1}$. Assume furthermore that $C$ satisfies (3.5). Then the unique optimal policy of the mean-CaR model (3.14) is*

$$\pi^*=(\varepsilon^*/\theta)\,(\sigma\sigma')^{-1}(b-r\mathbf{1}), \tag{3.15}$$

*where*

$$\varepsilon^*=(\ln(C/w)-rT)\,/(\theta T). \tag{3.16}$$

*The corresponding expected terminal wealth is $E[W^{\pi^*}(T)]=C$ and Capital-at-Risk is*

$$CaR_1(\pi^*)=w\exp(rT)-C\Phi(z_\alpha-\varepsilon^*\sqrt{T})/\alpha. \tag{3.17}$$

Consequently, the efficient frontier of the mean-CaR model associated with $CaR_1$ in mean-CaR space is given by

$$CaR_1(\xi) = we^{rT} - \frac{\xi}{\alpha}\Phi\left(z_\alpha - \frac{\ln\frac{\xi}{w} - rT}{\theta\sqrt{T}}\right) \tag{3.18}$$

for $\xi := E[W^{\pi^*}(T)] \geq w\exp(rT + (\theta\sqrt{T} + z_\alpha)^+\theta\sqrt{T})$.

It should be pointed out that although Emmer, Klüppelberg and Korn [7] also obtained a solution to (3.2) that has the same representation as (3.15), the parameter $\varepsilon^*$ however was not obtained explicitly as in (3.16). In fact, in their formulation $\varepsilon^*$ is estimated as a value between two expressions representing two real numbers.

### 3.3 Mean-$CaR_0$ portfolio selection

Consider the following mean-CaR model associated with $CaR_0$:

$$\min_{\pi\in\mathbb{R}^n} CaR_0(\pi) \quad \text{subject to} \quad E[W^\pi(T)] \geq C, \tag{3.19}$$

where $C$, as in problem (3.3), is again the predetermined level of the expected terminal wealth $E[W^\pi(T)]$ and satisfies condition (3.4).

The solution to the above optimization problem (3.19) is summarized in the following theorem. We omit the proof since it is very similar to the proof of Theorem 3.1.

**Theorem 3.3** *Assume that $b \neq r\mathbf{1}$. Then the unique optimal policy of mean-CaR model* (3.19) *is*

$$\pi^* = (\varepsilon^*/\theta)\,(\sigma\sigma')^{-1}(b - r\mathbf{1}), \tag{3.20}$$

*where*

$$\varepsilon^* = \max\left\{(\ln(C/w) - rT)/(\theta T), \theta + z_\alpha/\sqrt{T}\right\}. \tag{3.21}$$

*The corresponding expected terminal wealth is*

$$E[W^{\pi^*}(T)] = w\exp(\varepsilon^*\theta T + rT) = \max\left\{C, w\exp\left(rT + \theta T\left(\theta + z_\alpha/\sqrt{T}\right)\right)\right\} \tag{3.22}$$

*and the Capital-at-Risk is*

$$CaR_0(\pi^*) = w\exp(rT)\left[1 - \exp\left(\varepsilon^*\theta T - {\varepsilon^*}^2 T/2 + z_\alpha\varepsilon^*\sqrt{T}\right)\right]. \tag{3.23}$$

Based on this result, the efficient frontier of the mean-CaR model associated with $CaR_0$ in mean-CaR space is given by

$$CaR_0(\xi) = w\exp(rT) - \xi\exp\left(\frac{\ln(\xi/w) - rT}{\theta T}\left(z_\alpha\sqrt{T} - \frac{\ln(\xi/w) - rT}{2\theta}\right)\right) \tag{3.24}$$

for $\xi := E[W^{\pi^*}(T)] \geq w\exp\left(rT + \left(\theta + z_\alpha/\sqrt{T}\right)^+\theta T\right)$.

We noted that the part of the efficient frontier corresponding to those $C$ satisfying

$$w\exp(rT) \leq C \leq w\exp\left(rT + \left(\theta + z_\alpha/\sqrt{T}\right)^+\theta T\right)$$

degenerates to a single point where $\xi = w\exp\left(rT + \left(\theta + z_\alpha/\sqrt{T}\right)^+\theta T\right)$ in mean-CaR space. Hence the whole efficient frontier starts from this point.

## 4 A comparison of the mean-CaR models

Based on the results in the previous section, in this section we compare the optimal behaviors of our mean-$CaR_0$, mean-$CaR_1$, and mean-$CaR_2$ models.

(1) For any given expected terminal wealth level $C \geq C_0 := w \exp\left(rT + \theta\sqrt{T}\left(\theta\sqrt{T} + z_\alpha\right)^+\right)$, the three mean-CaR models have the same optimal strategy which does not depend on the confidence level $\alpha$ and the same expected terminal wealth which is equal to the lowest permissible wealth $C$. When the given expected terminal wealth level $C$ is lower than $C_0$, the optimal policy of the mean-$CaR_0$ model does not dependent on the expected terminal wealth level $C$ but depends on the the confidence level $\alpha$.

(2) For each mean-CaR model, the optimal fraction of wealth invested in risky assets $\pi^*$ is increasing with the expected terminal wealth level $C$, indicating that a higher expected terminal wealth level requires more investment in risky assets. (In the low level region $C \leq C_0$, the optimal stock weights of the mean-$CaR_0$ model are invariant with the expected terminal wealth level.)

(3) For the mean-$CaR_2$ and the mean-$CaR_1$ models, the optimal fraction of wealth invested in risky assets $\pi^*$ is decreasing with the investment horizon $T$, exhibiting the reverse time-diversification effect: an investor allocates less to stocks when confronted with a longer investment horizon. For the mean-$CaR_0$ model, however, the optimal fraction of wealth invested in stocks first decreases with $T$ in the region $T \leq T_0 := \left(\frac{-z_\alpha\theta + \sqrt{(z_\alpha\theta)^2 + 4(r+\theta^2)\ln(C/w)}}{2(r+\theta^2)}\right)^2$, exhibiting the reverse time-diversification effect in the region of short investment horizons $T \leq T_0$, and then increases with $T$ in the region $T \geq T_0$, exhibiting the time-diversification effect in the region of long investment horizons $T \geq T_0$.

(4) For each mean-CaR model, CaR of the optimal strategy is decreasing with confidence level $\alpha$; that is, smaller risk measured by CaR is exposed at the expense of higher confidence level.

(5) For each mean-CaR model, roughly the CaR of the optimal strategy is first increasing and then decreasing with time horizon $T$, implying that more (less) risk measured by CaR is exposed as the horizon extends in the small (large) region of short (long) horizons. This will be illustrated in the example of the next section.

(6) As to be expected, in mean-CaR spaces, the three mean-CaR efficient frontiers are all strictly increasing and concave, where the concavity of the mean-$CaR_0$ efficient frontier is true at least in the region

$$\xi \geq w \exp\left(rT + \left(\theta\sqrt{T} + z_\alpha\right)\theta\sqrt{T} + \left(\sqrt{1/4 + 1/(\theta^2 T)} - 1/2\right)\theta^2 T\right).$$

(7) The mean-$CaR_1$ efficient frontier is higher than the mean-$CaR_2$ efficient frontier, which, in turn, is higher than the mean-$CaR_0$ efficient frontier; that is, for each $\xi = E[W^{\pi^*}(T)] \geq w \exp\left(rT + \left(\theta\sqrt{T} + z_\alpha\right)^+ \theta\sqrt{T}\right)$, $CaR_1(\xi) \geq CaR_2(\xi) \geq CaR_0(\xi)$. In other words, for the same expected terminal wealth level, the optimal strategy of the mean-$CaR_1$ model has larger CaR than the one of the mean-$CaR_2$ model, which in turn has larger CaR than the one of the mean-$CaR_0$ model. In fact, it holds that $CaR_1(\pi) \geq CaR_2(\pi) \geq CaR_0(\pi)$ for general strategies $\pi$; see Corollary 2.4 of Emmer, Klüppelberg and Korn [7].

(8) Each of the three mean-CaR efficient frontiers depends only on the stocks via the norm $\|\sigma^{-1}(b - r\mathbf{1})\|$ and has no explicit dependence on the number of different stocks. Therefore, Theorems 3.1, 3.2 and 3.3 can be interpreted as a kind of *mutual fund theorems* since there is no difference between investment in our multi-stock market and a market consisting of the bond and just one stock with appropriate market coefficients $b$ and $\sigma$, as observed by Emmer, Klüppelberg and Korn [6] for their mean-CaR model.

## 5 An example

In this section, a numerical example is presented to demonstrate the results stated in the previous section.

**Example 5.1** Consider a market that consists of the bond and just one stock (i.e., $n = 1$). Assume that the rate of interest of the bond is $r = 0.05$, the stock-appreciation rate is $b = 0.1$, and the stock-volatility is $\sigma = 0.2$, implying $\theta = 0.25$. And assume that the initial wealth of an investor is $w = 1000$.

Figures 5.1 and 5.2 show the dependence of the optimal fraction of wealth invested in the stock on the time horizon $T$, the expected terminal wealth level $C$ and the confidence levels $\alpha$. Figure 5.1 exhibits the reverse time-diversification effect, the increasingness with the expected terminal wealth level, and the invariance with the confidence level of the optimal stock fraction to the mean-$CaR_2$ and the mean-$CaR_1$ models. In Figure 5.2, the optimal stock fraction of the mean-$CaR_0$ model displays the reverse time-diversification effect in a large time horizon region (e.g., $0 < T \leq 16.48$ for $\alpha = 0.20$), the time-diversification effect in a small time horizon region (e.g., $16.48 \leq T \leq 20$ for $\alpha = 0.20$), the increasingness with the expected terminal wealth level, and the increasingness with the confidence level.

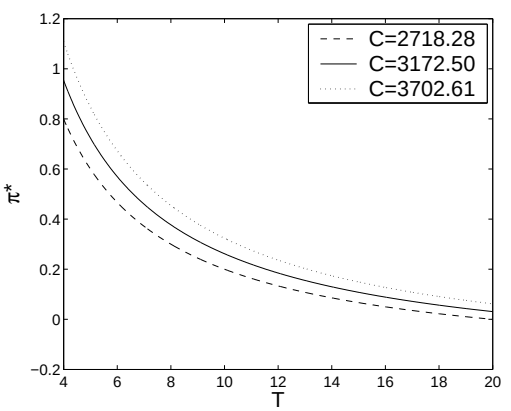


**Figure 5.1:** The optimal stock fraction of the mean-$CaR_2$ and the mean-$CaR_1$ models with any confidence level $\alpha < 0.13$ as a function of the time horizon $T$ ($0 < T \leq 20$) for different expected terminal wealth levels $C$.

The CaR of the optimal strategy as a function of the time horizon $T$ is illustrated graphically in Figure 5.3 for mean-$CaR_2$, Figure 5.4 for mean-$CaR_1$, and Figure 5.5 for mean-$CaR_0$ models, which indicates that more (less) CaR risk is exposed as the horizon extends in a small (large) region of short (long) horizons for each of the mean-CaR models.

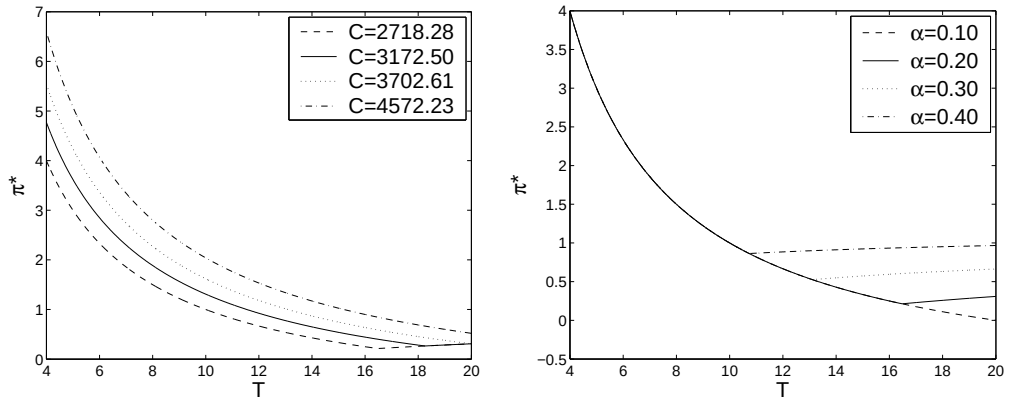


(a) with a confidence level $\alpha = 0.20$ for different expected terminal wealth levels $C$

(b) with a expected terminal wealth level $C = w\exp(20r) = 2718.28$ for different confidence levels $\alpha$

**Figure 5.2:** The optimal stock fraction of the mean-$CaR_0$ model as a function of the time horizon $T$ $(0 < T \leq 20)$.

Figures 5.5(a) and 5.5(b) also display some difference of $CaR_0$ of the optimal strategy to the mean-$CaR_0$ model with the same expected terminal wealth levels between different confidence levels. Figure 5.6 plots the CaR of the three mean-CaR models in the same plane to compare them, showing that the optimal $CaR_1$ is larger than the optimal $CaR_2$ which is larger than the optimal $CaR_0$ for the same time horizon.

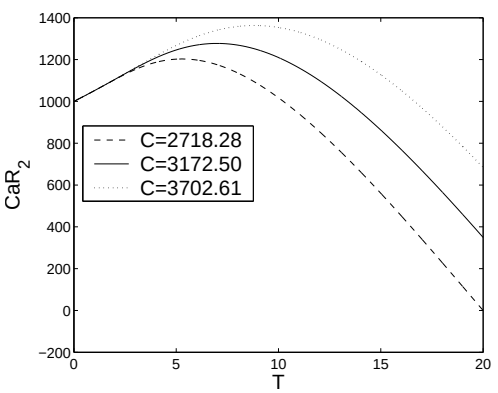


**Figure 5.3:** $CaR_2$ of the optimal strategy to the mean-$CaR_2$ model with a confidence level $\alpha = 0.05$ as a function of the time horizon $T$ $(0 < T \leq 20)$ for different expected terminal wealth levels $C$.

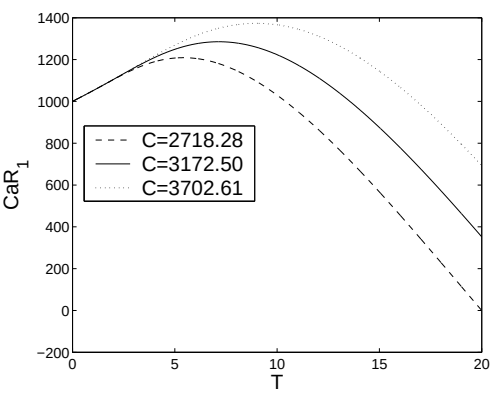


**Figure 5.4:** $CaR_1$ of the optimal strategy to the mean-$CaR_1$ model with a confidence level $\alpha = 0.05$ as a function of the time horizon $T$ $(0 < T \leq 20)$ for different expected terminal wealth levels $C$.

The mean-$CaR_2$, the mean-$CaR_1$ and the mean-$CaR_0$ efficient frontiers are depicted respectively in Figure 5.7, Figure 5.8 and Figure 5.9 with the mean on the horizontal axis and the CaR on the vertical axis for confidence levels $\alpha = 0.01$ (dashed line), $\alpha = 0.05$ (solid line) and $\alpha = 0.1$ (dotted line). Clearly, all the efficient frontiers are increasing

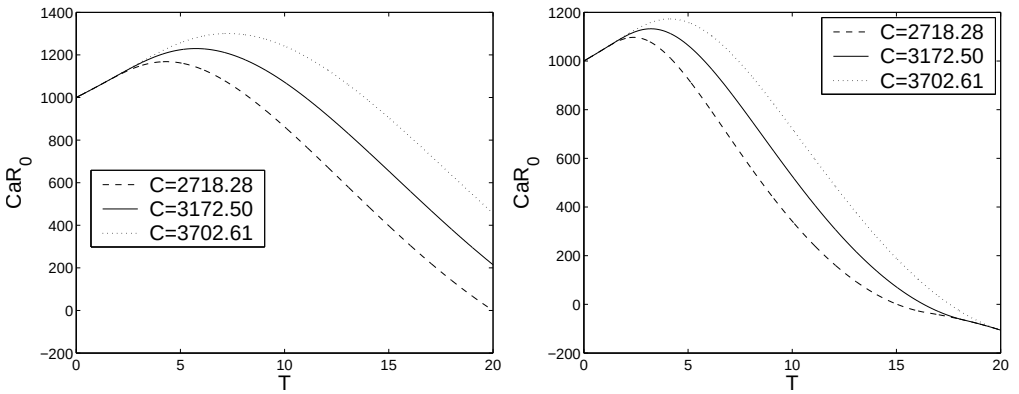


(a) with a confidence level $\alpha = 0.05$ (b) with a confidence level $\alpha = 0.20$

**Figure 5.5:** $CaR_0$ of the optimal strategy to the mean-$CaR_0$ model as a function of the time horizon $T$ $(0 < T \leq 20)$ for different expected terminal wealth levels $C$.

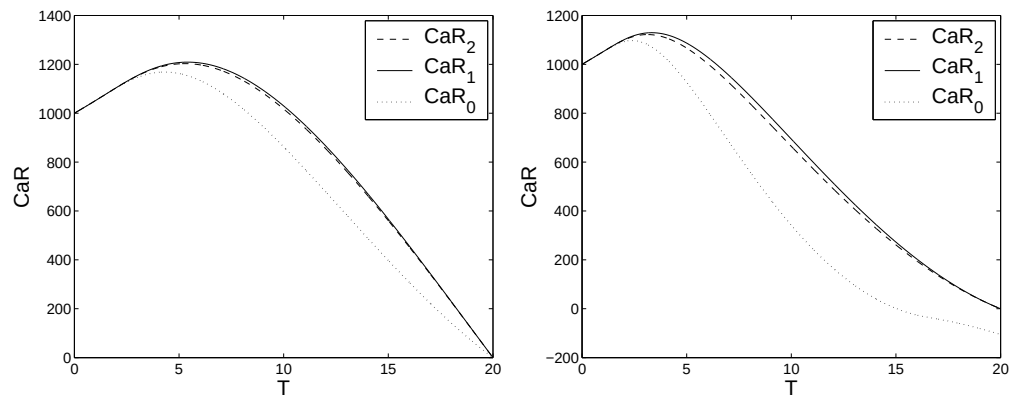


(a) with a confidence level $\alpha = 0.05$ and a expected terminal wealth level $C = 2718.28$ (b) with a confidence level $\alpha = 0.20$ and a expected terminal wealth level $C = 2718.28$

**Figure 5.6:** CaR of the optimal strategies to the mean-$CaR_k$ $(k = 0, 1, 2)$ models as a function of the time horizon $T$ $(0 < T \leq 20)$.

and concave; and the higher is the confidence level $\alpha$, the lower is the efficient frontier for each of the three mean-CaR models, implying that CaR of the optimal strategy for each mean-CaR model decreases as the confidence level increases. Furthermore, in order to demonstrates the difference of the three efficient frontiers, the efficient frontiers of mean-$CaR_2$ (dashed line), mean-$CaR_1$ (solid line) and mean-$CaR_0$ (dotted line) models are plotted in the same plane, see Figure 5.10. Obviously, the efficient frontiers of the mean-$CaR_1$, the mean-$CaR_2$ and the mean-$CaR_0$ models fall in turn, again implying that the risk measured by $CaR_1$ is the largest and the one by $CaR_0$ is the smallest, among the three.

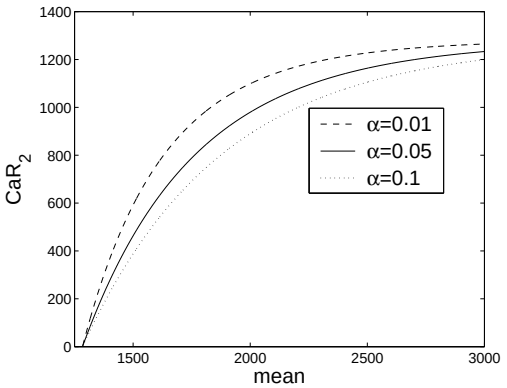


**Figure 5.7:** Mean-$CaR_2$ efficient frontiers for different confidence levels.

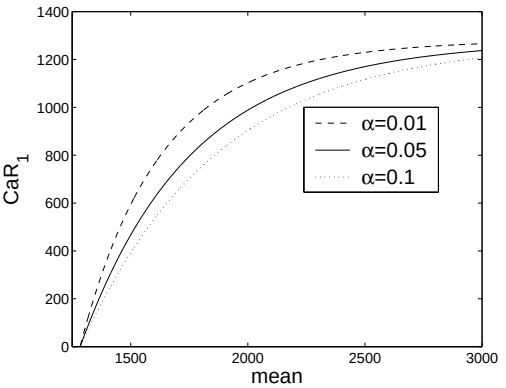


**Figure 5.8:** Mean-$CaR_1$ efficient frontiers for different confidence levels.

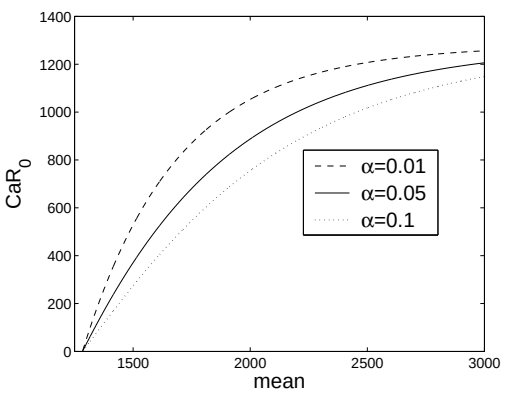


**Figure 5.9:** Mean-$CaR_0$ efficient frontiers for different confidence levels.

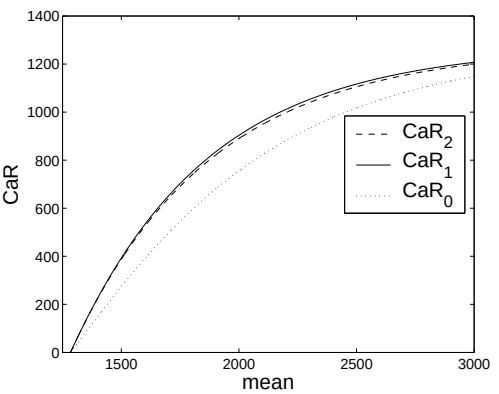


**Figure 5.10:** The mean-$CaR_k$ efficient frontiers with $k = 0, 1, 2$ for $\alpha = 0.10$.

## 6 Conclusions

This paper investigates three continuous-time mean-CaR portfolio selection models under the setting of Black-Scholes financial markets and CRP investment strategies. After

converting the portfolio optimization problems we obtain closed-form explicit expressions of optimal strategies and efficient frontiers by virtue of a decomposition of the feasible solution set. This approach facilitates computation and the comparison of results and can be easily used in practice. It unifies the framework of dealing with different mean-CaR portfolio selection models. In an analogous way, it can be shown that the approach can be applied to a mean-variance model, a mean-VaR model, and some expected utility models with a shortfall constraint to obtain closed-form solutions. We also believe that the approach can be applied to some other continuous-time portfolio selection problems.

Note that the derived optimal strategies of the three mean-CaR models are nonnegative under the assumption that each stock-appreciation rate is not smaller than the riskless interest rate. In this case, our results are valid for continuous-time mean-CaR portfolio selection problems where short-selling of risky assets is not allowed. (However, short-selling the riskless asset is still allowed.)

CRP strategies have a variety of optimality properties associated with them for ordinary portfolio problems (see, e.g., Merton [15, 16]) showed that this form of strategies are optimal to portfolio selection problems of maximizing expected utility with constant relative risk-aversion.) and are widely used in asset allocation practice (see, e.g., Perold and Sharpe [17] and Black and Perold [3]). However, since such strategies may not be feedback strategies under general models, the optimal CRP strategy for our models or for the models in Emmer, Klüppelberg and Korn [6, 7] may not be globally optimal in the set of all dynamic strategies. Removing the restriction to strategies with constant proportions would be both mathematically harder and more interesting.

## Acknowledgements

Authors would like to thank the referees for careful reading of the paper and helpful comments. This work is partially supported by Program for New Century Excellent Talents in University of China (NCET-04-0798), a grant of Foundation for the Author of National Excellent Doctoral Dissertation of China (No. 200267), grants of the National Natural Science Foundation of China (Nos. 70471018, 70518001), and a grant of Hong Kong Research Grant Council (CityU 1156/04E).

## References

[1] Artzner, P., Delbaen, F., Eber J., and Heath, D. Coherence measures of risk. *Mathematical Finance* **9** (1999) 203–228.

[2] Basak, S., and Shapiro, A. Value-at-Risk-based risk management: optimal policies and asset prices. *The Review of Financial Studies* **14** (2001) 371–405.

[3] Black, F., and Perold, A. F. Theory of constant proportion portfolio insurance. *Journal of Economic Dynamics and Control* **16** (1992) 403–426.

[4] Chen, A. H. Y., Jen, F. C., and Zionts, S. The optimal portfolio revision policy. *Journal of Business* **44** (1971) 51–61.

[5] Fishburn, P. Mean-risk analysis with risk associated with below-target returs. *American Economic Review* **67** (1977) 116–125.

[6] Emmer, S., Klüppelberg, C., and Korn, R. Optimal portfolios with bounded capital-at-risk. *Mathematical Finance* **11** (2001) 365–384.

[7] Emmer, S., Klüppelberg, C., and Korn, R. Optimal portfolios with bounded downside risks. Working Paper 2000, http://www-m4.mathematik.tu-muenchen.de/m4/pers/cklu/cklu.shtml

[8] Gänssler, P., and Stute, W. *Wahrscheinlichkeitstheorie*. Spinger, Berlin, 1977.

[9] Harlow, W. Asset allocatio in a downside risk framework. *Financial Analysis Journal* **47** (1991) 28–40.

[10] Helmbold, D. P., Schapire, R. E., Singer Y., and Warmuth, M. K. On-line portfolio selection using multiplicative updates. *Mathematical Finance* **8** (1998) 325–347.

[11] Jorion, P. *Value at Risk: The New Benchmark for Controlling Market Risk*. McGraw-Hill, New York, 1997.

[12] Li D., and Ng, W.L. Optimal dynamic portfolio selection: multiperiod mean-variance formulation. *Mathematical Fiance* **10** (2000) 387–406.

[13] Markowitz, H. Portfolio selection. *The Journal of Finance* **7** (1952) 77–91.

[14] Markowitz, H. *Portfolio Selection: Efficient Diversification of Investments*. Wiley, New York, 1959.

[15] Merton, R. C. Lifetime portfolio selection under uncertainty: the continuous-time model. *Review of Economics and Statistics* **51** (1969) 247–256.

[16] Merton, R. C. Optimum consumption and portfolio rules in a continuous-time model. *Journal of Economic Theory* **3** (1971) 373–413.

[17] Perold, A. F., and Sharpe, W. F. Dynamic strategies for asset allocation. *Financial Analyst Journal* **Jan/Feb** (1988) 16–27.

[18] Samuelson, P. A. Lifetime portfolio selection by dynamic stochastic propramming. *The Review of Economics and Statistics* **51** (1969) 239–246.

[19] Schweizer, M. Approximating random variables by stochastic integrals. *The Annals of Applied Probability* **22** (1994) 1536–1575.

[20] Smith, K. A transition model for portfolio revision. *Journal of Finance* **22** (1967) 425–439.

[21] Zhou X. Y., and Li, D. Continuous-time mean-variance portfolio selection: a stochastic LQ Framework. *Applied Mathematics and Optimization* **42** (2000) 19–33.

Nonlinear Dynamics and Systems Theory, **7** (1) (2007) 51–67

# A Simple Nonlinear Adaptive-Fuzzy Passivity-Based Control of Power Systems

H.E. Psillakis and A.T. Alexandridis *

*Department of Electrical & Computer Engineering, University of Patras, Rion 26500, Patras, Greece*

Received: November 30, 2005; Revised: March 12, 2006

**Abstract:** A new intelligent nonlinear control for power system stabilizers that improves the transient stability is proposed. To guarantee high performance with low complexity cost, new concepts on the passivity design under unknown disturbance inputs, as well as on the adaptive fuzzy logic rule extraction are introduced. This permits the most possible simple design implementation of an adaptive-fuzzy logic passivity-based controller which is developed on an equivalent model of the system obtained by a suitable use of the backstepping technique. The overall scheme is decentralized providing local output feedback controllers, supported by a very simple adaptive-fuzzy scheme of only three rules. A detailed analysis proves that the proposed control scheme ensures uniform ultimate boundedness of all the error variables in an arbitrarily small region around the origin. Extensive simulations on a two machine infinite bus power system on which a permanent serious fault occurs, confirm the theoretical results and verify an excellent system performance.

**Keywords:** *Adaptive control; fuzzy logic control; passivity; power system control.*

**Mathematics Subject Classification (2000):** 93D05, 93C42.

## 1 Introduction

Advanced intelligent control designs are increasingly used in high technology applications to solve practical problems in nonlinear systems. Among others, a characteristic example of a highly nonlinear system is the power system where these techniques are recently applied. Particularly, power systems are nonlinear, large scale, distributed systems that include a number of synchronous machines as producers. One of the main goals of the excitation control of each machine is the enhancement of power system stability especially

* Corresponding author: a.t.alexandridis@ee.upatras.gr

 

after faults such as short-circuits or significant power disturbances. To this end, power system stabilizers (PSS) are widely used as supplementary excitation control devices.

Last decade nonlinear control theory has been extensively used to account for the nonlinearities of the controlled power systems. Early designs are based on the feedback linearization technique [1]. Alternatively, the sliding-mode control technique has been applied on power systems providing rather simple control schemes [2, 3]. Nonlinear control techniques have been crucially enhanced by using robust control designs such as $H_\infty$ control and $L_2$ disturbance attenuation [4, 5, 6, 7]. In recent years new approaches have been proposed for power stability designs based on advanced nonlinear schemes such as adaptive control [8, 9, 10], neuro-control [11] and fuzzy logic [12].

Fuzzy logic designs have been employed as promising controllers, since they provide a convenient method in nonlinear design via the use of qualitative rules characterizing the power system performance. However, due to different operating conditions a large rule base is needed to ensure an acceptable performance. In order to obtain a better performance, as compared to the standard design, an adaptive fuzzy logic stabilizer has been proposed [13, 14]. Although this on-line adaptation mechanism overcomes many of the drawbacks, the whole control scheme of each machine cannot be considered as a simple one; at least 9 rules for the two-input single-output fuzzy system are required while a 9-order adaptive system is needed [14].

In this paper, a new approach to the design of decentralized adaptive fuzzy excitation control is proposed that acts in coordination with the automatic voltage regulator. The design is based on the nonlinear third-order model of each machine [5]. On this model a suitable backstepping technique is applied that modifies the original $n$-machine system into $n$ separate systems that are interconnected through highly nonlinear links. Each of these systems is a single-input single-output (SISO) minimum phase system with relative degree one. However, due to the highly nonlinear interconnections, it is shown that the system can be passive by output feedback anywhere in $\mathbf{R}^n$ except for a compact region $\Omega$ containing the origin. To describe this property the concept of $\Omega^-$ -passivity is introduced. As a result a simple standard passivity-based output feedback control design with negative gain [15, 16] can be applied that provides uniform ultimate boundedness (UUB). The size of $\Omega$ depends on the unknown nonlinear interconnections. In order to avoid high gains and large regions $\Omega$, a very simple SISO adaptive fuzzy logic scheme is included to approximate these nonlinearities. As shown in the paper, the qualitative principle that holds for the fuzzy logic rule extraction has a SISO linguistic form with input, a fixed linear combination of the power angle deviation, the nominal frequency deviation and the accelerating power. Including additionally an adaptation mechanism that provides on-line the fuzzy logic output parameters, i.e. the centers of gravity of the membership functions, a very simple rule base of only three IF-THEN SISO statements accompanied by a 3-order adaptation scheme is proposed.

Hence, by the proposed scheme, a completely decentralized excitation control is achieved. Furthermore, exploiting some inherent structure properties of power systems, a passivity-based control scheme is developed that in turn is combined with advanced control techniques in a manner that results in an extremely simple form. Extensive stability analysis proves that the system becomes UUB while the estimated parameter errors remain bounded. The region around the origin inside which the variables converge can be arbitrarily small by suitably tuning the passivity control gain and the design parameters. Finally, the effectiveness of the proposed controller is successfully verified by simulation tests on a two machine infinite bus power system.

## 2 Preliminaries and system formulation

Before proceeding with our approach we give some definitions assuming that the concepts of relative degree and normal form of a dynamical system are familiar to the reader (see [15] and the references therein for details).

**Definition 2.1** *The zero dynamics of a dynamical system with output $y$, represent those internal dynamics which are consistent with the constraint that the output is identically equal to zero. If the zero dynamics of a dynamical system are asymptotically stable, then this system is called a minimum-phase system.*

**Definition 2.2** *A dynamical system with state vector $x \in \mathbf{R}^n$, input $u \in \mathbf{R}^m$ and output $y \in \mathbf{R}^m$ is said to be passive if there exists a positive definite radially unbounded storage function $V(x)$ and a positive definite function $S(x)$ such that for all $u \in U$ where $U$ is the set of all admissible inputs holds true that*

$$V(x(t)) - V(x(0)) = \int_0^t y^T(s)u(s)ds - \int_0^t S(x(s))ds \quad \text{for all } t \geq 0 \text{ and } x \in \mathbf{R}^n.$$

Obviously from Definition 2.2, the following proposition can be made.

**Proposition 2.1** *A dynamical system with state vector $x \in \mathbf{R}^n$, input $u \in \mathbf{R}^m$ and output $y \in \mathbf{R}^m$ has the passivity property if there exists a positive definite radially unbounded function $V(x)$ and a positive scalar $c > 0$ such that*

$$\dot{V} < -cV + y^T u \quad \forall x \in \mathbf{R}^n.$$

### 2.1 $\Omega^-$-passivity

At this point, the following definition is introduced.

**Definition 2.3** *A dynamical system with state vector $x \in \mathbf{R}^n$, input $u \in \mathbf{R}^m$ and output $y \in \mathbf{R}^m$ is said to be $\Omega^-$-passive (read:* Omega minus passive*) if there exists a positive definite radially unbounded storage function $V(x)$ and a positive definite function $S(x)$ such that for all $u \in U$ where $U$ is the set of all admissible inputs, it holds true that*

$$V(x(t)) - V(x(0)) = \int_0^t y^T(s)u(s)ds - \int_0^t S(x(s))ds$$
$$\text{whenever } x(\tau) \in \mathbf{R}^n \backslash \Omega, \forall\, \tau \in [0,t],$$

*where $\Omega$ is a compact set, $\Omega \subset \mathbf{R}^n$, containing the origin.*

Obviously from Definition 2.3, the following proposition (analogous to Proposition 2.1) is given.

**Proposition 2.2** *A dynamical system with state vector $x \in \mathbf{R}^n$, input $u \in \mathbf{R}^m$ and output $y \in \mathbf{R}^m$ has the $\Omega^-$-passivity property if there exists a positive definite radially unbounded function $V(x)$ and a positive scalar $c > 0$ such that*

$$\dot{V} < -cV + y^T u \quad \forall x \in \mathbf{R}^n \backslash \Omega,$$

*where $\Omega$ is a compact set, $\Omega \subset \mathbf{R}^n$, containing the origin.*

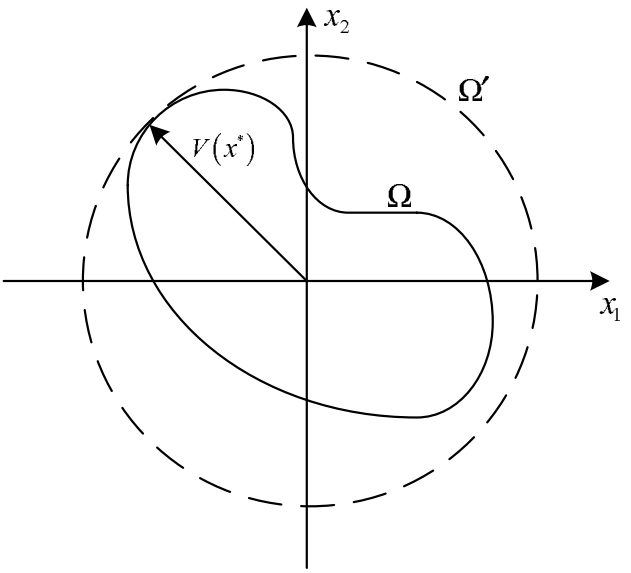


**Figure 2.1:** The regions $\Omega$ and $\Omega'$ for a Lyapunov function $V(x_1, x_2) = x_1^2 + x_2^2$.

From Definition 2.2 it is deduced that any passive unforced system ($u \equiv 0$) is asymptotically stable. On the other hand, one can easily see from Definition 2.3 that any unforced system that is $\Omega^-$-passive, ensures finite-time convergence of the state vector inside the region $\Omega$. Particularly, in accordance to Definition 2.3, since $S$ is positive definite, $\frac{\partial S}{\partial x} \neq 0 \quad \forall x \neq 0$ and therefore a local minimum of $S$ does not exist in $\mathbf{R}^n \backslash \Omega$; hence the minimum of $S$ in the closure of $\mathbf{R}^n \backslash \Omega$ is on $\partial\Omega$ where $\partial\Omega$ is the boundary surface of $\Omega$. If we define $S_\ell := \min_{x \in \partial\Omega} S(x) \neq 0$ then the system trajectories starting from the region $\mathbf{R}^n \backslash \Omega$ will insert inside the region $\Omega$ in a finite-time less than $T = V_0 / S_\ell$ , since $0 - V_0 = -\int_0^t S(x(s))ds \leq -S_\ell \cdot T$ with $V_0 = V(x(0))$. Define now the point $x^* := \arg\max_{x \in \partial\Omega} V(x)$ and the compact set $\Omega' := \{x \in \mathbf{R}^n | V(x) \leq V(x^*)\}$. It is straightforward that the state trajectories remain in $\Omega'$ for all $t \geq T$ (obviously it is $\Omega \subset \Omega'$, see Figure 2.1).

The stability analysis based on the concept of $\Omega^-$-passivity generalizes the results of [17, 18] on quasi-dissipative systems and constitutes an effective tool in this field.

## 2.2 System Model

Now, we are ready to proceed with the system model. In the model used, the multimachine power system is reduced into a network with generator nodes only. For the design of the excitation controller the classical third-order single-axis dynamic generator model is used whereas differential equations that represent dynamics with very short time constants have been neglected. In general, for a $n$-generator power system, the dynamic model of the $i$-th generator is

$$\dot{\delta}_i(t) = \omega_i(t) - \omega_0, \tag{1}$$

$$\dot{\omega}_i(t) = -\frac{D_i}{M_i}(\omega_i(t) - \omega_0) + \frac{\omega_0}{M_i}(P_{mi} - P_{ei}(t)), \tag{2}$$

$$\dot{E}'_{qi}(t) = \frac{1}{T'_{d0i}}(E_{fi}(t) - E_{qi}(t)), \tag{3}$$

where

$$E_{qi}(t) = E'_{qi}(t) + (x_{di} - x'_{di})I_{di}(t), \tag{4}$$

$$E_{fi}(t) = k_{ci}u_{fi}(t), \tag{5}$$

$$I_{qi}(t) = \sum_{j=1}^{n} E'_{qj}\Big(B_{ij}\sin\delta_{ij}(t) + G_{ij}\cos\delta_{ij}(t)\Big), \tag{6}$$

$$I_{di}(t) = \sum_{j=1}^{n} E'_{qj}\Big(G_{ij}\sin\delta_{ij}(t) - B_{ij}\cos\delta_{ij}(t)\Big), \tag{7}$$

$$P_{ei}(t) = E'_{qi}(t)I_{qi}(t), \tag{8}$$

$$Q_{ei}(t) = E'_{qi}(t)I_{di}(t), \tag{9}$$

$$E_{qi}(t) = x_{adi}I_{fi}(t), \tag{10}$$

$$V_{tqi}(t) = E'_{qi}(t) - x'_{di}I_{di}(t), \tag{11}$$

$$V_{tdi}(t) = x'_{di}I_{qi}(t), \tag{12}$$

$$V_{ti}(t) = \sqrt{V^2_{tqi}(t) + V^2_{tdi}(t)}. \tag{13}$$

Applying the backstepping technique used in [9, 10], the following state transformation for the $i$-th machine is obtained

$$\begin{bmatrix} z_{i1} \\ z_{i2} \\ z_{i3} \end{bmatrix} = \begin{bmatrix} 1 & 0 & 0 \\ c_{i1} & 1 & 0 \\ -\frac{M_i}{\omega_0}(1 + c_{i1}c_{i2}) & -\frac{M_i}{\omega_0}(c_{i1} + c_{i2} - \frac{D_i}{M_i}) & 1 \end{bmatrix} \begin{bmatrix} \Delta\delta_i \\ \Delta\omega_i \\ \Delta P_{ei} \end{bmatrix}, \tag{14}$$

where $c_{i1} > 0$ and $c_{i2} > 0$.

Defining for each machine the excitation control law $E_{fi} = k_{ci}u_{fi}$ with $k_{ci} = 1$ and

$$u_{fi}(t) = \frac{T'_{d0i}}{I_{qi}}(k_{i1}\Delta\omega_i + k_{i2}\Delta P_{mi} + v_i) \tag{15}$$

with gains given by

$$k_{i1} = \frac{M_i}{\omega_0}[c_{i1}c_{i2} + 1 - \frac{D_i}{M_i}(c_{i1} + c_{i2} - \frac{D_i}{M_i})],$$
$$k_{i2} = c_{i1} + c_{i2} - \frac{D_i}{M_i}, \tag{16}$$

the dynamics of each machine with respect to the new $z$ variables are given by

$$\begin{bmatrix} \dot{z}_{i1} \\ \dot{z}_{i2} \\ \dot{z}_{i3} \end{bmatrix} = \begin{bmatrix} -c_{i1} & 1 & 0 \\ -1 & -c_{i2} & -\frac{\omega_0}{M_i} \\ 0 & 0 & 0 \end{bmatrix} \begin{bmatrix} z_{i1} \\ z_{i2} \\ z_{i3} \end{bmatrix} + \begin{bmatrix} 0 \\ 0 \\ 1 \end{bmatrix} v_i - \begin{bmatrix} 0 \\ 0 \\ f_i \end{bmatrix}, \tag{17}$$

where

$$f_i(t) := \frac{1}{T'_{d0i}}\Big[E'_{qi}(t) + (x_{di} - x'_{di})I_{di}(t)\Big]I_{qi}(t) - E'_{qi}(t)\dot{I}_{qi}(t). \tag{18}$$

Thus, applying (14), the original system is transformed into (17), i.e. a system consisting of a linear part of the form $\dot{z}_i = A_i z_i + B_i v_i$ and a nonlinear term $f_i$ that affects the state equations wherein the input $v_i$ appears. As shown by (18), the nonlinear term cannot be reconstructed from the local $i$-th machines variables and therefore it can be considered as an unknown input function. Additionally, the unknown input $f_i(t)$ is considered to be bounded (this is always the case since the machine voltages and currents and their rates cannot take infinite values) , i.e.

$$|f_i(t)| \leq F_i < \infty. \tag{19}$$

If one considers the variable $z_{i3}$ as the output of the $i$-th subsystem, i.e.

$$y_i = Cz_i = \begin{bmatrix} 0 & 0 & 1 \end{bmatrix} \begin{bmatrix} z_{i1} \\ z_{i2} \\ z_{i3} \end{bmatrix} = z_{i3},$$

then it is obvious that the system is minimum phase i.e. it holds true that $z_{i1}, z_{i2} \to 0$ as $t \to \infty$ for $z_{i3} \equiv 0$. Moreover the system has relative degree one since the input appears directly in the first derivative of the output.

In the case where $f_i \equiv 0$, system (17) becomes a purely linear system and in accordance to [15] it can be feedback equivalent to a passive system, since it is minimum phase with relative degree one. However, since in this case relative degree one is equivalent to the nonsingularity of the system high frequency gain $CB$ and furthermore since $CB$ is positive definite then as it has been shown in [15] and [16] an output feedback $v_i = -k_i y_i + v_{fi}$ can be determined with large enough gain $k_i > 0$ that ensures passivity of the closed-loop system with new input $v_{fi}$ in accordance to Definition 2.2. In the case where $f_i \neq 0$ and since (19) holds true, we will prove in Section 4 that also for this case an output feedback

$$v_i = -k_i y_i + v_{fi} \tag{20}$$

can be determined with large enough gain $k_i > 0$ that ensures $\Omega^-$-passivity of the closed-loop system in accordance to Definition 2.3, where $v_{fi}$ in (20) is an external input.

## 3 The proposed control scheme

Incorporating the passivity-based controller (20) into the control scheme given by (15), the excitation input takes a rather simple mathematical form

$$E_{fi}(t) = \frac{T'_{d0i}}{I_{qi}}(K_{i1}\Delta\delta_i + K_{i2}\Delta\omega_i + K_{i3}\Delta P_{mi} + v_{fi}), \tag{21}$$

where the constant gains are now given by

$$\begin{aligned} K_{i1} &= \frac{M_i}{\omega_0} k_i (1 + c_{i1}c_{i2}), \\ K_{i2} &= \frac{M_i}{\omega_0}\left[\left(k_i - \frac{D_i}{M_i}\right)\left(c_{i1} + c_{i2} - \frac{D_i}{M_i}\right) + c_{i1}c_{i2} + 1\right], \\ K_{i3} &= c_{i1} + c_{i2} + k_i - \frac{D_i}{M_i}, \end{aligned} \tag{22}$$

and the $v_{fi}$ is an external input.

This control scheme requires only local measurements of $P_{ei}$, $\omega_i$, $\delta_i$ and of the current $I_{qi}$ that can be calculated from the measurements.

## 4 $\Omega^-$-passivity property of power systems

For the multimachine power system with the model of each machine described by the modified system (17), we consider the nonnegative candidate Lyapunov function

$$V_0 = \sum_{i=1}^{n} V_i \qquad \text{with} \qquad V_i = \frac{1}{2}\sum_{j=1}^{3} z_{ij}^2, \quad i = 1, 2, \ldots, n. \tag{23}$$

The time derivative of $V_i$ has the following form

$$\dot{V}_i = -c_{i1}z_{i1}^2 - c_{i2}z_{i2}^2 + z_{i3}\left[v_i(t) - f_i(t) - \frac{\omega_0}{M_i}z_{i2}\right]. \tag{24}$$

Then for the control law (21) we have

$$\dot{V}_i = -c_{i1}z_{i1}^2 - c_{i2}z_{i2}^2 - k_i z_{i3}^2 - \frac{\omega_0}{M_i}z_{i2}z_{i3} + z_{i3}(v_{fi} - f_i).$$

Using the inequality

$$F_i|z_{i3}| \le \rho_{fi}k_i z_{i3}^2 + \frac{F_i^2}{4\rho_{fi}k_i},$$

we arrive at

$$\dot{V}_i \le -c_{i1}z_{i1}^2 - \begin{bmatrix} z_{i2} & z_{i3} \end{bmatrix} \begin{bmatrix} c_{i2} & \frac{\omega_0}{2M_i} \\ \frac{\omega_0}{2M_i} & (1-\rho_{fi})k_i \end{bmatrix} \begin{bmatrix} z_{i2} \\ z_{i3} \end{bmatrix} + z_{i3}v_{fi} + \frac{F_i^2}{4\rho_{fi}k_i}$$

for arbitrary $\rho_{fi}:\ 0 < \rho_{fi} < 1$.

If the positive constants $c_{i2}, k_i$ are selected so that

$$P_i := \begin{bmatrix} c_{i2} & \frac{\omega_0}{2M_i} \\ \frac{\omega_0}{2M_i} & (1-\rho_{fi})k_i \end{bmatrix} > 0,$$

i.e. if

$$c_{i1} > 0\,, \qquad c_{i2}k_i > \frac{1}{1-\rho_{fi}}\left(\frac{\omega_0}{2M_i}\right)^2, \tag{25}$$

we result in

$$\dot{V}_i \le -c_{i1}z_{i1}^2 - \lambda_{\min}(P_i)z_{i2}^2 - \lambda_{\min}(P_i)z_{i3}^2 + z_{i3}v_{fi} + \frac{F_i^2}{4\rho_{fi}k_i}.$$

Defining $m_{fi} := \min\{c_{i1}, \lambda_{\min}(P_i)\}$, $i = 1, \cdots, n$ and $m_f := min_{1\le i\le n} m_{fi}$ , it is obvious that

$$\dot{V}_i \le -m_{fi}(z_{i1}^2 + z_{i2}^2 + z_{i3}^2) + z_{i3}v_{fi} + \frac{F_i^2}{4\rho_{fi}k_i}$$

or

$$\dot{V}_i \le -2m_{fi}V_i + z_{i3}v_{fi} + \frac{F_i^2}{4\rho_{fi}k_i}.$$

Let $m_f := min_{1\le i\le n} m_{fi}$, then for $V_0$ we have that

$$\dot{V}_0 \le -2m_f V_0 + \sum_{i=1}^{n}\left(z_{i3}v_{fi} + \frac{F_i^2}{4\rho_{fi}k_i}\right). \tag{26}$$

For every arbitrary parameter $\epsilon : 0 < \epsilon < 2$ and for $(z_{11}, z_{12}, z_{13}) \times \cdots \times (z_{n1}, z_{n2}, z_{n3}) \in \mathbf{R}^{3n}$ which do not belong to the compact set

$$\Omega_f := \left\{ (z_{11}, z_{12}, z_{13}) \times \cdots \times (z_{n1}, z_{n2}, z_{n3}) : \sum_{i=1}^{n} \sum_{j=1}^{3} z_{ij}^2 \leq \sum_{i=1}^{n} \frac{F_i^2}{2(2-\epsilon) m_f \rho_{fi} k_i} \right\} \quad (27)$$

it is immediately deduced that

$$\sum_{i=1}^{n} \frac{F_i^2}{4\rho_{fi} k_i} = (2-\epsilon) \sum_{i=1}^{n} \frac{m_f}{2} \frac{F_i^2}{2(2-\epsilon) m_f \rho_{fi} k_i} \leq (2-\epsilon) m_f \left( \frac{1}{2} \sum_{i=1}^{n} \sum_{j=1}^{3} z_{ij}^2 \right) = (2-\epsilon) m_f V_0.$$

Hence, (26) becomes

$$\dot{V}_0 \leq -\epsilon\, m_f V_0 + \sum_{i=1}^{n} z_{i3} v_{fi}.$$

Thus, in accordance to Proposition 2.2 we have proven that the closed-loop system is $\Omega_f^-$-passive with constant $c = \epsilon\, m_f$, input and output vectors $\begin{bmatrix} v_{f1} & v_{f2} & \cdots & v_{fn} \end{bmatrix}^T$ and $\begin{bmatrix} z_{13} & z_{23} & \cdots & z_{n3} \end{bmatrix}^T$, respectively. Hence, for the unforced system ($v_{fi} \equiv 0$, $i = 1, 2, \cdots, n$), the region $\Omega_f$ that defines the $\Omega_f^-$-passivity property is identical to the UUB region, i.e. $\Omega_f^-$-passivity guarantees UUB in the region $\Omega_f$. As can be easily seen from (27), as $\epsilon \to 0$ the region $\Omega_f$ decreases to its inferior limit. Also, as the feedback gain $k_i$ takes larger values for a given $F_i$ the region $\Omega_f$ becomes smaller. However, the unknown input $f_i$ may have large values; this consequently may imply a large region $\Omega_f$ around the origin in which the states of the system converge making the output feedback controller performance inefficient. To reduce $\Omega_f$, a high-gain controller is needed.

To avoid high-gain controls one can observe the following. The nonlinear term $f_i$ appears in the 3rd equation of (17) that provides the $z_{i3}$-dynamics, i.e.

$$\dot{z}_{i3} = -k_i z_{i3} + (v_{fi} - f_i). \quad (28)$$

From (28) and (27) one can see that the region $\Omega_f$ around the origin can be closer to the origin if $v_{fi}$ can effectively compensate $f_i$. In order to accommodate this requirement with a simple controller structure, we propose an adaptive fuzzy-logic controller for $v_{fi}$ as it is explained in the following.

## 5 Adaptive fuzzy-logic controller

A general fuzzy system includes four basic parts. A fuzzifier and a defuzzifier are the interface between the fuzzy system and the crisp system. The rule base is a database of IF THEN statements extracted from qualitative rules characterizing the operation of the system. For each rule, the inference engine maps the input fuzzy set to an output fuzzy set according to the relation defined by the rule. All four parts of a fuzzy logic system (FLS) can be mathematically formulated [19].

By choosing product inference and employing the centre of gravity method for defuzzification, the output of the fuzzy system is written as

$$y = \frac{\sum_{\ell=1}^{M} \theta_\ell \prod_{i=1}^{n} \mu_{F_i^\ell}(x_i)}{\sum_{\ell=1}^{M} \prod_{i=1}^{n} \mu_{F_i^\ell}(x_i)}, \quad (29)$$

where $M$ is the number of rules in the FLS, $n$ is the number of inputs to the FLS, $\theta_\ell$ is the center of gravity of the membership function corresponding to the $\ell$-th rule and $\mu_{F_i^\ell}$ is the membership function. Defining the fuzzy basis functions (FBF) $\phi_\ell(x)$ as

$$\phi_\ell(x) = \frac{\prod_{i=1}^{n} \mu_{F_i^\ell}(x_i)}{\sum_{\ell=1}^{M} \prod_{i=1}^{n} \mu_{F_i^\ell}(x_i)}, \tag{30}$$

then equation (29) can be expressed as $y = \sum_{\ell=1}^{M} \theta_\ell \phi_\ell(x) = \theta^T \Phi(x)$ where $\Phi(x) = \begin{bmatrix} \phi_1(x) & \cdots & \phi_\ell(x) & \cdots & \phi_M(x) \end{bmatrix}^T$ is the vector of FBFs and $\theta = \begin{bmatrix} \theta_1 & \cdots & \theta_\ell & \cdots & \theta_M \end{bmatrix}^T$ is the center of gravity vector.
The choice of control law (21) results in the $z_{i3}$-dynamics given by (28) where $v_{fi}$ is the output of a fuzzy logic controller.

*Rule base extraction:* From (28) one can immediately see that starting from $v_{fi} = f_i = 0$ then $z_{i3}$ approaches the origin where it remains. Now, in the case where $f_i$ takes a nonzero positive (negative) value and $v_{fi} = 0$, then $z_{i3}$ also takes a nonzero negative (positive) value, i.e. the value of $z_{i3}$ follows the value of $-f_i$. Therefore, in order to compensate the act of the unknown input $f_i$, so that $z_{i3}$ to approach the origin, a suitable $v_{fi}$ that follows $-z_{i3}$ can effectively compensate the action of $f_i$. This constitutes the basic qualitative principle for the rule base extraction of the fuzzy logic controller. Hence, a symmetrical fuzzy rule set can be implemented by a SISO fuzzy controller that needs only $z_{i3}$ as an input and $v_{fi}$ as an output, i.e. the linguistic rules can be of the simple form

$$\text{IF } z_{i3} \text{ is } F_i^\ell, \text{ THEN } v_{fi} \text{ is } G_i^\ell,$$

where $F_i^\ell$ and $G_i^\ell$ are suitable fuzzy sets selected in such a way that each of the input and output fuzzy variables assign linguistic values varying simultaneously from negative big to positive big values. Each linguistic value is associated with a normalized and symmetrical membership function.

The controller $v_{fi}$ can then be written in accordance to the FBF expansion as

$$v_{fi} = \frac{\sum_{\ell=1}^{M} \theta_\ell^i \mu_{F^\ell}(z_{i3})}{\sum_{\ell=1}^{M} \mu_{F^\ell}(z_{i3})} = \theta_i^T \Phi_i(z_{i3}), \tag{31}$$

where $\Phi_i(z_{i3}) = \begin{bmatrix} \phi_1^i(z_{i3}) & \cdots & \phi_\ell^i(z_{i3}) & \cdots & \phi_M^i(z_{i3}) \end{bmatrix}^T$ is the vector of FBFs and $\theta_i = \begin{bmatrix} \theta_1^i & \cdots & \theta_\ell^i & \cdots & \theta_M^i \end{bmatrix}^T$ the center of gravity vector. The membership functions are generally defined to be Gaussian of the form

$$\mu_F(x_i) = \exp\left[ -\left( \frac{x_i - a}{\sigma} \right)^2 \right],$$

where $x_i$ represents $z_{i3}$ or $v_{fi}$ and $a$ is the center and $s$ is the width of the fuzzy set "F". We note that the first and last membership functions are of the sigmoid form:

$$\mu_F(x_i) = \exp\left[ 1 + exp\left[ \pm \left( \frac{x_i - a}{\sigma} \right) \right] \right]^{-1}.$$

In accordance to the previous discussion, $v_{fi}$ is designed to compensate $f_i$. However, depending on the conditions under which excitation control acts (after faults or large

or small power disturbances), $f_i$ and consequently $v_{fi}$ may take values on a widely varying unknown range. Hence, in order to improve the performance of the fuzzy logic controller in such a way that the best possible approximation of $f_i$ to be achieved, an increased number of rules is needed. At this point, we note that a fuzzy system implementation with the smallest rule base is the concern of any efficient design. To this end, we effectively reduce the rule base by updating on-line the parameters of the FLS output. As a consequence, the minimum possible rule base involving only the following three rules is used:

$$\text{IF } z_{i3} \text{ is } N, \text{ THEN } v_{fi} \text{ is } P,$$

$$\text{IF } z_{i3} \text{ is } ZE, \text{ THEN } v_{fi} \text{ is } ZE,$$

$$\text{IF } z_{i3} \text{ is } P, \text{ THEN } v_{fi} \text{ is } N.$$

However, as it can be easily seen from (31), the FLS output parameters are determined through the centers of gravity $\theta_i$ of the membership functions, and therefore a suitable adaptation law is used to update on-line these parameters.
The adaptation law is chosen as

$$\dot{\theta}_i = \text{Proj}\{z_{i3}\Gamma_i\Phi_i(z_{i3})\} = z_{i3}\Gamma_i\Phi_i(z_{i3}) - \tau_i z_{i3}\frac{\theta_i\theta_i^T\Gamma i\Phi_i(z_{i3})}{\|\theta_i\|^2}, \tag{32}$$

where

$$\tau_i = \begin{cases} 0\,, & \text{if } \|\theta_i\| < M_\theta \text{ or } (\|\theta_i\| = M_\theta \text{ and } z_{i3}\theta_i^T\Gamma_i\Phi_i(z_{i3}) < 0) \\ 1\,, & \text{if } (\|\theta_i\| = M_\theta \text{ and } z_{i3}\theta_i^T\Gamma_i\Phi_i(z_{i3}) \geq 0) \end{cases} \tag{33}$$

and $\Gamma_i \in \mathbf{R}^{3\times 3}$ is a symmetric positive definite adaptation gain matrix.

This adaptation mechanism is a projection law which is commonly used in Lyapunov stability analysis.

## 6 Stability analysis

From the previous analysis, it is clear that without the FLS operation a particular region $\Omega_f$ is determined for a given $f_i$ and a reasonable gain $k_i$ ($i = 1, 2, \cdots, n$ ). Taking into account the FLS operation, let $\theta_i^*$ be defined so that $v_{fi}^* = \theta_i^{*T}\Phi_i(z_{i3})$ is the optimal approximation of $F_i$ [20], inside the compact subset $\Omega_f$ of $\mathbf{R}^{3n}$ (given by (27)) i.e.

$$\theta_i^* := \arg\min_{\theta_i}\left[\sup_{(z_{11},z_{12},z_{13})\times\cdots\times(z_{n1},z_{n2},z_{n3})\in\,\Omega_f} |f_i - \theta_i^T\Phi_i(z_{i3})|\right]. \tag{34}$$

Then there exists a $0 \leq \mu_i < 1$ such that

$$|f_i - \theta_i^{*T}\Phi_i(z_{i3})| \leq \mu_i F_i. \tag{35}$$

Let $\tilde{\theta}_i := \theta_i - \theta_i^*$, then from (31) it is

$$v_{fi} = \tilde{\theta}_i^T\Phi_i(z_{i3}) + \theta_i^{*T}\Phi_i(z_{i3}).$$

Choosing a Lyapunov function candidate as

$$V = V_0 + \frac{1}{2}\sum_{i=1}^{n}\tilde{\theta}_i^T\Gamma_i^{-1}\tilde{\theta}_i,$$

then for the control law (21), (31) we have

$$\dot{V} = -\sum_{i=1}^{n} c_{i1} z_{i1}^2 - \sum_{i=1}^{n} c_{i2} z_{i2}^2 - \sum_{i=1}^{n} k_i z_{i3}^2 - \sum_{i=1}^{n} \frac{\omega_0}{M_i} z_{i2} z_{i3} + \sum_{i=1}^{n} z_{i3}[f_i - \theta_i^{*T} \Phi_i(z_{i3})] - \sum_{i=1}^{n} \tilde{\theta}_i^T [z_{i3} \Phi_i(z_{i3}) - \Gamma_i^{-1} \dot{\theta}_i]$$

and

$$\dot{V} \leq -\sum_{i=1}^{n} c_{i1} z_{i1}^2 - \sum_{i=1}^{n} c_{i2} z_{i2}^2 - \sum_{i=1}^{n} k_i z_{i3}^2 - \sum_{i=1}^{n} \frac{\omega_0}{M_i} z_{i2} z_{i3} + \sum_{i=1}^{n} \mu_i F_i |z_{i3}| - \sum_{i=1}^{n} \tilde{\theta}_i^T [z_{i3} \Phi_i(z_{i3}) - \Gamma_i^{-1} \dot{\theta}_i]. \tag{36}$$

Now, one can see from the above inequality that (32), (33) is a reasonable choice of the update law since it cancels the last term in the right-hand side of (36) when $\|\theta_i\| \leq M_\theta$. Moreover, the boundedness of the parameter vectors $\theta_i$ is ensured from the projection law, in the sense that if $\theta_i(0) \in \Omega_\theta$ where $\Omega_\theta := \{\theta_i : \|\theta_i\| \leq M_\theta\}$ then $\theta_i(t) \in \Omega_\theta$, $\forall\, t \geq 0$ [21]. This means that the parameter errors $\tilde{\theta}_i$ are also bounded i.e.

$$\|\tilde{\theta}_i(t)\| \leq \varepsilon_\theta \ , \qquad \varepsilon_\theta = M_\theta + \max_{1 \leq i \leq n} \|\theta_i^*\|.$$

The basis functions are also bounded i.e. there exists a constant $\bar{\phi}_M$ such that

$$\|\Phi_i(z_{i3})\| \leq \bar{\phi}_M.$$

Due to the boundedness of the parameter errors $\tilde{\theta}_i$ we can proceed with the stability analysis by using the non-negative function $V_0$ instead of $V$. In this case its derivative is

$$\dot{V}_0 \leq -\sum_{i=1}^{n} c_{i1} z_{i1}^2 - \sum_{i=1}^{n} c_{i2} z_{i2}^2 - \sum_{i=1}^{n} k_i z_{i3}^2 - \sum_{i=1}^{n} \frac{\omega_0}{M_i} z_{i2} z_{i3} + \sum_{i=1}^{n} z_{i3}[f_i - \theta_i^T \Phi_i(z_{i3})]$$

and since it holds true that

$$z_{i3}[f_i - {\theta_i}^T \Phi_i(z_{i3})] \leq -\tilde{\theta}_i^T \Phi_i(z_{i3}) z_{i3} + \mu_i F_i |z_{i3}|,$$

we equivalently have

$$\dot{V}_0 \leq -\sum_{i=1}^{n} c_{i1} z_{i1}^2 - \sum_{i=1}^{n} c_{i2} z_{i2}^2 - \sum_{i=1}^{n} k_i z_{i3}^2 - \sum_{i=1}^{n} \frac{\omega_0}{M_i} z_{i2} z_{i3} + \sum_{i=1}^{n} |z_{i3}| \Big[ \|\tilde{\theta}_i\| \|\Phi_i(z_{i3})\| + \mu_i F_i \Big].$$

Using the inequality

$$(\varepsilon_\theta \bar{\phi}_M + \mu_i F_i)|z_{i3}| \leq \rho_{fi} k_i z_{i3}^2 + \frac{(\varepsilon_\theta \bar{\phi}_M + \mu_i F_i)^2}{4 \rho_{fi} k_i},$$

we arrive at

$$\dot{V}_0 \leq -2 m_f V_0 + \sum_{i=1}^{n} \frac{(\varepsilon_\theta \bar{\phi}_M + \mu_i F_i)^2}{4 \rho_{fi} k_i}. \tag{37}$$

Writing (37) as

$$\dot{V}_0 \leq -2m_f \left[ V_0 - \sum_{i=1}^{n} \frac{(\varepsilon_\theta \bar{\phi}_M + \mu_i F_i)^2}{8m_f \rho_{fi} k_i} \right]$$

and using the comparison principle, [22], we sequentially have

$$V_0(t) - \sum_{i=1}^{n} \frac{(\varepsilon_\theta \bar{\phi}_M + \mu_i F_i)^2}{8m_f \rho_{fi} k_i} \leq \left[ V_0(0) - \sum_{i=1}^{n} \frac{(\varepsilon_\theta \bar{\phi}_M + \mu_i F_i)^2}{8m_f \rho_{fi} k_i} \right] e^{-2m_f t},$$

$$V_0(t) \leq \sum_{i=1}^{n} \frac{(\varepsilon_\theta \bar{\phi}_M + \mu_i F_i)^2}{8m_f \rho_{fi} k_i} + V_0(0) e^{-2m_f t}. \tag{38}$$

From (38) one can see that for every $0 < \epsilon < 2$ there exists a $T = T(\epsilon) \geq 0$ such that

$$V_0(t) \leq \sum_{i=1}^{n} \frac{(\varepsilon_\theta \bar{\phi}_M + \mu_i F_i)^2}{4(2-\epsilon) m_f \rho_{fi} k_i} \qquad \forall\, t \geq T,$$

i.e. the state trajectories enter in finite-time in the compact set

$$\Omega_{fc} := \left\{ (z_{11}, z_{12}, z_{13}) \times \cdots \times (z_{n1}, z_{n2}, z_{n3}) : \sum_{i=1}^{n} \sum_{j=1}^{3} z_{ij}^2 \leq \sum_{i=1}^{n} \frac{(\varepsilon_\theta \bar{\phi}_M + \mu_i F_i)^2}{2(2-\epsilon) m_f \rho_{fi} k_i} \right\}, \tag{39}$$

wherein they remain thereafter. Thus, we have proven that the closed-loop system is UUB in the region $\Omega_{fc}$.

As the FLS output approaches the optimal i.e. as $\varepsilon_\theta \to 0$ and $\mu_i \ll 1$, the region $\Omega_{fc}$ is significantly reduced with respect to the initial region $\Omega_f$. We have therefore proven that as the FLS operates closer to its optimal, the error variables are UUB in a much smaller region.

## 7 Case study

A two-generator infinite bus power system is used to demonstrate the efficiency of the proposed controller. The power system is shown in Figure 7.1.
The system parameters are as follows:

| | | |
|---|---|---|
| $x_{T1} = 0.129$ p.u., | $x_{T2} = 0.11$ p.u., | $x_{12} = 0.55$ p.u., |
| $x_{13} = 0.53$ p.u., | $x_{23} = 0.6$ p.u., | $T'_{d01} = 6.9$ sec, |
| $x_{d1} = 1.863$ p.u., | $x'_{d1} = 0.257$ p.u., | $D_1 = 5.0$ p.u., |
| $M_1 = 8.0$ sec, | $M_2 = 10.2$ sec, | $D_2 = 3.0$ p.u., |
| $x_{d2} = 2.36$ p.u., | $x'_{d2} = 0.319$ p.u., | $T'_{d02} = 7.96$ sec, |
| $k_{c1} = 1.0$ p.u., | $k_{c2} = 1.0$ p.u.. | |

For a more accurate evaluation of the proposed controller, we take into account in the simulation the physical limits of the excitation voltage which are:

$$|k_{c1} u_{f1}| \leq 5.0\, p.u. \qquad |k_{c2} u_{f2}| \leq 5.0\, p.u.$$

A symmetrical three phase short circuit fault occurs on one of the two transmission lines

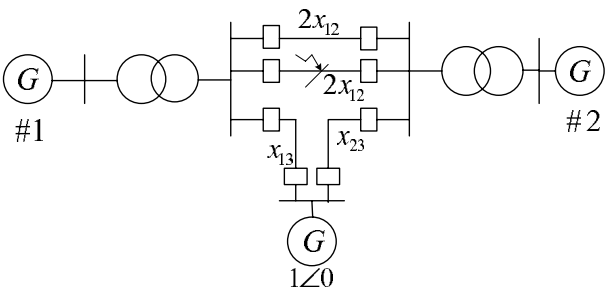


**Figure 7.1:** The two machine infinite bus test system.

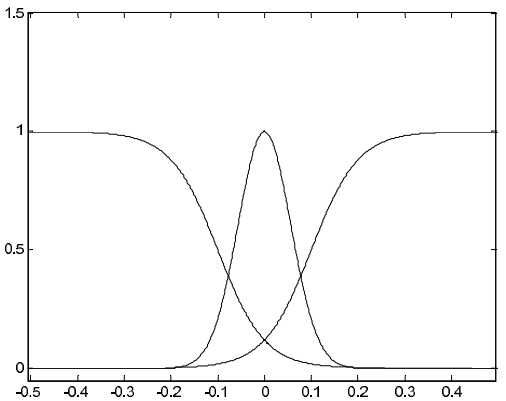


**Figure 7.2:** The input membership functions of FLS.

between Generator # 1 and Generator # 2 at $t = 20.1$ second. The fault is removed by opening the brakers of the faulted line at $t = 20.5$ second and the system is restored at $t = 21.5$ seconds. If we use $\lambda$ to represent the fraction of the fault, simulations are made for $\lambda = 0.6$ i.e. for a fault near the middle of the line and towards Generator # 2. The operating point considered in the simulation is:

$$\begin{aligned} &\delta_{10} = 40^o, \quad V_{t10} = 0.93, \quad P_{m10} = 0.95; \\ &\delta_{20} = 35^o, \quad V_{t20} = 0.937, \quad P_{m20} = 0.8. \end{aligned}$$

Most common used power system stabilizers are of fixed parameter lead-lag compensation type designed using linear control techniques. However, since power systems are extremely nonlinear and among the PSS tasks is to damp low frequency oscillations and to improve dynamic performance in a wide range of operating conditions, linear control schemes may be inefficient; this is clear especially in cases of large disturbances such as transmission line faults. Therefore, in order to better evaluate the performance of the proposed controller the case of a permanent serious fault is examined, since this can be considered as the worst case for the power system. The parameter *lambda* of the fault position is taken close to the center of the transmission line between generators #1 and #2, in order to create a balanced impact of the abnormal conditions on both the generators. Obviously, as $\lambda$ becomes smaller the impact is larger for generator #1 while the opposite occurs as $\lambda$ becomes larger.

Using the proposed method, the controllers parameters are selected as follows: As

shown by the state transformation (14) $c_{i1}$ and $c_{i2}$ determine the coupling of the states of the equivalent system. Hence, suitable positive values that determine a reasonable coupling must be used. In this case we select $c_{11} = c_{21} = 3$ , $c_{12} = c_{22} = 5$. For this parameter selection, the following gains $k_1 = k_2 = 100$ are selected that satisfy stability requirement (25) and avoid high-gain performance. Also the adaptation gains are $\Gamma_1 = \Gamma_2 = \text{diag}\{10, 40, 10\}$. Figure 7.2 shows the input membership functions used in FLS.

The response of the system is shown in Figures 7.3 – 7.6. One can clearly see that the system maintains stability after the fault. Additionally, the excitation control input of the proposed Passivity-based Adaptive Fuzzy (PAF) controller effectively penalizes the angle and speed deviations to relatively limited values. As clearly shown in Figures 7.3 and 7.4, a significantly improved dynamic performance of the angle and speed deviations is achieved by the proposed method compared to the performance obtained by a conventional simple linear PSS controller with form and parameters taken from [23]. Finally, the adaptation mechanism suitably adjusts the FLS center of gravity parameters.

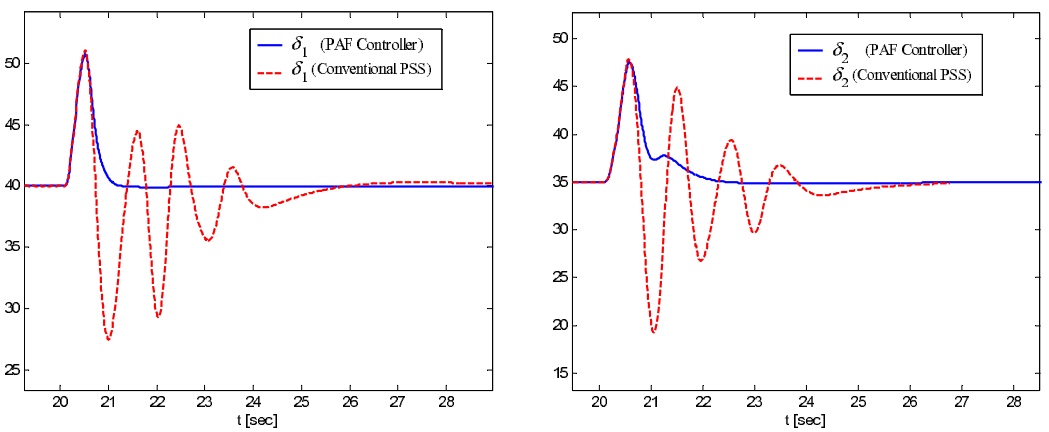


**Figure 7.3:** Power angle deviations for machines #1 and #2 (in deg).

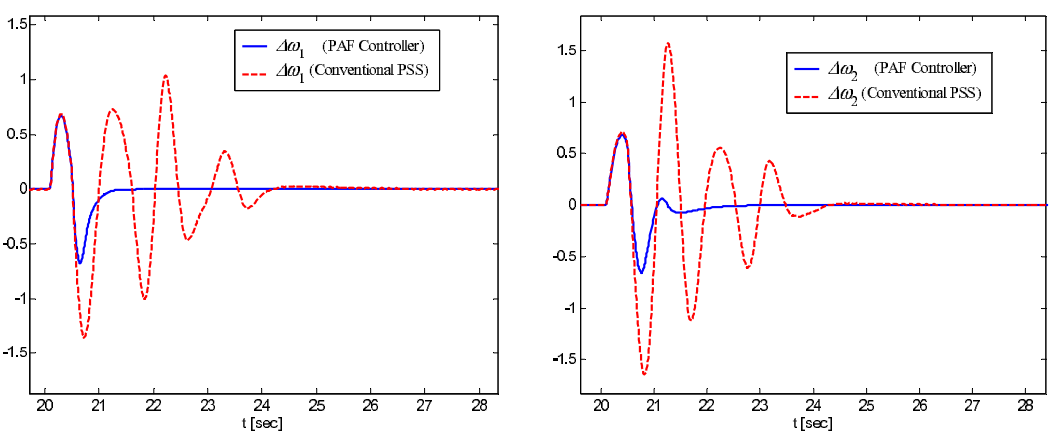


**Figure 7.4:** Speed deviations for machines #1 and #2 (in rad/sec) respectively.

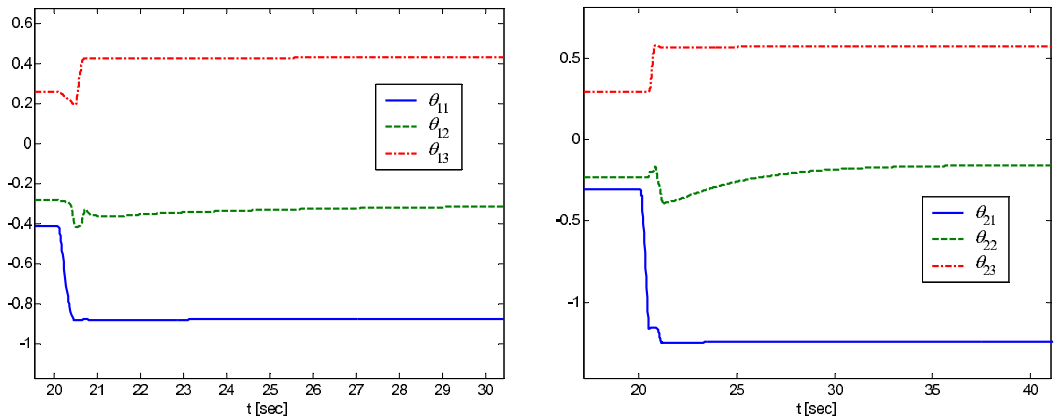


**Figure 7.5:** The centres of gravity for the FLS #1 and #2 respectively.

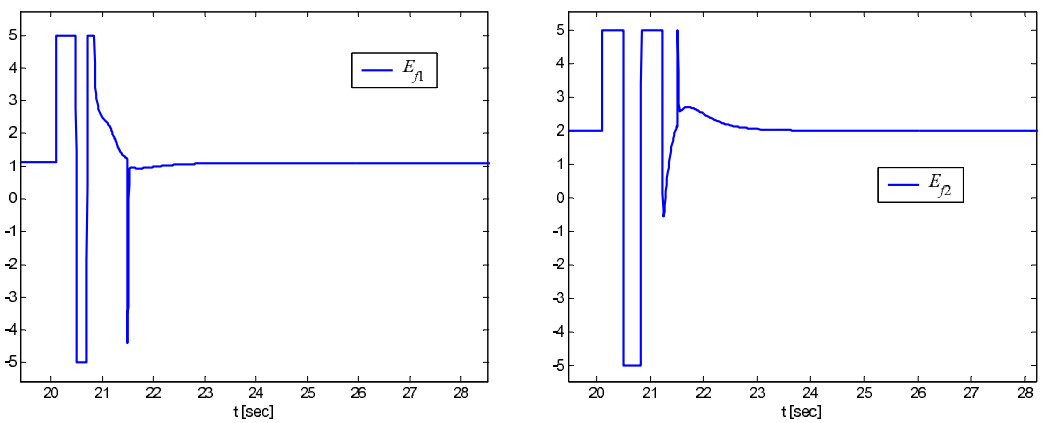


**Figure 7.6:** Excitation input for machines #1 and #2 respectively.

Comparing the proposed method with other similar advanced nonlinear control methods applied on power systems [9, 10, 13, 14] we can make the following remarks.

In [9, 10] the proposed adaptive scheme may result in high-gain controllers in order to obtain the bounds of the unknown nonlinearities included in $f_i$. In the present paper, we overcome this disadvantage by using a suitable FLS for the approximation of $f_i$ without increasing the complexity. In [13, 14] a self-learning model reference adaptive fuzzy algorithm is proposed to approximate the system model which is considered to be totally unknown. Therefore, a more complex algorithm is needed with a lot of fuzzy rules and a lot of parameters that must be estimated by adaptation techniques. In our case a simple SISO fuzzy logic controller with only three rules and adaptation loops is needed. This significantly reduces the on-line computational effort. A disadvantage is the requirement of an extra state measurement which however contributes to a better system performance.

## 8 Conclusions

An intelligent-based simple nonlinear passive control suitable for power system applications is proposed. Stability analysis and simulation tests verify the effectiveness in a variety of operating conditions resulting from large unknown disturbances such as short-circuit faults.

## 9 Notation

| | |
|---|---|
| $\delta_i(t)$ | : power angle, in radian; |
| $\omega_i(t)$ | : rotor speed, in rad/sec; |
| $\omega_0$ | : synchronous machine speed, in rad/sec; |
| $P_{mi}$ | : mechanical input power, in p.u; |
| $P_{ei}(t)$ | : active electrical power, in p.u.; |
| $D_i$ | : damping constant, in p.u.; |
| $M_i$ | : inertia coefficient, in seconds; |
| $E'_{qi}(t)$ | : transient EMF in the q-axis in p.u.; |
| $E_{qi}(t)$ | : EMF in the q-axis, in p.u.; |
| $E_{fi}(t)$ | : equivalent EMF in excitation coil, in p.u.; |
| $T'_{d0i}$ | : d-axis transient short circuit time constant, in sec; |
| $I_{fi}(t)$ | : excitation current, in p.u.; |
| $I_{qi}(t)$ | : q-axis current, in p.u.; |
| $I_{di}(t)$ | : d-axis current, in p.u.; |
| $Q_{ei}(t)$ | : reactive electrical power, in p.u.; |
| $V_{ti}(t)$ | : generator terminal voltage, in p.u.; |
| $k_{ci}$ | : gain of generator excitation amplifier, in p.u.; |
| $u_{fi}(t)$ | : input of the SCR amplifier, in p.u.; |
| $x'_{di}$ | : d-axis transient reactance, in p.u.; |
| $x_{di}$ | : d-axis reactance, in p.u.; |
| $x_{adi}$ | : mutual reactance between the excitation coil and the stator coil, in p.u.; |
| $Y_{ij} = G_{ij} + jB_{ij}$ | : the $i$-th row and $j$-th column element of nodal admittance matrix, in p.u.; |
| $\Delta\delta_i(t) = \delta_i(t) - \delta_{i0}$ | : nominal angle deviation, in deg; |
| $\Delta\omega_i(t) = \omega_i(t) - \omega_0$ | : nominal speed deviation, in rad/sec; |
| $\Delta P_{ei}(t) = P_{ei}(t) - P_{mi}$ $:= -\Delta P_{mi}$ | : where $\Delta P_{mi}$ the accelerating power, in p.u. |
| $\mathbf{R}^n \backslash \Omega$ | : $\mathbf{R}^n$except a region defined by the compact set $\Omega \subset \mathbf{R}^n$ containing the origin. |

## References

[1] Chapman, J., Ilic, M., King, C., Eng, L. and Kaufman, H. Stabilizing a multimachine power system via decentralized feedback linearizing excitation control. *IEEE Trans. Power Syst.* **8** (1993) 830–839.

[2] Pourboghrat, F., Farid, F., Hatziadoniu, C.J., Daneshdoost, M., Mehdian, F. and Lotfalian, M. Local sliding control for damping interarea power oscillations. *IEEE Trans. Power Syst.* **19** (2004) 1123–1134.

[3] Psillakis, H.E. and Alexandridis, A.T. Adaptive gain sliding mode control for multimachine power systems. *IFAC World Congress 05*, no. 3812. Prague, July 2005.

[4] Wang, Y., Guo, G. and Hill, D. Robust decentralized nonlinear controller design for multimachine power systems. *Automatica* **33**9 (1997) 1725–1733.

[5] Wang, Y., Hill, D. and Guo, G. Robust decentralized control for multimachine power systems. *IEEE Trans. Circ. & Syst.-I: Fund. Th. Appl.* **45** (1998) 271–279.

[6] Lu, Q., Mei, S., Hu, W., Wu, F.F., Ni, Y. and Shen, T. Nonlinear decentralized disturbance attenuation excitation control via new recursive design for multi-machine power systems. *IEEE Trans. Power Systems* **16**(4) (2001) 729–736.

[7] Wang, Y., Cheng, D., Li, C. and Ge, Y. Dissipative Hamiltonian realization and energy-based $L_2$-disturbance attenuation control of multimachine power systems. *IEEE Trans. Automat. Contr.* **48**(8) (2003) 1428–1433.

[8] Xi, Z. Adaptive stabilization of generalized Hamiltonian systems with dissipation and its application to power systems. *Int. J. of Syst. Sci.* **33** (2002) 839–846.

[9] Psillakis, H.E. and Alexandridis, A.T. A new excitation control for multimachine power systems. I: Decentralized nonlinear adaptive control design and stability analysis. *Int. J. Contr. Aut. Syst.* **3**(2) (2005) 278–287.

[10] Psillakis, H.E. and Alexandridis, A.T. A new excitation control for multimachine power systems. II: Robustness and disturbance attenuation analysis. *Int. J. Contr. Aut. Syst.* **3**(2) (2005) 288–295.

[11] Liu, W., Venayagamoorthy, G. K. and Wunsch, D. C. II. Design of an adaptive neural network based power system stabilizer. *Neural Netw.* **16** (2003) 891–898.

[12] El-Metwally, K. A. and Malik, O. P. Fuzzy logic power system stabilizer. *IEE Proc. on Gen. Transm. & Distr.* **142**(3) (1995) 277–281.

[13] Hosseinzadeh, N.and Kalam, A. A direct adaptive fuzzy power system stabilizer. *IEEE Trans. Energy Conv.* **14**(4) (1999) 1564–1571.

[14] Elshafei, A., El-Metwally, K. and Shaltout, A. A variable-structure adaptive fuzzy-logic stabilizer for single and multi-machine power systems. *Contr. Eng. Pract.* **13** (4) (2005) 413–423.

[15] Byrnes, C. I., Isidori, A. and Willems, J. Passivity, feedback equivalence, and the global stabilization of minimum phase nonlinear systems. *IEEE Trans. Automat. Contr.* **36**(11) (1991) 1228–1240.

[16] Huang, C. H., Ioannou, P.A., Maroulas, J. and Safonov, M.G. Design of strictly positive real systems using constant output feedback. *IEEE Trans. Automat. Contr.* **44**(3) (1999) 569–573.

[17] Polushin, I.G. Stability results for quasi-dissipative systems. *ECC95*, Rome, 1995.

[18] Polushin, I.G. and Marquez, H.J. Boundedness properties of nonlinear quasi-dissipative systems. *IEEE Trans. Aut. Contr.* **49**(12) (2004) 2257–2261.

[19] Wang, L. X. *A course in fuzzy systems and control*. Prentice Hall PTR, Upper Saddle River: NJ, 1997.

[20] Wang, L.X.and Mendel, J.M. Fuzzy basis functions, universal approximation, and orthogonal least squares learning. *IEEE Trans. Neural Networks* **3**(5) (1992) 807–814.

[21] Ioannou, P.A. and Sun, J. *Robust Adaptive Control*. Upper Saddle River, NJ: Prentice-Hall, 1996.

[22] Lakshmikantham, V. and Leela, S. *Differential and Integral Inequalities*. New York, NY: Academic, 1969.

[23] Cong, L., Wang, Y. and Hill, D.J. Transient stability and voltage regulation enhancement via coordinated control of generator excitation and SVC. *Electr. Pow. & Ener. Syst.* **27** (2005) 121–130.

Nonlinear Dynamics and Systems Theory, **7** (1) (2007) 69–83

# Performance Analysis of Communication Networks Based on Conditional Value-at-Risk

Jun Wu[1], Wuyi Yue[2] and Shouyang Wang[1]

[1] *School of Economics and Management, Beijing University of Posts and Telecommunications, Beijing 100876, China*
[2] *Department of Information Science and Systems Engineering, Konan University, 8-9-1 Okamoto, Kobe 658-8501 Japan*

Received: August 25, 2005; Revised: October 21, 2006

**Abstract:** In this paper, we present an analysis of optimization and risk calculation in Communication Networks (CNs). The model is proposed for offline traffic engineering optimization with bandwidth allocation and performance analysis. First, we introduce an optimization model in the CN and derive the optimal bandwidth capacity. Then, we analyze the profit shortfall risk in the CN by using a conditional value-at-risk approach for two typical arrival processes of traffic demand: Poisson arrival process and uniform distribution arrival process. Finally, we give numerical results to show the impact of risk averseness and compare how the characteristics of these two arrival processes of traffic demand affect the network performance.

**Keywords:** *Communication networks; performance analysis; stochastic traffic engineering; conditional value-at-risk; optimization.*

**Mathematics Subject Classification (2000):** 46N99, 90B15, 90B18.

## 1 Introduction

As we have presented in [1], traffic engineering in Communication Networks (CNs) is a process of controlling traffic demand in a network so as to optimize resource utilization and network performance [2], [3]. There are two forms of traffic engineering: online planning and offline planning. Online traffic engineering focuses on instantaneous network states and individual connections. Offline traffic engineering simultaneously examines each channel's resource constraints and studies what is needed of each Local Service Provider (LSP) in order to provide global calculations and solutions for the CNs by a centralized view. Traffic engineering has greatly improved network utilization and performance by using advanced technologies such as Multi-Protocol Label Switching (MPLS) and Optical Channel Trails (OCT) [4], [5].

 

Previously, the offline traffic engineering optimization problem was formulated as a deterministic Multi-Commodity Flow (MCF) model with the objective to optimize the network total revenue derived from transmitting traffic demand. In the deterministic MCF model, the demand of each channel was assumed to be a fixed quantity and the network revenue was a linearly increasing function of the amount of bandwidth allocated to the network [6]-[8]. This approach may be improper when dealing with the case that the input for off-line optimization was assumed to be stochastic demand. In view of this, recently, Mitra and Wang developed a stochastic traffic engineering framework and proposed new approaches for risk analysis in communication networks.

An important aspect of Mitra and Wang's model is the formulation of the demand and revenue under a two-tier market structure: one is the wholesale market, the other is the retail market. In the wholesale market, the demand is assumed to be deterministic and there is no risk in revenue. In the retail market, the demand is random and there exists the risk of revenue shortfall. The objective includes both the maximization of the mean revenue and the acceptable risk level [8]-[10].

Based on the two-tier market structure for demand and revenue, Mitra and Wang also analyzed the impacts of demand variability on various aspects of traffic engineering design in their numerical studies. They observed significant changes in shadow costs, link utilization, bandwidth provisioning and routing with demand variability, and explained their causes and implications [8].

In [9], Mitra and Wang developed an optimization model to support bandwidth management decision-making based on the mean-risk framework. They discussed the selection of risk indices and proposed the use of standard deviation of total profit. They investigated the service provider's risk averseness on various aspects of bandwidth management. They also discussed profit improvement brought about by the presence of the wholesale market under various market and network conditions [9].

In [10], Mitra and Wang furthered their studies in [8] and [9] and developed the efficient frontier of mean revenue and revenue risk. They discussed three different risk indices including variance, Tail value-at-risk, and standard deviation. They obtained conditions under which the optimization problem was an instance of convex programming and therefore efficiently solvable. They also studied the properties of the solution for the special case of Gaussian distributions of demands. They also analyzed the impact of demand uncertainty on various aspects of traffic engineering, such as link utilization, bandwidth provisioning and total revenue [10].

Based on the analysis framework presented in [8]-[10], Wu, Yue and Wang proposed a stochastic model for macro-level bandwidth management from the viewpoint that emphasizing the randomness and risk averseness and their impacts on the network's performance. First, they treated the whole network as an integrated service provider and did not consider the routing and capacity sharing within the communication network. They also removed the wholesale market with deterministic demand and only focused on the random demand in the retail market, which was also mentioned in [8]. Second, they emphasized the stochastic properties of the demand and the impact of risk averseness on the system performance, such as bandwidth capacity and profit function. Finally, they presented a loss rate constraint to guarantee the network performance.

In their model, the communication network was regarded as a service provider, who can charge revenue from transmitting demand and pay for the cost for bandwidth allocation. Since the profit function obtained by transmitting traffic load was a random variable and thus had the risk of deviation from the desired expected profit. They char-

acterized the risk by use of the variance of the profit function. In [1], Wu, Yue and Wang proposed a stochastic model for optimizing bandwidth allocation with a loss rate constraint. They analyzed the loss rate constraint and risk averseness in the CN optimization model and showed the impact of loss rate constraint and risk averseness on the network performance. Wu, Yue and Wang also introduced a penalty cost based on the model presented in [1] to guarantee the network performance. They analyzed penalty cost and risk averseness in the CN optimization model and showed the impact of penalty cost and risk averseness on the network performance [11].

In regard to the selection of risk index, Mitra and Wang had proposed several approaches including variance, standard deviation and Tail value-at-risk [8]-[10]. However, they also mentioned that they did not use Tail value-at-risk in their analysis because of the optimization computational difficulties [10]. In [1] and [11], the risk index was defined as the deviation from the expected profit and measured by variance of the profit function, which included the upside risk and downside risk.

In this paper, we define the risk to be the downside risk of the profit shortfall and use an equivalent definition of a risk analysis tool named conditional value-at-risk, which is similar to Tail value-at-risk. There are two advantages of using this approach: first, it can avoid the computational difficulties mentioned in [10] and thus obtain an explicit solution for this problem; second, it can avoid the disadvantage of equally penalizing the desirable upside and the undesirable downside outcomes that is inherent in the mean-variance approach.

In this paper, we first describe the basic model proposed in [1] and derive the optimal bandwidth capacity without risk. Then, we analyze the system performance and derive the optimal bandwidth capacity by using CVaR approach and show the impact of risk on the network performance by the analysis. We also compare the characteristics of network performance by using CVaR approach presented in this paper with the characteristics of network performance presented in [1], where the mean-variance approach was used. Finally, numerical results are given to show the impact of risk on network performance.

The rest of this paper is organized as follows. In Section 2, we present the system model, notations and preliminaries. In Section 3, we present the optimization model and derive the optimal bandwidth capacity. In Section 4, we analyze the network profit shortfall risk by using the CVaR approach and also derive the optimal bandwidth capacity for two typical arrival processes of traffic demand: Poisson arrival process and uniform distribution arrival process. In Section 5, we give some numerical results to show the impact of risk averseness on the network performance. Conclusions are given in Section 6.

## 2 System Model

A Communication Network (CN) is formulated as a collection of nodes and links that should derive its revenue by delivering traffic load to and from its users. A unit cost is charged for unit bandwidth capacity allocated to the network. The objective of this system is to maximize the expected profit of the whole network. To guarantee the optimal network performance, we present performance analyses for the loss rate constraint and the risk of profit shortfall where the model presented in this paper is the same as the one presented in [1].

Similar to the description in [8], let $(N, L)$ denote a CN composed of nodes $n_i$ ($n_i \in N,\ 1 \leq i \leq N$) and links $l$ ($l \in L$), where $N$ is the total number of nodes and $L$ is the

total number of links in the network. Let $V$ denote the set of all node pairs, and $n \in V$ denote an arbitrary node pair where $n = (n_i, n_j)$ and $n_i, n_j \in N$. Let $C_l$ denote the maximal bandwidth capacity of link $l$, $R(n)$ denote an admissible route set for $n \in V$, $\xi_s$ ($s \in R(n)$) denote the amount of capacity provided on route $s$, $D_n$ ($n \in V$) denote the traffic load on an arbitrary node pair $n \in V$, and $b_n$ ($n \in V$) denote the amount of bandwidth capacity provided to an arbitrary node pair $n$. Since between two node pairs $n_i$ and $n_j$, there may be more than one route to be routed, then $b_n = \sum_{s \in R(n)} \xi_s$.

In this paper, we consider the CN to be a whole system. We let $b$ denote the amount of bandwidth capacity provided to the CN, then we have $b = \sum_{n \in V} b_n$. If we let $D$ denote the traffic demand in the CN, then we have $D = \sum_{n \in V} D_n$, which is characterized by a random distribution with its probability density function $f(x)$ and cumulative distribution function $F(x)$. $b \wedge D$ is the actual traffic load transmitted in the CN, where " $\wedge$ " represents the choice of the smaller value between $b$ and $D$. Let $r$ denote the unit revenue by serving the traffic demand, so the total revenue of the CN is $r \times (b \wedge D)$. Let $c$ denote the unit cost for unit bandwidth capacity allocated in the CN, so the total cost is $c \times b$.

To avoid unrealistic and trivial cases, we make the following assumptions:

**(1)** Probability density function of the random traffic load is $f(x) \geq 0$.

**(2)** Cumulative distribution function of the random traffic load is $F(x)$ and $F(x)$ is strictly increasing in $x$.

**(3)** Traffic demand $D$ in the CN is assumed to be positive, i.e., $D > 0$.

**(4)** Total bandwidth capacity $b$ provided to the CN is assumed to be positive, i.e., $b > 0$.

**(5)** Maximal capacity $C_{max}$ that can be allocated to the CN is assumed to be positive, i.e., $C_{max} > 0$.

**(6)** System parameters are as follows: unit revenue $r$ and unit cost $c$ satisfy $r > c > 0$.

## 3 Optimal Bandwidth Capacity without Risk

In this section, we present the model for the network bandwidth allocation problem and derive the optimal bandwidth capacity that can be attained without incurring any risk (see [1]).

Let $\pi(b, D)$ denote the random profit function by transmitting messages in the network, namely,

$$\pi(b, D) = r(b \wedge D) - cb. \tag{1}$$

Let $\Pi(b, D)$ denote the mean profit function as follows:

$$\Pi(b, D) \quad = \quad E[\pi(b, D)] = r \int_0^b x f(x) dx + rb \int_b^{+\infty} f(x) dx - cb. \tag{2}$$

By using the method of integral by parts, Eq. (2) can be obtained as follows:

$$E\left[\pi(b, D)\right] = (r - c)b - r \int_0^b F(x) dx. \tag{3}$$

The objective function of the system is given by

$$\Pi^* = \max_{b>0}\{\Pi(b, D)\}, \tag{4}$$

subject to

$$P(b \geq \alpha D) \geq \beta \tag{5}$$

and

$$b \leq C_{max}, \tag{6}$$

where $\Pi^*$ is the optimal profit function.

Eq. (5) is the loss rate constraint proposed in [1] adopted from [12]. In the loss rate constraint, $\alpha$ $(0 \leq \alpha \leq 1)$ is the percentage of satisfied users and $1-\alpha$ is the loss rate. As $\alpha$ increases, the loss rate $1-\alpha$ deceases. The higher $\alpha$ is, the better the network performance is. $\beta$ $(0 \leq \beta \leq 1)$ is the confidence level, which represents the probability of $b \geq \alpha D$. As $1-\beta$ decreases, the confidence level $\beta$ increases. A higher confidence level $\beta$ guarantees a higher probability of achieving a better network performance. The loss rate constraint enables us to control the network performance by properly setting the system parameters.

With the above assumptions, we can derive the optimal bandwidth capacity that should be allocated to the CN. First, we analyze the property of the mean profit function $\Pi(b, D)$ without any constraints.

The first order derivative of $\Pi(b, D)$ of Eq. (2) with respect to $b$ is given as follows:

$$\frac{d\Pi(b, D)}{db} = (r-c) - rF(b). \tag{7}$$

The second order derivative of $\Pi(b, D)$ presented in Eq. (2) with respect to $b$ is given as follows:

$$\frac{d^2\Pi(b, D)}{db^2} = -rf(b). \tag{8}$$

From the assumptions in Section 2, we know that $f(b) \geq 0$ and $r > 0$, hence,

$$\frac{d^2\Pi(b, D)}{db^2} \leq 0. \tag{9}$$

Therefore, we can say that $\Pi(b, D)$ is a concave function of $b$. So, the optimal bandwidth capacity that should be allocated to the CN is given by

$$F^{-1}\left(\frac{r-c}{r}\right), \tag{10}$$

where $F^{-1}(\cdot)$ is the inverse function of $F(\cdot)$.

Next, we analyze the loss rate constraint. Note that the loss rate constraint is equivalent to

$$P\left(b \geq \alpha D\right) = P\left(D \leq \frac{b}{\alpha}\right) \geq \beta. \tag{11}$$

By the definition of cumulative distribution function $F(x)$, Eq. (11) becomes

$$P\left(D \leq \frac{b}{\alpha}\right) = \int_0^{\frac{b}{\alpha}} f(x)dx = F\left(\frac{b}{\alpha}\right) \geq \beta. \tag{12}$$

So the loss rate constraint is equivalent to

$$b \in \left[\alpha F^{-1}(\beta), +\infty\right). \tag{13}$$

Thus, the optimal bandwidth capacity $b^*$ for the CN bandwidth allocation with loss rate constraint is given as follows:

$$b^* = F^{-1}\left(\frac{r-c}{r}\right) \vee \alpha F^{-1}(\beta), \tag{14}$$

where "$\vee$" represents the choice of the larger value between $F^{-1}\left(\frac{r-c}{r}\right)$ and $\alpha F^{-1}(\beta)$.

Finally, if we consider the maximal capacity constraint, then the optimal bandwidth capacity for the network is given as follows:

$$b^* \wedge C_{max}, \tag{15}$$

where "$\wedge$" represents the choice of the smaller value between $b^*$ and $C_{max}$.

## 4 Risk Analysis in Communication Networks

The term risk plays an important role in the literature on economic, financial and technological issues. There are various attempts to define and to characterize the risk for descriptive as well as prescriptive purpose. In general, we regard risk as random profit or loss of a position. It can be positive (gains) as well as negative (losses) [13].

In the presence of demand uncertainty, maximizing only the mean revenue in the network, which is implied in the earlier deterministic models, may be incomplete for the random demand case. Mitra and Wang had proposed a broader optimization objectives in financial area to address the issue of risk averseness. In this paper, we use CVaR as the risk measurement which is adopted from financial risk management. In the following, we give a brief introduction on risk management.

The mean-variance analysis, which was first introduced by Markowitz [14], has been a standard tool in risk management. It involves a systematic tradeoff between the mean and the variance [15]. Value-at-Risk (VaR), introduced in 1994, has been extensively used for measuring risk and has become a part of the financial regulations in the world [16]. It allows a manager to specify a confidence level (a certain level of probability) for attaining a certain level of the wealth. Recently, Rockafellar and Uryasev presented an alternative measure of risk with the CVaR approach [17]. It measures the average value of the profit below the $\gamma$-quantile ($0.0 < \gamma < 1.0$) level. Some empirical evidence proposed by [18] showed that the CVaR approach had superior computational characteristics when it is compared with the VaR approach and the mean-variance approach.

In [8]-[10], Mitra and Wang had proposed several approaches including variance, standard deviation and Tail value-at-risk. However, they also mentioned that they did not use Tail value-at-risk in their analysis because of the optimization computationally difficult [10]. In [1] and [11], the risk index was measured by the variance of the profit

function. In this paper, we use CVaR as the risk analysis tool, which can transform the original problem into a two step optimization problem.

By using CVaR approach as the risk index, we have the objective function given as follows [19]:

$$\max_{b>0} C_\gamma \left\{\pi(b,D)\right\}, \tag{16}$$

where

$$C_\gamma \left\{\pi(b,D)\right\} = \max_{v\in R}\left\{v + \frac{1}{\gamma}E\left[(\pi(b,D)-v)^-\right]\right\}, \tag{17}$$

where $(\cdot)^{-1}$ is the negative part of $(\cdot)$, $\pi(b,D)$ is the random profit function given by Eq. (1), $v$ belongs to the real number set $R$ and $\gamma$ is a risk parameter.

Then, the objective function using the CVaR approach can be obtained as follows:

$$\max_{b>0}\left\{\max_{v\in R}\left\{v + \frac{1}{\gamma}E\left[(\pi(b,D)-v)^-\right]\right\}\right\}. \tag{18}$$

We define a jointly concave function as follows:

$$g(v,b) = \left\{v + \frac{1}{\gamma}E\left[(\pi(b,D)-v)^-\right]\right\}. \tag{19}$$

By using the definition of expectation, we can get that

$$g(v,b) \quad = \quad v + \frac{1}{\gamma}\left\{\int_0^b (rx-cb-v)^- dF(x) + \int_b^\infty (rb-cb-v)^- dF(x)\right\}, \tag{20}$$

where $r$, $c$ and $b$ are defined in Section 2.

According to the objective function given by Eq. (18), we know that to find the optimal bandwidth capacity $b^*$ is equivalent to a two-step optimization. The first step is to maximize $g(v,b)$ with $v \in R$ as follows:

$$\max_{v\in R}\left\{g(v,b)\right\}. \tag{21}$$

The second step is to maximize $\max_{v\in R}\{g(v,b)\}$ with $b>0$ as follows:

$$\max_{b>0}\left\{\max_{v\in R}\left\{g(v,b)\right\}\right\}. \tag{22}$$

With respect to the first-step optimization, we illustrate four cases to derive the optimal solution $v^*$.

(1) For $v < -cb$:

In this case, $(rx-cb-v)^- = 0$ and $(rb-cb-v)^- = 0$. Both the two terms in large parenthesis of Eq. (20) vanish. Consequently, $g(v,b) = v$, thus $\dfrac{\partial g(v,b)}{\partial v} = 1 > 0$.

(2) For $-cb < v < rb-cb$:

In this case, $(rb-cb-v)^- = 0$. The second term in large parenthesis of Eq. (20) vanishes while the first term in large parenthesis of Eq. (20) remains, consequently,

$$g(v,b) = v + \frac{1}{\gamma}\int_0^b (rx-cb-v)dF(x). \tag{23}$$

Since $rx - cb - v < 0$, we have

$$x < \frac{v + cb}{r}. \tag{24}$$

So, Eq. (23) becomes as follows:

$$g(v, b) = v + \frac{1}{\gamma} \int_0^{\frac{v+cb}{r}} (rx - cb - v) dF(x). \tag{25}$$

Thus,

$$\begin{aligned} \frac{\partial g(v,b)}{\partial v} &= 1 + \frac{1}{\gamma} \int_0^{\frac{v+cb}{r}} (-1) dF(x) + \frac{1}{\gamma} \cdot \frac{1}{r} \left[ (rx - cb - v) f(x) \right] |_{x=0}^{x=\frac{v+cb}{r}} \\ &= 1 - \frac{1}{\gamma} F(\frac{v + cb}{r}) + \frac{1}{\gamma} \cdot \frac{1}{r} (0 - 0) \\ &= 1 - \frac{1}{\gamma} F(\frac{v + cb}{r}). \end{aligned} \tag{26}$$

(3) For $rb - cb < v$:

In this case, both the two terms in large parenthesis of Eq. (20) remain, consequently,

$$g(v, b) = v + \frac{1}{\gamma} \left\{ \int_0^b (rx - cb - v) dF(x) + \int_b^\infty (rb - cb - v) dF(x) \right\}. \tag{27}$$

Thus,

$$\begin{aligned} \frac{\partial g(v,b)}{\partial v} &= 1 + \frac{1}{\gamma} \int_0^b (-1) dF(x) + \frac{1}{\gamma} \int_b^\infty (-1) dF(x) \\ &= 1 - \frac{1}{\gamma} < 0. \end{aligned} \tag{28}$$

(4) Let us consider about what happened when $v$ approaches $-cb$ from the right, and also when $v$ approaches $rb - cb$ from the left as follows:

Let $v = -cb + \Delta$ for a sufficiently small positive number $\Delta$ ($\Delta > 0$), then

$$\begin{aligned} \frac{\partial g(v,b)}{\partial v} &= 1 - \frac{1}{\gamma} F\left(\frac{\Delta}{r}\right) \\ &= 1 - \frac{1}{\gamma} \int_0^{\frac{\Delta}{r}} f(x) dx > 0. \end{aligned} \tag{29}$$

In the same way, for $v = rb - cb - \Delta$,

$$\frac{\partial g(v,b)}{\partial v} = 1 - \frac{1}{\gamma} F\left(b - \frac{\Delta}{r}\right). \tag{30}$$

We cannot say whether Eq. (30) is negative or not for a sufficiently small positive number $\Delta$. But the sufficient condition for Eq. (30) is negative to be given by

$$b > F^{-1}(\gamma). \tag{31}$$

Note that $b$ is an unknown value in the first-step optimization. Let $v^*(b)$ denote the optimal solution of the first-step optimization. We illustrate two cases to investigate the optimal bandwidth capacity $b^*$.

(1) For $b \geq F^{-1}(\gamma)$:

In this case, $v^*(b) = rF^{-1}(\gamma) - cb$. Hence,

$$g(v^*(b), b) = rF^{-1}(\gamma) - cb - \frac{r}{\gamma}\int_0^{F^{-1}(\gamma)} F(x)dx. \tag{32}$$

Thus,

$$\frac{dg(v^*(b), b)}{db} = -c. \tag{33}$$

From Eq. (33), we know that $g(v^*(b), b)$ is a monotone function of $b$. So, the optimal solution in this case is the boundary value $b = F^{-1}(\gamma)$.

(2) For $b \leq F^{-1}(\gamma)$:

In this case, $v^*(b) = rb - cb$. Hence,

$$g(v^*(b), b) = rb - cb - \frac{r}{\gamma}\int_0^{b} F(x)dx. \tag{34}$$

Thus,

$$\frac{dg(v^*(b), b)}{db} = r - \frac{r}{\gamma}F(b) - c. \tag{35}$$

So, the optimal solution in this case is

$$b^* = F^{-1}\left(\gamma\frac{r-c}{r}\right), \tag{36}$$

which is also the optimal solution of this problem.

From the analysis above, we can say that:

**(1)** Compared with the model without risk presented in [1], the result presented in this paper enlarges the dimension of the problem without risk and provides more insight for those network managers who has a different risk preference:

- **(i)** When the parameter $\gamma \to 1$, the result of the model with risk in this paper is the same as that of the model without risk presented in [1].
- **(ii)** When the parameter $\gamma \to 0$, it means that there is no bandwidth allocated in the CN, i.e., the network manager is unwilling to provide any service.
- **(iii)** When the parameter $0 < \gamma < 1$, the optimal bandwidth obtained in this paper is less than the optimal bandwidth obtained without risk presented in [1]. It means that the optimal bandwidth capacity that is allocated in a network with risk is always less than that without risk.

**(2)** Compared with the mean-variance analysis model presented in [1], the result presented in this paper reveals advantages of using the CVaR approach over the mean-variance approach. It avoids the disadvantage of the mean-variance approach,

which equally penalizes the desirable upside and the undesirable downside outcomes. It also provides a closed-form solution, $F^{-1}\left(\gamma \cdot \frac{r-c}{r}\right)$, which has superior computational characteristics than the mean-variance approach.

In the following, we are going to present two typical arrival processes to express the random arrival processes of traffic demand in a CN. One is the Poisson arrival process; the other is the uniform distribution process.

### 4.1 Poisson arrival process

In this subsection, we consider a fully distributed communication network, where the traffic demand offered to the whole CN forms a Poisson process with arrival rate $\lambda > 0$, since in most of the system models in CNs, the arrival process of traffic demand is assumed to form a Poisson process.

The interarrival times are exponentially distributed with rate $\lambda$. Let $X$ be a random variable representing the time between successive demand arrivals in the Poisson process, then we have the probability distribution function $F_X(x)$ and the probability density function $f_X(x)$ of $X$ as follows:

$$F_X(x) = \begin{cases} 1 - e^{-\lambda x}, & x > 0 \\ 0, & x \leq 0, \end{cases} \tag{37}$$

$$f_X(x) = \begin{cases} \lambda e^{-\lambda x}, & x > 0 \\ 0, & x \leq 0. \end{cases} \tag{38}$$

The mean and variance of the exponential distribution are $1/\lambda$ and $1/\lambda^2$, respectively.

Based on the assumption of the traffic demand, the optimal bandwidth of Eq. (36) can be obtained as follows:

$$b^* = -\frac{Ln\left[1 - \gamma\frac{r-c}{r}\right]}{\lambda}, \tag{39}$$

where $Ln[\cdot]$ is the natural logarithm function based on $e$. The optimal mean profit of Eq. (2) can be obtained as follows:

$$\Pi^*(b, D) = \frac{r}{\lambda}\left(1 - e^{-\lambda b^*}\right) - cb^*, \tag{40}$$

where $b^*$ is given by Eq. (39).

### 4.2 Process with uniform distribution

In this subsection, we consider the same fully distributed communication network, but the traffic demand offered to the whole CN forms a uniform distribution on some interval $[m, n]$ $(-\infty < m < n < +\infty)$. Without loss of generality, we choose the interval $[0, 1]$ and the distribution function is denoted as $U[0, 1]$. (This assumption is sometimes used in some of the system models of CNs, such as ATM system). The arrival process of traffic demand is assumed to form a uniform distribution with the probability distribution function $F_X(x)$ and the probability density function $f_X(x)$ given as follows:

$$F_X(x) = \begin{cases} 1, & x > 1 \\ x, & 0 \le x \le 1 \\ 0, & x < 0, \end{cases}, \tag{41}$$

$$f_X(x) = \begin{cases} 1, & 0 \le x \le 1 \\ 0, & \text{otherwise.} \end{cases}. \tag{42}$$

The mean and variance of the uniform distribution are 1/2 and 1/12, respectively.

Based on the assumption of the traffic demand, the optimal bandwidth of Eq. (36) can be obtained as follows:

$$b^* = \gamma \frac{r-c}{r}. \tag{43}$$

The optimal mean profit of Eq. (2) can be obtained as follows:

$$\Pi^*(b, D) = (r-c)b^* - \frac{r}{2}(b^*)^2, \tag{44}$$

where $b^*$ is given by Eq. (43).

From Eqs. (39) and (43), we can obtain that the value of optimal bandwidth capacity with risk increases linearly to reach the value of the optimal bandwidth capacity without risk as the risk parameter $\gamma$ increases from 0.0 to 1.0, i.e., the risk parameter has a linear impact on the bandwidth capacity.

## 5 Numerical Results

With the same system parameters as in [1] and assumptions of arrival processes of traffic demand as presented in Section 4, we give some numerical results to show the impact of loss rate constraint and the impact of risk averseness on the network performance and compare the characters of network performance obtained in [1] and in this paper.

According to the engineering experience, we choose three different arrival rates following Poisson arrival process to represent the different cases of traffic load in the CN as: $\lambda = 0.1, 0.5, 0.9$ where $\lambda = 0.1$ represents the case that the traffic load in the CN is low, $\lambda = 0.5$ represents the case that the traffic load in the CN is normal, and $\lambda = 0.9$ represents the case that the traffic load in the CN is heavy.

### 5.1 Impact of risk averseness on bandwidth capacity

We give some numerical results to show the impact of risk averseness on the network bandwidth capacity.

Note that the optimal bandwidth capacity without risk, which is presented in [1], is $F^{-1}\left(\frac{r-c}{r}\right)$. However, in this paper the optimal bandwidth capacity with risk is given by Eq. (36). They are different ones.

Figure 5.1 shows the optimal bandwidth $b^*$ as a function of the risk parameter $\gamma$ with two different arrival processes of the Poisson arrival process and the uniform distribution process.

The ordinate axis $b^*$ of Figure 5.1 corresponds to the optimal bandwidth capacity given by Eq. (36). $b^*$ means the value of optimal bandwidth capacity provisioned in the

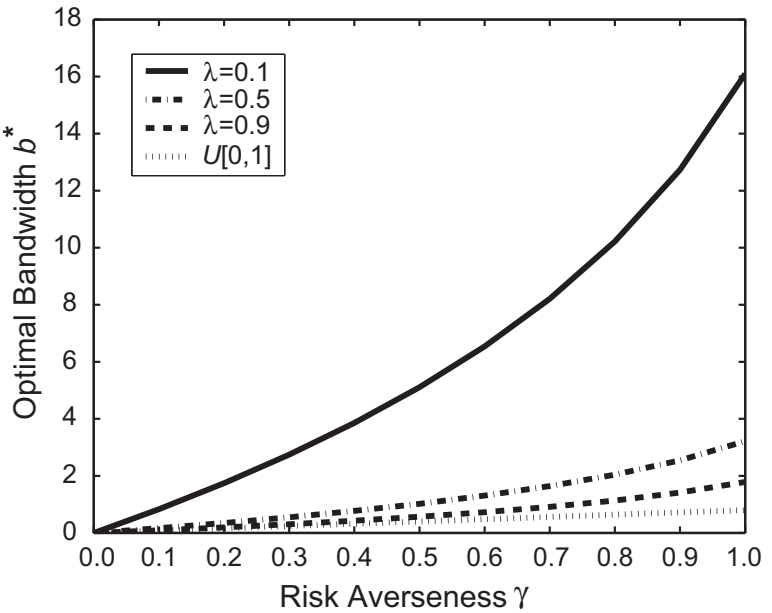


**Figure 5.1:** Impact of risk on the CN optimal bandwidth.

CN with risk. The smaller the value of $b^*$ is, the less the amount of bandwidth capacity will be. So, it clearly reflects the impact of risk averseness on the network performance.

The horizontal axis $\gamma$ of Figure 5.1 corresponds to the risk parameter $\gamma$ taking values from 0.0 to 1.0 by 0.1 each step. $\gamma = 0.0$ denotes the special case of most averse to risk. $\gamma = 1.0$ denotes the special case of risk neutrality. When $\gamma$ increases from 0.0 to 1.0, it indicates the CN manager's risk attitude changes from risk-averse to risk-neutral.

From Figure 5.1, we can discuss the impact of risk averseness on the network performance. When $\gamma$ increases from 0.0 to 1.0, the CN manager becomes less risk averse and he is inclined to bear more risk and sacrifice less profit to hedge risk. So, the value of $b^*$ becomes larger as the increase of $\gamma$. The less risk averse (with larger values of $\gamma$) the CN manager is, the more the optimal bandwidth capacity $b^*$ is.

Our numerical results include the optimal bandwidth capacity obtained without risk averseness presented in [1], which is one point in the curves with the value of $\gamma = 1.0$ in the horizontal axis of Figure 5.1.

From the numerical results in Figure 5.1, we can conclude that:

**(1)** In all curves, the optimal bandwidths with risk are always less than that without risk and the bandwidth capacity increases as the risk averseness decreases. This is because the values that the risk parameter $\gamma$ takes are less than 1.0.

**(2)** The curves with smaller arrival rates as $\lambda = 0.1, 0.5$ have quicker bandwidth capacity increasing speed than the curve with a larger arrival rate $\lambda = 0.9$. This is because the bandwidth $b$ is a decreasing function of arrival rate $\lambda$, which can be easily obtained by Eq. (39).

**(3)** With the same risk averseness, all the curves with the assumption of exponential distribution reveal a larger impact than the curve with the assumption of uniform

distribution. This is because the inverse function of the probability cumulative function of the Poisson arrival process is always larger than the inverse function of the probability cumulative function of the arrival process following the uniform distribution in the system, it results in a direct impact on the bandwidth capacity.

Compared with the results presented in [1] without risk, the numerical results in our paper reveal a distinct impact of risk on the network bandwidth capacity.

### 5.2 Impact of risk averseness on mean profit function

With the same system parameters and assumptions of traffic demand for Figure 5.1, we give some numerical results to show the impact of risk averseness on the network mean profit.

Figure 5.2 shows the optimal mean profit $\Pi^*(b, D)$ as a function of the risk parameter $\gamma$ with two different arrival processes of the Poisson arrival process and the uniform distribution process.

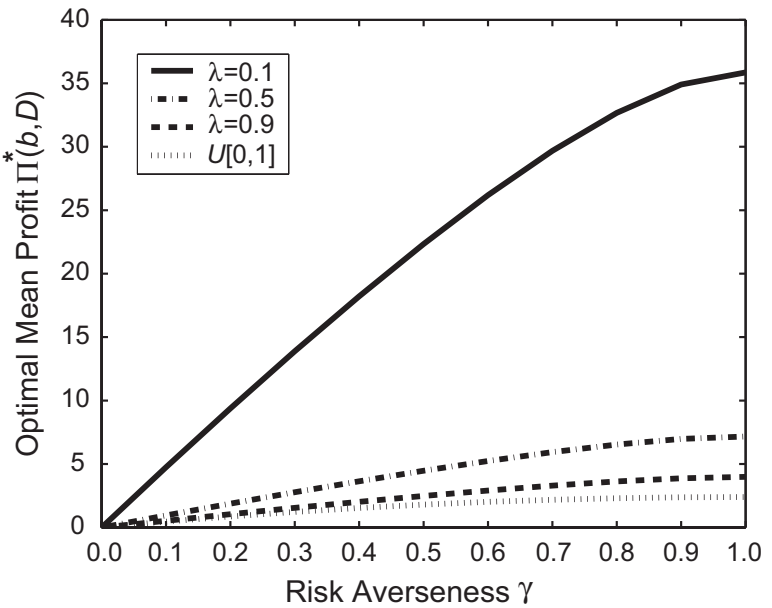


**Figure 5.2:** Impact of risk on the CN optimal profit.

The horizontal axis $\gamma$ of Figure 5.3 has the same meaning as that of Figure 5.1. The ordinate axis $\Pi^*(b, D)$ of Figure 5.2 corresponds to the optimal mean profit given by Eq. (2).

$\Pi^*(b, D)$ means the value of optimal profit obtained by the CN with risk. The smaller the value of $\Pi^*(b, D)$ is, the less the amount of optimal profit obtained by the CN will be. So, it clearly reflects the impact of risk averseness on the network performance.

From Figure 5.2, we can discuss the impact of risk averseness on the network performance. When $\gamma$ increases, the CN manager becomes less risk averse and he is inclined to bear more risk and sacrifice less profit to hedge risk. So, the value of $\Pi^*(b, D)$ becomes

larger as the increase of $\gamma$. The less risk averse the CN manager is, the more the optimal mean profit $\Pi^*(b, D)$ is.

Our numerical results include the optimal profit obtained without risk averseness presented in [1], which is one point in the curves with the value of $\gamma = 1.0$ in the ordinate axis of Figure 5.2.

Similarly, as we concluded in Subsection 5.1, from the numerical results shown in Figure 5.2, we can conclude that:

**(1)** In all curves, the profits with risk are always less than the profit without risk and the profit increases as risk averseness decreases. This is because the values that the risk parameter $\gamma$ takes are less than 1.0.

**(2)** The curves with smaller arrival rates as $\lambda = 0.1, 0.5$ have quicker mean profit increasing speeds than the curve with a larger arrival rate $\lambda = 0.9$. This is because the profit $\Pi^*(b, D)$ is a decreasing function of arrival rate $\lambda$, which can be easily obtained by Eq. (40).

**(3)** With the same risk averseness, all the curves with the assumption of exponential distribution reveal a larger impact than the curve with the assumption of uniform distribution. This is because the inverse function of the probability cumulative function of the Poisson arrival process is always larger than the inverse function of the probability cumulative function of the arrival process following the uniform distribution in the system, which results in a direct impact on the mean profit.

Compared with the results without risk presented in [1] without risk, the numerical results in our paper reveal a distinct impact of risk on the network profit function.

## 6 Conclusions

In this paper, we presented a stochastic model for bandwidth allocation and performance analysis in Communication Networks (CNs) with risk analysis included. We have derived the optimal bandwidth allocation capacity with risk averseness. We have analyzed the risk averseness in CNs by using the conditional value-at-risk approach. We have given numerical results to compare our model with the previous model presented in [1] and shown the impact of the risk on the network performance for two arrival processes of traffic demand. We can conclude that risk averseness has a distinct impact on the network performance. The implications presented in this paper provided insight for traffic engineering design and planning.

## Acknowledgment

This project was supported in part by MADIS, China Postdoctoral Science Foundation (No. 2005037010), National Natural Science Foundation of China (No. 70502001) and was supported in part by MEXT.ORC (2004-2008), Japan.

## References

[1] Wu J., Yue W. and Wang S. Stochastic model and analysis for capacity optimization in communication networks. *Journal of Computer Communications* **29**(12) (2006) 2377–2385.

[2] Awduche, D., Chiu, A., Elwalid, A., Widjaja, I. and Xiao, X. Overview and principles of internet traffic engineering. *RFC 3272, IETF* (2002).

[3] Xiao, X., Hannan, A., Bailey, B. and Ni, L. M. Traffic engineering with MPLS in the Internet. *IEEE Network* **14**(2) (2000) 28–33.

[4] Aukia, P., et al. RATES: a server for MPLS traffic engineering. *IEEE Network* **14**(2) (2000) 34–41.

[5] Elwalid, A., Jin, C., Low, S. and Widjaja, I. Mate: MPLS adaptive traffic engineering. In: *Proc. of IEEE INFOCOM*, 2001, 1300–1309.

[6] Mitra, D. and Ramakrishnan, K. G. A case study of multiservice multipriority traffic engineering design for data networks. In: *Proc. of IEEE GLOBECOM*, 1999, 1077–1083.

[7] Suri, S., Waldvogel, M., Bauer, D. and Warkhede, P. R. Profile-based routing and traffic engineering. *Journal of Computer Communications* **26**(4) (2003) 351–365.

[8] Mitra, D. and Wang, Q. Stochastic traffic engineering, with applications to network revenue management. In: *Proc. of IEEE INFOCOM*, 2003.

[9] Mitra, D. and Wang, Q. Risk-aware network profit management in a two-tier market. In: *Proc. of 18th International Telegraffic Congress*, 2003.

[10] Mitra, D. and Wang, Q. Stochastic traffic engineering for demand uncertainty and risk-aware network revenue management. *IEEE Transactions on Network* **13**(2) (2005) 221–233.

[11] Wu, J., Yue, W. and Wang, S. Optimization modeling and analysis for bandwidth allocation in communication networks with penalty cost. *IEICE Technical Report* **104** (2005) 7–12.

[12] Sethi, S., Yan, H., Zhang, H. and Zhou, J. Information updated supply chain with service-level constraints. *Journal of Industrial and Management Optimization* **1**(4) (2005) 513–531.

[13] Cheng, S., Liu, Y. and Wang, S. Progress in risk measurement. *Advanced Modelling and Optimization* **6**(1) (2004) 1–20.

[14] Markowitz, H. *Portfolio Selection, Efficient Diversification of Investments.* New Haven, Yale University Press, 1959.

[15] Wang, S. and Xia, Y. *Portfolio Selection and Asset Pricing.* Springer-Verlag, Berlin, 2002.

[16] Jorion, P. *Value At Risk: the New Benchmark for Controlling Derivative Risk.* Irwin, 2000.

[17] Rockafellar, R. and Uryasev, S. Optimization of conditional value-at-risk. *Journal of Risk* **2** (2000) 21–42.

[18] Bertsimas, D., Laupreteb, G. and Samarovc, A. Shortfall as a risk measure: properties, optimization and applications. *Journal of Economic Dynamics and Control* **28** (2004) 1353–1381.

[19] Chen, X., Sim, M., Simichi-Levi, D. and Sun, P. Risk aversion in inventory management. *Working paper*, 2003.

Nonlinear Dynamics and Systems Theory, **7** (1) (2007) 85–96

# Analysis of Network Revenue Management under Uncertainty **

Yifan Xu [1*], Shu-Cherng Fang [2] and Youyi Feng [3]

[1] *Department of Management Science, Fudan University, Shanghai, 200433, China*
[2] *Department of Industrial Engineering, NC State University, Raleigh, NC 27695*
[3] *Department of System Engineering and Engineering Management, Chinese University of Hong Kong, Shatin, NT, Hong Kong*

Received: June 16, 2005; Revised: November 15, 2006

**Abstract:** This paper investigates robust dynamic policies for network revenue management problems with uncertainty involved. We formulate such a problem in a setting of semi-definite programming and propose a heuristic procedure to find robust solutions. We also derive sufficient conditions for finding an approximation of the value function. Numerical experiments are included to illustrate the proposed approach.

**Keywords:** *Robust optimization; dynamic programming; revenue management; uncertainty.*

**Mathematics Subject Classification (2000):** 90B36, 90B15.

## 1 Introduction

This paper studies the revenue management problem on a given network in which all involved variables allow uncertainty. The optimal policy of the problem is investigated which determines what a quantity of resource should be offered at each different rate. The problem is important since we can find its broad applications, especially in airline network.

Revenue management is a technique concerned with a number of capacity constrained service industries such as airline, hotel, media, transposition, car rental, tourism and so on. Following the airline deregulation in 1970s, revenue management technique has

* Corresponding author: yfxu@fudan.edu.cn

** This research is supported by National Natural Science Foundation of China, No 70471012 and "Golden Spike" Foundation of Fudan University.

 

obtained a great progress both in theory and methodology. This progress further pushes the development of service industries.

No matter the difference in the definitions on revenue management, most researchers agree that the primary goal of revenue management is to maximize the revenues in the industry. They also agree that price is a major control tool to achieve this goal among various mechanisms. In the literature of revenue management, Littlewood [16] first proposed a marginal seat revenue principle and applied it to a single leg problem with two fare classes. Belobaba [1] developed a stochastic seat inventory control model to solve the multi-fare-class single leg problem. His model generalized the marginal seat revenue concept to the expected marginal seat revenue principle. The multi-fare-class problem was also studied by Brumelle and McGill [4] and Robinson [19].

There have been various studies of pricing policies in the continuous-time revenue management framework. In a two-fare model that allows a single price change, Feng and Gallego [12] proposed an optimal threshold control policy in 1995. Later, Feng and Xiao [13] generalized their result by considering risk analysis. Using the dynamic programming approach, Liang [15] showed that a threshold control policy is optimal for a continuous-time dynamic yield management model. In 1999, Subramanian et al. [21] incorporated the overbooking control on a single-leg flight into a Markov decision process. In the same year, Chatwin [10] discussed a continuous-time airline-overbooking model with time-dependent fares and refunds. To capture the time dependency of demand, most of airline revenue management models need an assumption of nonhomogeneous demand intensities.

A natural extension of single-leg problem is the network revenue management. A major concept in the study of network revenue management, bid price control, was proposed by Simpson [20] in 1989 and further studied by Williamson [25] and Talluri and Van Ryzin [24].

Up to now, the models that we list above are all based on the certain environment. However, in real applications, circumstances are variable and the data we obtain is uncertain because of various complications. Developing a model to deal with the revenue management under uncertainty is an interesting problem. In 2000, Bertsimas and Popescu [3] proposed a dynamic programming model with demand uncertainty only. But the general procedure for the network revenue management under uncertainty is still an open problem.

We know that optimization technique is the base of research in revenue management. With the recent advances in conic and robust optimization theory [5, 6], we can see its various applications in industries such as mechanical structure design [7], VLSI circuit design [11], systems and control [8] and signal processing [17].

In the paper, we incorporate the robust optimization technique into network revenue management and establish a robust dynamic model to deal with uncertainty produced by demand uncertainty, data perturbation and variable errors. We transform the problem into a robust semi-definite programming and provide a heuristic procedure to obtain the optimal solution of the problem. Furthermore, we discuss the Hamilton-Jacobi-Bellman equation under uncertainty, which establishes a sufficient condition for an optimal solution existing.

This paper is organized as follows. In the next section, we will introduce the background of our problem and establish a robust dynamic model for the problem. In Section 3, we propose a method to determine the optimal policy and provide a heuristic algorithm. In section 4, we establish a sufficient optimal condition under uncertainty. In Section 5,

we report some numerical results. Finally, in Section 6, we give our conclusion.

## 2 Dynamic Model under Uncertainty

### 2.1 Problem under Uncertainty

We are given an airline network which is composed of $m$ legs providing $n$ origin-destination itineraries. Let $a_{ij}$ be the number of units on leg $i$ used by itinerary $j$, which induces a $m \times n$ matrix $A = (a_{ij})$. The $j$-th column of $A$, denoted by $A^j$, is a multiple of the incidence vector for itinerary $j$. Here, we do not restrict that $A$ is a 0-1 matrix, which means that group demand is permitted. $a_{ij} = 0$ implies that leg $i$ is not a part of itinerary $j$.

The inventory state of the network is described by a vector $x = (x^1, x^2, \ldots, x^m)^T$ of leg capacities. We have $0 \leq x \leq X$, where $X = (X^1, X^2, \ldots, X^m)^T$ is the capacity limit vector of the system. If itinerary $j$ is sold, the state of the network changes to $x - A^j$. To simplify our analysis, we do not consider such problems involving cancellations, no-shows or overbooking. In our problem, time is discrete. We assume a finite booking horizon of length $T$, with time line being partitioned sufficiently fine such that almost surely at most one request appears at each period.

Time is counted backward: time $T$ is the beginning of the booking horizon and time 0 is the end of booking horizon. We assume that ticketing operation will stop when $t = 0$. At time $0 \leq t \leq T$, all booking events are denoted as a random vector $d(t) = (d_1(t), ..., d_n(t))$. $d_j(t) > 0$ for $1 \leq j \leq n$ indicates that a requirement for itinerary $j$ occurs at time $t$ while $d_j(t) = 0$ means no requirement for itinerary $j$ at time $t$. The tickets for each itinerary $j = 1, 2, ..., n$ can be sold at $h$ fares $p_j^r, r = 1, ..., h$. $p_j^r = 0$ implies that the fare $p_j^r$ is unavailable for itinerary $j$ and $p_j = 0$ the itinerary $j$ is unavailable. Suppose that demands for different fares are independent of one another. Let $D_j^r(t)$, $1 \leq r \leq h$ and $1 \leq j \leq n$, be the demand flow for the $r$-th fare on the $j$-th itinerary, which is a nonhomogeneous Poisson process about time $0 \leq t \leq T$. The intensity of $D_j^r(t)$ is $\lambda_j^r(t)$, a deterministic function of time $t$.

We know that in the dynamic world, any unexpected sudden affair would bring a corresponding perturbation to circumstance. For example, weather condition such as fog or storm often cause airlines to adjust their flight schedule. Some flights may be cancelled and some additional flights may be added. Hence, any model, if it would like to simulate the reality, must consider the uncertainty within its parameters.

Let us denote by $\Delta A$ the perturbation to itinerary network and $\Delta x$ the perturbation to the state of inventory. Then, the itinerary-leg matrix under uncertainty should be $A + \Delta A$. The capacity vector under uncertainty should be $x + \Delta x$. Here, $\Delta x$ also can be observed as overbooking.

Airlines often offer a variety of fares in each fare class of itinerary and also pay varying commissions on these fares. In other industries such as advertising, broadcasting and hotel, the fare negotiation also cause the uncertainty in fares. Thus, we suppose that revenue from selling a ticket on itinerary $j \in \{1, ..., n\}$ at class $r \in \{1, ..., h\}$ is $p_j^r + \Delta p_j^r$, where $\Delta p_j^r$ is the perturbation to fare $p_j^r$. In vector, $p^r = (p_1^r, \cdots, p_n^r)^T$ and $\Delta p^r = (\Delta p_1^r, \cdots, \Delta p_n^r)^T$.

In general, demand is concerned with the price. The uncertainty in fares would cause the requirement for itineraries at these fares is uncertain. Another reason for requirement uncertainty is the data error produced in our approaches for requirement forecast. Hence, we suppose that demand flow for class $r \in \{1, ..., h\}$ on itinerary $j \in \{1, ..., n\}$ at time $t$

is a nonhomogeneous Poisson process with intensity $\lambda_j^r(t) + \Delta\lambda_j^r(t)$, where $\Delta\lambda_j^r(t)$ is the perturbation to $\lambda_j^r(t)$.

Suppose there is an upper bound $\epsilon > 0$ such that for any $r$, $\|(\Delta x, \Delta A, \Delta p^r)\| \leq \epsilon$ holds for all perturbations, where $\|\cdot\|$ is the norm under Euclidian. Given the time-to-go, $k$, we call $S(k, x, A, p, \epsilon)$, or simply $S(k, x, \epsilon)$, the *current state* of system.

Our problem is that: Under the current state $S(k, x, \epsilon)$, should we accept or refuse the current request?

### 2.2 Dynamic Model

To answer the question proposed in the end of the last subsection, we establish a dynamic programming model in the subsection. Then, we solve the model to decide whether the current request is accepted or not.

Let $u_k = \{u_k^{r,j}\}$ denote the decision at time $k$, where

$$u_k^{r,j} = \begin{cases} 1, & \text{if } p_j^r \text{ is accepted at time } k; \\ 0, & \text{otherwise.} \end{cases}$$

In general, the decision $u_k$, accepting or refusing, is the function of time $k$, the capacity vector $x$ and perturbation bound $\epsilon$. Thus, $u_k = u_k(x, \epsilon)$. From our assumption, there is at most one request at each sufficiently small period, i.e., $\sum_{r,j} u_k^{r,j} \leq 1$. The feasible set for $u_k$ at current state is defined as:

$$U_k(x, \epsilon) = \{u_k : \sum_{r,j} u_k^{r,j} \leq 1, u_k^{r,j} \in \{0, 1\}, (A + \Delta A)u_k \leq (x + \Delta x), \\ \text{for all } \|(\Delta A, \Delta x)\| \leq \epsilon\}, \tag{1}$$

where $(A + \Delta A)u_k := \sum_{r,j}(A^j + \Delta A^j)u_k^{r,j}$ and $\epsilon > 0$ is a given scalar.

Let $J_k(x + \Delta x)$ denote the maximum expected revenue at current system state $S(k, x, \epsilon)$. Then $J_k(x + \Delta x)$ should satisfy the Bellman equation [2]:

$$J_k(x + \Delta x) = \max_{u_k \in U_k(x,\epsilon)} E[(p + \Delta p)u_k + J_{k-1}((x + \Delta x) - (A + \Delta A)u_k)], \tag{2}$$

where $(p + \Delta p)u_k := \sum_{r,j}(p_j^r + \Delta p_j^r)u_k^{r,j}$, with the boundary conditions:

$$J_0(x + \Delta x) = 0, \quad \forall x,\ \Delta x. \tag{3}$$

We call $J_k(x + \Delta x)$ satisfying (2) and (3) the *value function* under a given state $S(k, x, \epsilon)$. Define the *minimum acceptable fare* (MAF) [12] for itinerary $j$ under state $S(k, x, \epsilon)$ as follows:

$$G_j(x + \Delta x, k) = J_{k-1}(x + \Delta x) - J_{k-1}(x + \Delta x - (A^j + \Delta A^j)).$$

In view of [23], the request for class $r$ on itinerary $j$ at current state $S(k, x, \epsilon)$ is accepted if and only if

$$(p_j^r + \Delta p_j^r) - G_j(x + \Delta x, k) \geq 0 \text{ and } (A^j + \Delta A^j) \leq (x + \Delta x). \tag{4}$$

The intuition of formulation (4) is clear: Under uncertainty, we only accept a fare exceeding the MAF while we have sufficient remaining capacity.

## 3 Computation of MAF

In the section, we develop a robust linear programming model to obtain the approximation of value function under uncertainty.

Over the remaining period from $k$ to 0, the expected accumulation demand for itinerary $j$ at fare class $r$ can be calculated as $D_j^r(k)+\Delta D_j^r(k) := \sum_{t=1}^{k}(\lambda_j^r(t)+\Delta\lambda_j^r(t))$. Similar as [25, 3], we consider following deterministic integer programming:

$$\begin{aligned} J_k(x+\Delta x) \quad = \quad & \max_{y^r} \min_{\|\Delta p^r\|} \sum_{r=1}^{h}(p^r+\Delta p^r)^T y^r \\ s.t. \quad & (A+\Delta A)(\sum_{r=1}^{h} y^r) \le (x+\Delta x), \\ & 0 \le y^r \le (D^r(k)+\Delta D^r(k)), \quad \forall r, \\ & y^r \text{ integer vector}, \quad \forall r \\ & \text{for all } \|(\Delta x, \Delta A, \Delta p^r, \Delta D^r(k))\| \le \epsilon, \quad \forall r, \end{aligned} \tag{5}$$

where $y^r = (y_1^r, ..., y_n^r)^T$. This is a robust linear integer optimization problem. In formulation (5), variable $y_j^r$ denotes the amount of accepted demands for itinerary $j$ at fare class $r$ over the remaining horizon. The first inequality in the constrain means that the total amount of accepted demands can not exceed the current capacity. The second inequality means that the amount of accepted demands for various itineraries at fare class $r$ over the remaining horizon should be less then or equal to the expected accumulation demand for various itineraries at fare class $r$. We want to maximize the revenue under bounded perturbations.

Let $z^r = y^r - \Delta z^r$, where $\Delta z^r := \Delta D^r(k)$. Then, problem (5) can be transformed as a robust linear programming problem in following form:

$$\begin{aligned} L_k(x+\Delta x) \quad = \quad & \max_{\epsilon_0 \le z^r \le D^r(k)} \min_{\|\Delta z^r\| \le \epsilon_0} \sum_{r=1}^{h}(p^r+\Delta p^r)^T(z^r+\Delta z^r) \\ s.t. \quad & (A+\Delta A)[\sum_{r=1}^{h}(z^r+\Delta z^r)] \le (x+\Delta x), \\ & \text{for all } \|(\Delta x, \Delta A, \Delta p^r)\| \le \epsilon, \ \forall r, \end{aligned} \tag{6}$$

where $\epsilon > 0$ and $\epsilon_0 > 0$ are perturbation bounds given by the problem we consider.

In formulation (6), the integral requirement on variables is relaxed and the perturbation on expected accumulation demand is transformed as that on variables. Thus, problem (6) is a relaxation of problem (5). We assume that both $\epsilon > 0$ and $\epsilon_0 > 0$ are small. The reason we make such an assumption is based on following analysis. First, $\|\Delta p^r\|$ denotes the price perturbation. This perturbation is small in general. Second, $\|\Delta A\|$ and $\|\Delta x\|$ denote variations of flight and capacity caused by some emergent affairs. Although these variations may be great in case of copping with the unexpected emergency, the unexpected accident affair happens at a low probability. It is unimaginable that we always treat routine affairs by the standard for emergency. From the view of long run, the average infection to flight and capacity should be small. Third, we hope to find an optimal solution with small perturbation to itself. Hence, (6) provides us a possible approximation of the allocation of inventory.

Problem (6) is a max-min problem with perturbations to all parameters and variables. To simplify the problem, we transform it to a semi-definite programming just with perturbation to variable via S-lemma in [26, 18].

We call a solution $\epsilon_0 \le z^r \le D^r(k), r = 1, ...h$ is *robust feasible* for problem (6) if

$$(A_i + \Delta A_i)[\sum_{r=1}^{h}(z^r + \Delta z^r)] \le (x_i + \Delta x_i), \quad i = 1, ..., m$$

hold for all $\|(\Delta p^r, \Delta A, \Delta x, )\| \le \epsilon,\ \|\Delta z^r\| \le \epsilon_0,\ r = 1, ..., h$, where $A_i$ is the $i-$th row of $A$. In view of [6], $\epsilon_0 \le z^r \le D^r(k), r = 1, ..., h$ is robust feasible if and only if for each $i$,

$$-A_i \sum_r z^r + x_i - \epsilon \sqrt{\| \sum_r z^r + \sum_r \Delta z^r \|^2 + 1} \ge 0 \tag{7}$$

holds for all $\|\Delta z^r\| \le \epsilon_0$. The formulation of (7) can be reformulated as:

$$\begin{pmatrix} I & \sqrt{\epsilon}\begin{pmatrix} \sum_r z^r + \sum_r \Delta z^r \\ 1 \end{pmatrix} \\ \sqrt{\epsilon}\begin{pmatrix} (\sum_r z^r + \sum_r \Delta z^r)^T & 1 \end{pmatrix} & -A_i(\sum_r z^r + \sum_r \Delta z^r) + x_i \end{pmatrix} \succeq 0 \tag{8}$$

holds for each $i$ and all $\|\Delta z^r\| \le \epsilon_0$, where $A \succeq 0$ implies that $A$ is a positive semi-definite matrix.

Now consider the objective function of problem (6). By introducing an additional variable $v \ge 0$ to be maximized, we obtain a new constraint: $\sum_{r=1}^{h}(p^r + \Delta p^r)^T(z^r + \Delta z^r) - v \ge 0$ for all $\|\Delta p^r\| \le \epsilon, \|\Delta z^r\| \le \epsilon_0, r = 1, ..., h$. Since both $(z^r + \Delta z^r) \ge 0$ and $(p^r + \Delta p^r) \ge 0$, this constraint is equivalent to $(p^r + \Delta p^r)^T(z^r + \Delta z^r) - v_r \ge 0$ for all $\|\Delta p^r\| \le \epsilon, \|\Delta z^r\| \le \epsilon_0, r = 1, ..., h$. Furthermore, each constraint is equivalent to

$$\begin{pmatrix} I & \sqrt{\epsilon}(z^r + \Delta z^r) \\ \sqrt{\epsilon}(z^r + \Delta z^r)^T & (p^r)^T(z^r + \Delta z^r) - v_r \end{pmatrix} \succeq 0, \quad for\ all\ \|\Delta z^r\| \le \epsilon_0. \tag{9}$$

In view of S-Lemma in [26, 18], we can obtain the conclusion: (8) holds if and only if there exists a $\mu_i \ge 0$ for each $i$ such that

$$\begin{pmatrix} I & \sqrt{\epsilon}\begin{pmatrix} \sum_r z^r \\ 1 \end{pmatrix} & \sqrt{\epsilon}\begin{pmatrix} I \\ 0 \end{pmatrix} \\ \sqrt{\epsilon}\begin{pmatrix} (\sum_r z^r) \\ 1 \end{pmatrix}^T & -A_i(\sum_r z^r) + x_i & -\frac{1}{2}A_i \\ \sqrt{\epsilon}\begin{pmatrix} I \\ 0 \end{pmatrix}^T & -\frac{1}{2}A_i^T & 0 \end{pmatrix} - \mu_i \begin{pmatrix} 0 & 0 & 0 \\ 0 & \epsilon_0 & 0 \\ 0 & 0 & -I \end{pmatrix} \succeq 0. \tag{10}$$

Similarly, (9) holds if and only if there exists a $\mu_r \ge 0$ for each $r$ such that

$$\begin{pmatrix} I & \sqrt{\epsilon}\sum_r z^r & \sqrt{\epsilon}I \\ \sqrt{\epsilon}(\sum_r z^r)^T & (p^r)^T z^r - v_r & -\frac{1}{2}p^r \\ \sqrt{\epsilon}I & -\frac{1}{2}(p^r)^T & 0 \end{pmatrix} - \mu_r \begin{pmatrix} 0 & 0 & 0 \\ 0 & \epsilon_0 & 0 \\ 0 & 0 & -I \end{pmatrix} \succeq 0. \tag{11}$$

Combining (7)–(11), we can obtain following theorem.

**Theorem 3.1** *The robust linear programming (6) is equivalent to the following problem:*

$$\begin{aligned} &\text{maximize} && \sum_{r=1}^{h} v_r, \\ &\textit{subject to} && (10), (11) \text{ and } \epsilon_0 \le z^r \le D^r(k), \forall r. \end{aligned} \tag{12}$$

Problem (12) is a typical semi-definite programming. There are many effective methods [22, 14] to solve this problem.

Now we present a robust heuristic algorithm for network revenue management under uncertainty based on the robust optimization technique.

**Robust Heuristic Algorithm (RHA):**

*At any current state $S(k, x, \epsilon)$, where $\epsilon$ is the perturbation bound for all parameters.*

1. *For a request for itinerary $j$ at class $r$, computer MAF via solving (12).*
2. *Sell to itinerary $j$ if and only if its fare $p_j^r$ exceeds its MAF, i.e., $p_j^r \ge G_j(x, k)$.*
3. *Back to step 1 for next request.*

## 4 Hamilton-Jacobi Equation

In this section, we further explore the property of value function and prove that Hamilton-Jacobi equation [9] still holds under uncertainty.

From (2) and (4), the value function can be expressed an inductive formulation as follows:

$$\begin{aligned} J_k(x+\Delta x) &= \max_{u_k \in U_k(x,\epsilon)} E[(p+\Delta p)u_k + J_{k-1}((x+\Delta x) - (A+\Delta A)u_k)] \\ &= J_{k-1}(x+\Delta x) + \max_{u_k \in U_k(x,\epsilon)} E[(p+\Delta p)u_k - G_j(x+\Delta x, k)u_k]^+ \\ &= J_{k-1}(x+\Delta x) + \sum_{r,j} (\lambda_j^r(k) + \Delta\lambda_j^r(k))[(p_j^r + \Delta p_j^r) - G_j(x+\Delta x, k)]^+, \end{aligned}$$

where $[\cdot]^+ := \max\{0, \cdot\}$. Let $\Delta J_k(x+\Delta) = J_{k-1}(x+\Delta x) - J_k(x+\Delta x)$. We obtain the difference equation as follows:

$$0 = \Delta J_k(x+\Delta x) + \sum_{r,j} (\lambda_j^r(k) + \Delta\lambda_j^r(k))[(p_j^r + \Delta p_j^r) - G_j(x+\Delta x, k)]^+.$$

We call $f(x)$ is an $\epsilon$-*approximation* of $F(x)$ on $X$ if there exists $\epsilon > 0$ and a constant $\alpha$ such that $\|f(x) - F(x)\| \le \alpha\epsilon$ for all $x \in X$. In view of Hamilton-Jacobi equation [9], if take $\Delta J_k(x+\Delta x)$ as an $\epsilon$-approximation of derivation, then we have following approximately sufficient optimality condition.

**Theorem 4.1** *Suppose $\lambda_j^r(t)$ is continuous about $0 \le t \le T$. Partition $[0, T]$ into $K$ sufficiently small intervals and arbitrarily take a point $k$ from each small interval $T_k, k = 1, ..., K$. If for any given $\eta > 0$, there exist continuous function $J_t(x)$ such that $\Delta J_k(x+\Delta x)$ is an $\epsilon$-approximation of $\frac{\partial J_t(x)}{\partial t}$ and satisfies*

$$\left| \sum_{r,j} (\lambda_j^r(k) + \Delta\lambda_j^r(k))[(p_j^r + \Delta p_j^r) - G_j(x+\Delta x, k)]^+ + \Delta J_k(x+\Delta x) \right| \le \eta \tag{13}$$

*and*

$$J_0(x + \Delta x) = 0$$

*for all* $\|(\Delta x, \Delta A, \Delta p, \Delta\lambda)\| \leq \epsilon$, *where* $\epsilon > 0$ *is a given parameter. Then,* $J_k(x + \Delta x)$ *is an* $\epsilon$*-approximately value function.*

***Proof*** Since $J_t(x)$ is continuous and $T_k$ is sufficiently small, we only need to prove that $J_t(x)$ satisfies Hamilton-Jacobi equation [9].

From $|\Delta J_k(x + \Delta x) - \frac{\partial}{\partial t} J_t(x)| \leq \epsilon$, the continuity of $\lambda_j^r(t)$ and $J_t(x)$ and (13), we have

$$|\sum_{r,j} \lambda_j^r(t)[(p_j^r - J_{t-1}(x) + J_{t-1}(x - A^j)]^+ + \frac{\partial}{\partial t} J_t(x)| \leq \rho_1\eta + \rho_2\epsilon,$$

where $\rho_1, \rho_2$ are constants. Taking $\epsilon = \eta$ will finish the proof. □

Theorem 4.1 has an important meaning: The value function under uncertainty determined by (13) is the $\epsilon$-approximation of value function in certainty.

## 5 Numerical Experiments

In the section, we will exhibit some numerical examples on the optimal booking control by the following example.

**Example 5.1** *Consider the airline network whose leg-itinerary matrix is given as follows:*

$$A = \begin{pmatrix} 1 & 0 & 1 & 0 \\ 0 & 1 & 1 & 0 \\ 0 & 0 & 0 & 1 \end{pmatrix}.$$

*The current state we consider is* $S = (x, T, \epsilon)$, *where the capacity vector* $x = (600, 500, 280)^T$ *and* $T = 200$. *There are* $h = 2$ *fare classes for itinerary* $i = 1, 2, 3, 4$ *in the problem. The fares and their demand rates are tabulated in Table 5.1.*

We take $\mu_1 = 0.75, \mu_2 = 0.8$ in (12) and calculate by Robust Heuristic Algorithm the value function for each $j$ at various $\epsilon$. The results are presented in Figure 5.1 – Figure 5.4 as follows. The figures display the monotone evolution of the MAFs of disparate itineraries. The curves in the figures do not intersect with each other, which numerically depicts the corresponding monotone behaviors. This example shows the algorithm RHA is effective for a kind of robust revenue management problems.

| Itinerary | 1 | 2 | 3 | 4 |
|---|---|---|---|---|
| $p_i^1$ | 400 | 300 | 560 | 320 |
| $p_i^2$ | 350 | 260 | 400 | 280 |
| $\lambda_i^1$ | $50 + 25t$ | $60 + 10t$ | $30 + 15t$ | $25 + 12t$ |
| $\lambda_i^2$ | $40 + 5t$ | $60 + 10t$ | $50 + 10t$ | $20 + 11t$ |

**Table 5.1:** The data for Example 5.1.

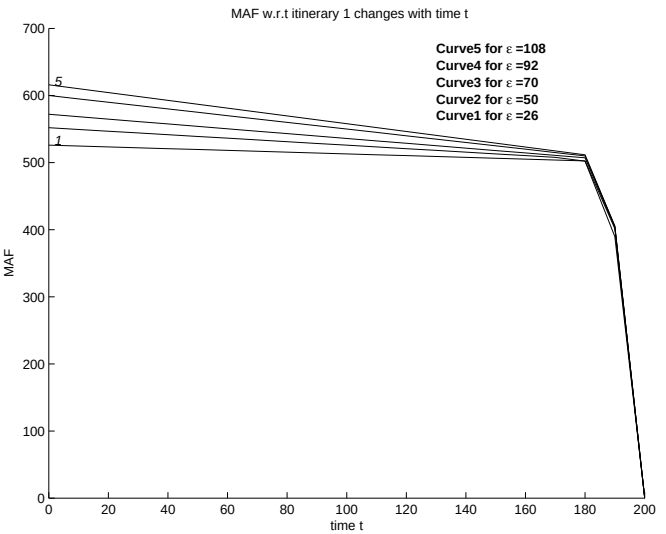


**Figure 5.1:** Picture of MAF for itinerary 1 changes with $t$ for various $\epsilon$.

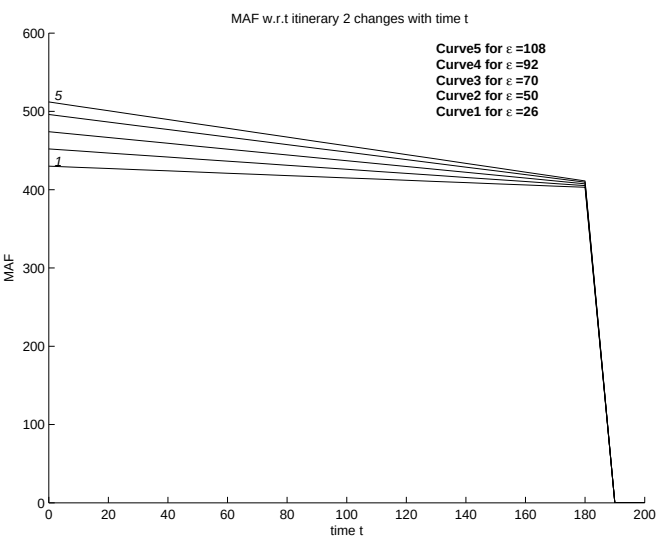


**Figure 5.2:** Picture of MAF for itinerary 2 changes with $t$ for various $\epsilon$.

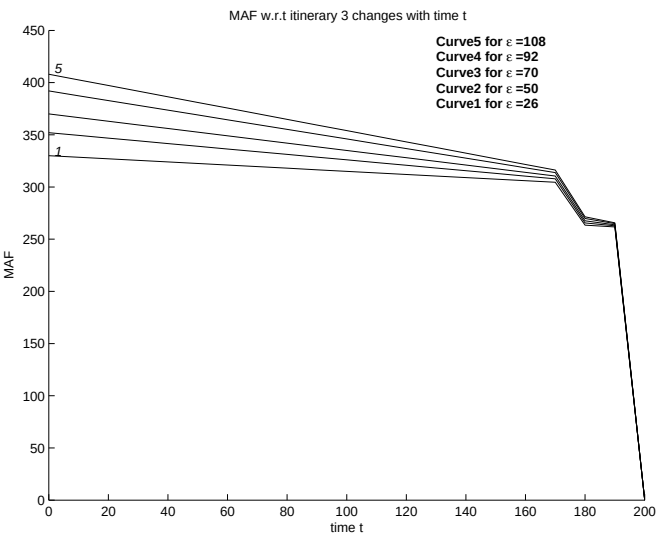


**Figure 5.3:** Picture of MAF for itinerary 3 changes with $t$ for various $\epsilon$.

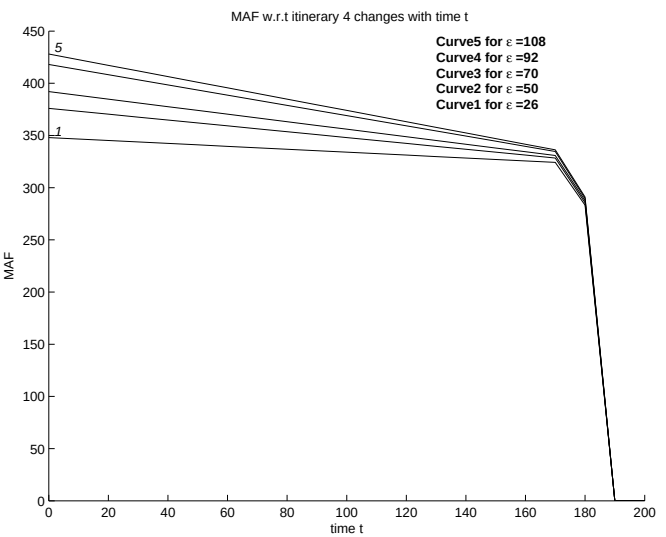


**Figure 5.4:** Picture of MAF for itinerary 4 changes with $t$ for various $\epsilon$.

## 6 Conclusion

This paper studies the network revenue management under uncertainty. A robust dynamic model for the problem is established and a heuristic is provided to find the robust solutions. Some numerical results are given to show that the algorithm is efficient. From the figures, we can observe that MAF is monotone of time for small $\epsilon$. We estimate that MAF is also monotone of remaining capacity $x$ for small $\epsilon$.

## Acknowledgements

This research was partially supported by the National Sciences Foundation of China, No.70471012.

## References

[1] Belobaba, P. Airline travel demand and airline seat inventory management. PhD thesis, MIT, 1987.

[2] Bertsekas, D. P. *Dynamic Programming and Optimal Control, Volume I*. Athena Sciences, Belmont, MA, 1995.

[3] Bertsimas, D. and Popesecu, I. Revenue management in a dynamic network environment. Working paper, 2000.

[4] Brumelle, S. L. and McGill, J. I. Allocation of airline sears between stochastically dependent demand. *Transportation Sciences* **24** (1990) 183–192.

[5] Ben-Tal, A., Ghaoui, L. E. and Nemirovskii, A. Robust semideinite programming. *Handbook of semidefinite programming* (H.Wolkowicz, R.Saigal, and L.Vandenberghe, eds). Kluwer Academic Publishers, March 2000.

[6] Ben-Tal, A. and Nemirovskii, A. Robust convex optimization. *Mathematics of Operations Research* **23** (1998) 769–805.

[7] Ben-Tal, A. and Nemirovskii, A., Structural Design. In: *Handbook of semidefinite programming, theory, algorithm and applications* (H.Wolkowicz, R.Saigal and L.Vandenberghe, eds). Kluwer Academic Press, 2000.

[8] Boyd, S., Ghaoui, L. E., Feron, E. and Balakrishnan, V. *Linear matrix inequalities in system and control theory*. SIAM Studies in Applied Mathematics, SIAM, Philadelphia, 1994.

[9] Bremaud, P. *Point processes and queue, martingale dynamics*. Springer-Verlag, 1980.

[10] R. E. Chatwin, Continuous-time airline overbooking with time-dependent fares and refund, *Transportation Sciences*, 33 (1999) 182-191.

[11] C. Choi and Y. Ye, Application of semidefinite programming to circuit partitioning, In: *Approximation and complexity in numerical optimization* (P. Pardalos, ed.). Kluwer Academics Publishers, 2000.

[12] Feng, Y. and Gallego, G. Optimal stopping times for end of season sales and optimal stopping times for promotional fares. *Management Sciences* **41** (1995) 1371–1391.

[13] Feng, Y. and Xiao, B. Maximizing revenue of perishable asset with risk analysis. *Operations Research* **47** (1999) 337–341.

[14] Henrion, D. and Lasserre, J. B. GloptiPoly - global optimization over polynomials with Matlab and SeDuMi. LAAS-CNRS Research Report, February 2002.

[15] Liang, Y. Solution to the continuous time dynamic yield management model. *Transportation Sciences* **33** (1999) 117–123.

[16] Littlewood, K. Forecasting and control of passenger booking. *AGIFORS Symposium Proceedings* **12** (1972) 95–117.

[17] Luo, Z. Q. Applications of convex optimization in signal processing and digital communication, Working paper. Department of Electrical and Computer Engineering, McMaster University, 2003.

[18] Luo, Z. Q., Sturm, J. and Zhang, S. Multivariate nonnegative quadratic mappings, Manuscript. Department of Electrical and Computer Engineering, McMaster University, 2002.

[19] Robinson, L. W. Optimal and approximate control policies for airline booking with sequential fare classes. *Operations Research* **43** (1995) 252–263.

[20] Simpton, R. W. Using network flow techniques to find shadow prices for market and seat inventory control, Memorandum M89-1. MIT Flight Transportation Lab., Cambridge, MA, 1989.

[21] Subramanian, J., Stidham, S., Lautenbacher, J. Airline yield management with overbooking, cancellations and no-shows. *Transportation Sciences* **33** (1999) 147–167.

[22] Sturm, J. Implementation of interior point methods for mixed semidefinite and second order cone optimization problems, Tecnical Report. Tilburg University, The Netherlands, August 2002.

[23] Talluri, K. and Ryzin, G. V. An analysis of bid-price controls for network revenue management. *Management Science* **44:11** (1998) 1577–1593.

[24] Talluri, K. and G. Van Ryzin. An analysis of bid-price controls for network revenue management. *Management Sciences* **44** (1998) 1577–1593.

[25] Williamson, E. L. Airline network seat control, PhD Dissertation. MIT, Cambridge, MA, 1992.

[26] Yakubovich, V. A. S-Procedure in nonlinear control theory. Vestnik Leningrad University **4** (1977) 73–93.

Nonlinear Dynamics and Systems Theory, **7** (1) (2007) 97–112

# An Online Learning Algorithm with Adaptive Forgetting Factors for Feedforward Neural Networks in Financial Time Series Forecasting

Lean Yu [ac], Shouyang Wang [ab] and Kin Keung Lai [bc*]

[a] *Institute of Systems Science, Academy of Mathematics and Systems Sciences, Chinese Academy of Sciences, Beijing 100080, China*
[b] *College of Business Administration, Hunan University, Changsha 410082, China*
[c] *Department of Management Sciences, City University of Hong Kong, Tat Chee Avenue, Kowloon, Hong Kong*

Received: July 15, 2005; Revised: September 11, 2006

**Abstract:** In this study, an online learning algorithm for feedforward neural networks (FNN) based on the optimized learning rate and adaptive forgetting factor is proposed for online financial time series prediction. The new learning algorithm is developed for online predictions in terms of the gradient descent technique, and can speed up the FNN learning process substantially relative to the standard FNN algorithm, with simultaneous preservation of stability of the learning process. In order to verify the effectiveness and efficiency of the proposed online learning algorithm, two typical financial time series are chosen as testing targets for illustration purposes.

**Keywords:** *Online learning algorithm; adaptive forgetting factor; optimal learning rate; feedforward neural network; financial time series forecasting.*

**Mathematics Subject Classification (2000):** 93C55, 92B20, 91B99.

## 1 Introduction

The financial market is a complex, evolutionary, and nonlinear dynamical system [1]. Financial time series are inherently noisy, non-stationary, and deterministically chaotic [2]. This means that the distribution of financial time series changes over time. Not only a single data series is non-stationary in the sense of the mean and variance of the series, but the relationship of the data series to other related data series may also be continuously changing. Modeling such dynamical and non-stationary time series is a

* Corresponding author: mskklai@cityu.edu.hk

 

challenging task. Over the past few years, neural networks have been successfully used to model financial time series ranging from options prices [3], corporate bond ratings [4] and stock index trading [5] to currency exchange [6]. Neural networks are universal function approximators that can map any nonlinear function without any *a priori* assumption about the data [7]. Unlike traditional statistical models, neural networks are data-driven, non-parametric weak models, and they let "the data speak for themselves". So neural networks are less susceptible to the model mis-specification problem than most parametric models are, and they are more powerful in describing the dynamics of financial time series than traditional statistical models are [6, 8].

Among these neural network models, the multilayer feedforward neural network (FNN) is widely used for financial time series prediction due to its approximations to nonlinear functions and its self-learning capability [7]. However, the FNN has several limitations. For example, the convergence speed of the FNN algorithm is often slow because the learning rate is fixed [12], thus increasing the network learning time. Therefore, some faster training FNN algorithms, such as adaptive learning algorithms [9-10], real-time learning algorithms [11-12] and other fast learning algorithms [13-15], have been developed in an attempt to reduce these shortcomings. But two main limitations still remain so far.

Firstly, most FNN models do not use the optimized instantaneous learning rates except the work of [11]. In studies in which these are introduced, the learning rate is set to a fixed value. It is, however, critical to determine a proper fixed learning rate for the FNN applications. If the learning rate is large, learning may occur quickly, but it may also become unstable and may even not learn at all [11]. To ensure stable learning, the learning rate must be sufficiently small, but a small learning rate may lead to a long learning time and a slow convergence speed. Also, it is unclear just how small the learning rate should be. In addition, the best fixed learning rate is problem-independent, and it varies with different neural network structure for different applications.

Secondly, in the existing literature, almost all fast algorithms are batch learning algorithms. Although neural network batch learning is highly effective, the computation involved in each learning step is very big, especially when large sample data sets are presented. Furthermore, the neural networks must re-learn from the beginning as new data become available. Therefore, this may overly affect the overall computational efficiency of batch learning. In this sense, batch learning is unsuitable for real-time or online prediction when neural networks are used as a predictor.

For the first problem, an optimized instantaneous learning rate is derived from the gradient descent rule based on optimization techniques. For the second problem, an online learning algorithm should be created to overcome the drawbacks of batch learning algorithm. Actually, there is a difference between online learning algorithm and batch learning algorithm in the neural networks models. In the online learning algorithm, the weight vectors are updated recursively after the presentation of each input vector. While in the batch learning algorithm, the weight vectors of neural networks are updated only at the end of each epoch, which will be further illustrated later. Usually, in the neural networks, a single pass over the input data set is called as an epoch. Furthermore, the weight sequence should be chosen to given a higher weight to more recent data in the time series prediction. So an adaptive forgetting factor is also introduced into the proposed online learning algorithm. In order to verify the effectiveness and efficiency of the proposed online learning algorithm, two typical financial time series, S&P 500 and the exchange rate of euros against US dollars (EUR/USD), are chosen for testing.

The rest of this work is organized as follows. In Section 2, the proposed online learning algorithm with adaptive forgetting factor is first presented in terms of the gradient descent algorithm and optimization techniques. For further illustration, an empirical analysis is then given in Section 3. Finally, some concluding remarks are drawn in Section 4.

## 2 The Proposed Online Learning Algorithm

In this study, we use a matrix-vector notation of the neural network description in order to be able to express the later by simple formula. Consider a three-layer FNN, which has $p$ nodes in the input layer, $q$ nodes in the hidden layer and $k$ nodes in the output layer. Mathematically, the basic structure of the FNN model is described by

$$Y(t+1) = \begin{bmatrix} y_1(t+1) \\ y_2(t+1) \\ \cdots \\ y_k(t+1) \end{bmatrix} = \begin{bmatrix} f_2[\sum_{i=1}^{q} f_1(\sum_{j=1}^{p} w_{ij}(t)x_j(t) + w_{i0}(t))v_{1i}(t) + v_{10}(t)] \\ f_2[\sum_{i=1}^{q} f_1(\sum_{j=1}^{p} w_{ij}(t)x_j(t) + w_{i0}(t))v_{2i}(t) + v_{20}(t)] \\ \cdots \\ f_2[\sum_{i=1}^{q} f_1(\sum_{j=1}^{p} w_{ij}(t)x_j(t) + w_{i0}(t))v_{ki}(t) + v_{k0}(t)] \end{bmatrix}$$

$$= \begin{bmatrix} f_2[\sum_{i=0}^{q} f_1(\sum_{j=0}^{p} w_{ij}(t)x_j(t))v_{1i}(t)] \\ f_2[\sum_{i=0}^{q} f_1(\sum_{j=0}^{p} w_{ij}(t)x_j(t))v_{2i}(t)] \\ \cdots \\ f_2[\sum_{i=0}^{q} f_1(\sum_{j=0}^{p} w_{ij}(t)x_j(t))v_{ki}(t)] \end{bmatrix} = \begin{bmatrix} f_2[V_1^T F_1(W(t)X(t))] \\ f_2[V_2^T F_1(W(t)X(t))] \\ \cdots \\ f_2[V_k^T F_1(W(t)X(t))] \end{bmatrix}$$

$$= F_2[V^T(t)F_1(W(t)X(t))], \tag{1}$$

where $x_j(t)$, $j = 1, 2, \ldots, p$, are the inputs of the FNN; $y_j(t+1)$, $j = 1, 2, \ldots, k$, are the output of the FNN; $w_{ij}(t)$, $i = 1, 2, \ldots, q$, $j = 1, 2, \ldots, p$, are the weights from the input layer to the hidden layer; $w_{i0}(t)$, $i = 1, 2, \ldots, q$, are the biases of the hidden nodes; $v_{ij}(t)$, $i= 1, \ldots, q$, $j = 1, \ldots, k$, are the weights from the hidden layer to the output layer; $v_{i0}(t)$, $i = 1, \ldots, k$, are the bias of the output node; $t$ is a time factor; $f_1$ is the activation function of the nodes for the hidden layer and $f_2$ is the activation function of the nodes for the output layer. Generally, the activation function for nonlinear nodes is assumed to be a symmetric hyperbolic tangent function, i.e. $f_1(x) = \tanh(u_0^{-1}x)$, and its first- and second-order derivatives are $f_1'(x) = u_0^{-1}[1 - f_1^2(x)]$, $f_1''(x) = -2u_0^{-1}f_1(x)[1 - f_1^2(x)]$, respectively, where $u_0$ is the shape factor of the activation function. Specially, some notations in Equation (1) are defined as follows:

$$X = (x_0, x_1, \cdots, x_p)^T \in R^{(p+1)\times 1}, \quad Y = (y_1, y_2, \cdots, y_k)^T \in R^{k\times 1},$$

$$W = \begin{pmatrix} w_{10} & w_{11} & \cdots & w_{1p} \\ w_{20} & w_{21} & \cdots & w_{2p} \\ \cdots & \cdots & \cdots & \cdots \\ w_{q0} & w_{q1} & \cdots & w_{qp} \end{pmatrix} = (W_0, W_1, \cdots, W_p) \in R^{q\times(p+1)},$$

$$V = \begin{pmatrix} v_{10} & v_{20} & \cdots & v_{k0} \\ v_{11} & v_{21} & \cdots & v_{k1} \\ \cdots & \cdots & \cdots & \cdots \\ v_{1q} & v_{2q} & \cdots & v_{kq} \end{pmatrix} = (V_1, V_2, \cdots, V_k) \in R^{(q+1)\times k},$$

$$F_1(W(t)X(t))$$
$$= \begin{pmatrix} F_1(\sum_{j=1}^{p} w_{0j}(t)x_j(t)) & F_1(\sum_{j=1}^{p} w_{1j}(t)x_j(t)) & \cdots & F_1(\sum_{j=1}^{p} w_{qj}(t)x_j(t)) \end{pmatrix}^T.$$

$$F_1(W(t)X(t)) \in R^{(q+1)\times 1}.$$

For simplification, let $net_i(t) = \sum_{j=0}^{p} w_{ij}(t)x_j(t), \quad i = 0, 1, \ldots, q$, then

$$F_1(W(t)X(t)) = \begin{pmatrix} F_1(net_0(t)) & F_1(net_1(t)) & \cdots & F_1(net_q(t)) \end{pmatrix}^T \in R^{(q+1)\times 1}.$$

Usually, through estimating the model parameter vectors ($W$, $V$) via FNN learning, we can realize the corresponding tasks such as function approximation, system identification or prediction. In fact, the model parameter vectors ($W$, $V$) can be obtained by iteratively minimizing a cost function $E(X\colon W, V)$. In general, $E(X{:}W, V)$ is a sum of the error squares cost function with $k$ output nodes and $N$ training pairs, i.e.,

$$E(X : W, V) = \frac{1}{2}\sum_{j=1}^{N}\sum_{i=1}^{p} e_i^2(j) = \frac{1}{2}\sum_{j=1}^{N} e^T(j)e(j)$$

$$= \frac{1}{2}\sum_{j=1}^{N} [y_j - \hat{y}_j(X : W, V)]^T[y_j - \hat{y}_j(X : W, V)], \tag{2}$$

where $e(j) = [e_1(j), e_2(j), \cdots, e_k(j)]^T \in R^{k\times 1}$, $y_j$ is the $j$th actual value and $\hat{y}_j(X : W, V)$ is the $j$th estimated value, $j = 1, \ldots, N$.

However, the learning algorithm based on Equation (2) is batch learning of neural networks. As earlier mentioned, the computation of the batch learning algorithm is very large if big sample data sets are given. Also, the neural networks must re-learn when new data are available. To overcome the shortcomings, the neural network learning should be iterative or recursive, allowing the network parameters to be updated at each sample interval as new data become available. This idea will be activated to create a new online learning algorithm. In addition, a weighting sequence should be chosen to give a higher weight for more recent data in order to perform online prediction. To arrive at this goal, an adaptive forgetting factor is introduced to this problem. In this study, an exponential forgetting mechanism in the cost function, like a recursive algorithm with the forgetting factor, is used, and then Equation (2) can be rewritten as

$$E(t) = \frac{1}{2}\sum_{j=1}^{t} \lambda^{t-j}\sum_{i=1}^{k} e_i^2(j) = \frac{1}{2}\sum_{j=1}^{t} \lambda^{t-j} e^T(j)e(j)$$

$$= \frac{1}{2}\sum_{j=1}^{t} \lambda^{t-j}[y(j) - \hat{y}_i(j)]^T[y(j) - \hat{y}_i(j)], \tag{3}$$

where $\lambda$ is the forgetting factor, $0 < \lambda \leqslant 1$, $e(j) = [e_1(j), e_2(j), \cdots, e_k(j)]^T \in R^{k\times 1}$, $j = 1, \ldots, t$; t is a time factor, representing the number of training pairs here.

By applying the steepest descent method to the error cost function $E(t)$ (i.e., Equation (3)), we can obtain the gradient of $E(t)$ with respect to parameters $W$ and $V$, respectively.

$$\nabla_W E(t) = \frac{\partial E(t)}{\partial W(t)} = \sum_{j=1}^{t} \lambda^{t-j}\sum_{i=1}^{k} e_i(j)\frac{\partial e_i(j)}{\partial W(j)} = -\sum_{j=1}^{t} \lambda^{t-j}\sum_{i=1}^{k} e_i(j)\frac{\partial \hat{y}_i(j)}{\partial W(j)}$$

$$= -\sum_{j=1}^{t} \lambda^{t-j} \bar{F}_1'(j)\bar{V}(j)F_2'(j)e(j)x^T(j) = \lambda\nabla_W E(t-1) - \bar{F}_1'(t)\bar{V}(t)F_2'(t)e(t)x^T(t), \tag{4}$$

$$\nabla_V E(t) = \frac{\partial E(t)}{\partial V(t)} = \sum_{j=1}^{t} \lambda^{t-j} \sum_{i=1}^{k} e_i(j)\frac{\partial e_i(j)}{\partial V(j)} = -\sum_{j=1}^{t} \lambda^{t-j} \sum_{i=1}^{k} e_i(j)\frac{\partial \hat{y}_i(j)}{\partial V(j)}$$

$$= -\sum_{j=1}^{t} \lambda^{t-j} F_1(j)e^T(j)F_2'(j) = \lambda\nabla_V E(t-1) - F_1(t)e^T(t)F_2'(t). \tag{5}$$

So, the updated formulae of weights are given by, respectively

$$\Delta W(t) = -\eta\nabla_W E(t) = -\eta\left(\lambda\nabla_W E(t-1) - \bar{F}_1'(t)\bar{V}(t)F_2'(t)e(t)x^T(t)\right), \tag{6}$$

$$\Delta V(t) = -\eta\nabla_V E(t) = -\eta\left(\lambda\nabla_V E(t-1) - F_1(t)e^T(t)F_2'(t)\right), \tag{7}$$

where $\eta$ is the learning rate; $\lambda$ is the forgetting factor; $\Delta$ is the incremental operator; $\nabla$ is the gradient operator; $\Delta W$ and $\Delta V$ are the weight adjustment increments;

$$\bar{F}_{1(j)}' = diag[f_{1(1)}' \ f_{1(2)}' \ \cdots \ f_{1(q)}'] \in R^{q\times q};$$

$$F_2' = diag[f_{2(1)}' \ f_{2(2)}' \ \cdots \ f_{2(k)}'] \in R^{k\times k};$$

$$f_{1(i)}' = f_1'(net_i) = \frac{\partial f_1(net_i)}{\partial net_i}, i = 1, 2, \cdots, q;$$

$$f_{2(i)}' = f_2'[v_i^T F_1(WX)] = \frac{\partial f_2[v_i^T F_1(WX)]}{\partial[v_i^T F_1(WX)]}, i = 1, 2, \cdots k;$$

$$\bar{V} = \begin{bmatrix} v_{11} & v_{21} & \cdots & v_{k1} \\ v_{12} & v_{22} & \cdots & v_{k2} \\ \cdots & \cdots & \cdots & \cdots \\ v_{1q} & v_{2q} & \cdots & v_{kq} \end{bmatrix} = [\bar{v}_1 \ \bar{v}_2 \ \cdots \ \bar{v}_k] \in R^{q\times p};$$

$$\bar{v}_i = [v_{i1} \ \cdots \ v_{iq}]^T \in R^{q\times 1}, i = 1, 2, \cdots, q.$$

To derive the optimal learning rate, consider the following error increment equation:

$$\Delta e(t+1) = e(t+1) - e(t) = y(t+1) - \hat{y}(t+1) - y(t) + \hat{y}(t). \tag{8}$$

Let $\Delta y(t+1) = y(t+1) - y(t)$ be the change of the actual series and let $\Delta\hat{y}(t+1) = \hat{y}(t+1) - \hat{y}(t)$ be the change of the neural network output. Here we assume that the absolute value of the change of the actual series is much smaller than the absolute value of the change of the neural network output, i.e., $|\Delta y(t+1)| << |\Delta\hat{y}(t+1)|$. This implies that the value $y(t)$ can approximate $y(t+1)$ locally during the training process, that is to say, the change of the actual series can be ignored comparing with the change of neural network output during the learning process. This assumption is realistic for many processes of actual series due to energy constraints in practical systems, while no constraints are imposed to the output of the neural networks [11]. Also, if this condition is not satisfied, then the neural network prediction system will not be able to adapt

sufficiently fast to change in the actual series and the prediction of the actual series will be impossible. With the above assumption, the increment in Equation (8) can be approximated as

$$\Delta e(t+1) = e(t+1) - e(t) = \Delta y(t+1) - \Delta \hat{y}(t+1) \approx -\Delta \hat{y}(t+1). \tag{9}$$

Usually, in the recursive algorithm, the change of output of neural networks with adaptive forgetting factors can be represented as

$$\Delta \hat{y}(t+1) = -\eta \lambda \zeta(t-1) + \eta \xi(t) e(t), \tag{10}$$

where $\zeta(t-1) = F_2'[\nabla_V^T E(t-1) F_1 + \bar{V}^T \bar{F}_1' \nabla_W E(t-1) X]$, $\xi(t) = F_2'[(F_1^T F_1) I_{k^2} + \bar{V}^T F_1' F_1' \bar{V} X^T X] F_2'$ with

$$F_2' = \begin{bmatrix} F_{2(1)}' & 0 & \cdots & 0 \\ 0 & F_{2(2)}' & \cdots & 0 \\ \cdots & \cdots & \cdots & \cdots \\ 0 & 0 & \cdots & F_{2(N)}' \end{bmatrix},$$

$$F_1^T F_1 = \begin{bmatrix} F_{1(1)}^T F_{1(1)} & F_{1(1)}^T F_{1(2)} & \cdots & F_{1(1)}^T F_{1(N)} \\ F_{1(2)}^T F_{1(1)} & F_{1(2)}^T F_{1(2)} & \cdots & F_{1(2)}^T F_{1(N)} \\ \cdots & \cdots & \cdots & \cdots \\ F_{1(N)}^T F_{1(1)} & F_{1(N)}^T F_{1(2)} & \cdots & F_{1(N)}^T F_{1(N)} \end{bmatrix},$$

$$X^T X = \begin{bmatrix} x_1^T x_1 & x_1^T x_2 & \cdots & x_1^T x_N \\ x_2^T x_1 & x_2^T x_2 & \cdots & x_2^T x_N \\ \cdots & \cdots & \cdots & \cdots \\ x_N^T x_1 & x_N^T x_2 & \cdots & x_N^T x_N \end{bmatrix},$$

$$F_1' F_1' = \begin{bmatrix} \bar{F}_{1(1)}' \bar{F}_{1(1)}' & \bar{F}_{1(1)}' \bar{F}_{1(2)}' & \cdots & \bar{F}_{1(1)}' \bar{F}_{1(N)}' \\ \bar{F}_{1(2)}' \bar{F}_{1(1)}' & \bar{F}_{1(2)}' \bar{F}_{1(2)}' & \cdots & \bar{F}_{1(2)}' \bar{F}_{1(N)}' \\ \cdots & \cdots & \cdots & \cdots \\ \bar{F}_{1(N)}' \bar{F}_{1(1)}' & \bar{F}_{1(N)}' \bar{F}_{1(2)}' & \cdots & \bar{F}_{1(N)}' \bar{F}_{1(N)}' \end{bmatrix}.$$

In order to prove Equation (10), a lemma must be introduced firstly.

**Lemma 2.1** *The total time derivative of the FNN single output $V^T F_1(WX)$is given by*

$$\frac{d[V^T F_1(WX)]}{dt} = F_1(WX)\frac{dV}{dt} + \bar{V}^T \bar{F}'_1(WX)\frac{dW}{dt}X$$

$$= \frac{dV^T}{dt} F_1(WX) + \bar{V}^T \bar{F}'_1(WX)\frac{dW}{dt}X,$$

*where $V^T F_1(WX)$ is the single output of FNN; $\frac{dW}{dt}$ and $\frac{dV}{dt}$ are the derivatives with*

*respect to timet; $W$, $V$ are the weight vectors; $X$ is the input vector; and*

$$F_1(WX) = [f_1(net_0), f_1(net_1), \cdots, f_1(net_q)]^T; X = [x_0, x_1, \cdots, x_p]^T;$$

$$\bar{F'}_1(WX) = \begin{bmatrix} f'(net_1) & \cdots & 0 \\ \cdots & \cdots & \cdots \\ 0 & \cdots & f'(net_q) \end{bmatrix}; \quad \frac{dW}{dt} = \begin{bmatrix} \frac{dw_{00}}{dt} & \frac{dw_{01}}{dt} & \cdots & \frac{dw_{0p}}{dt} \\ \frac{dw_{10}}{dt} & \frac{dw_{11}}{dt} & \cdots & \frac{dw_{1p}}{dt} \\ \cdots & \cdots & \cdots & \cdots \\ \frac{dw_{q0}}{dt} & \frac{dw_{q1}}{dt} & \cdots & \frac{dw_{qp}}{dt} \end{bmatrix};$$

$$\bar{V} = [v_1, v_2, \cdots, v_q]^T; \quad \frac{dV}{dt} = \begin{bmatrix} \frac{dv_0}{dt} & \frac{dv_1}{dt} & \cdots & \frac{dv_q}{dt} \end{bmatrix}^T.$$

***Proof*** Derivation of $\frac{d[V^T F_1(WX)]}{dt}$ is as follows:

$$\begin{aligned}
&\frac{d[V^T F_1(WX)]}{dt} = \frac{d\left[\sum_{i=0}^{q} v_i f_1\left(\sum_{j=0}^{p} w_{ij} x_j\right)\right]}{dt} \\
&= \sum_{i=0}^{q} \frac{\partial\left[\sum_{i=0}^{q} v_i f_1\left(\sum_{j=0}^{p} w_{ij} x_j\right)\right]}{\partial v_i} \frac{dv_i}{dt} + \sum_{i=0}^{q}\sum_{j=0}^{p} \frac{\partial\left[\sum_{i=0}^{q} v_i f_1\left(\sum_{j=0}^{p} w_{ij} x_j\right)\right]}{\partial w_{ij}} \frac{dw_{ij}}{dt} \\
&= \sum_{i=0}^{q} f_1\left(\sum_{j=0}^{p} w_{ij} x_j\right) \frac{dv_i}{dt} + \sum_{i=0}^{q}\sum_{j=0}^{p} v_i f'_1\left(\sum_{j=0}^{p} w_{ij} x_j\right) x_j \frac{dw_{ij}}{dt} \\
&= f_1(net_0)\frac{dv_0}{dt} + f_1(net_1)\frac{dv_1}{dt} + \cdots + f_1(net_q)\frac{dv_q}{dt} \\
&\quad + v_0 f'_1(net_0)[x_0 \frac{dw_{00}}{dt} + x_1 \frac{dw_{01}}{dt} + \cdots + x_p \frac{dw_{0p}}{dt}] \\
&\quad + v_1 f'_1(net_1)[x_0 \frac{dw_{10}}{dt} + x_1 \frac{dw_{11}}{dt} + \cdots + x_p \frac{dw_{1p}}{dt}] + \cdots \\
&\quad + v_q f'_1(net_q)[x_0 \frac{dw_{q0}}{dt} + x_1 \frac{dw_{q1}}{dt} + \cdots + x_p \frac{dw_{qp}}{dt}] \\
&\quad = [f_1(net_0)\ f_1(net_1)\ \cdots\ f_1(net_q)] \left[\frac{dv_0}{dt}\ \frac{dv_1}{dt}\ \cdots\ \frac{dv_q}{dt}\right]^T \\
&\quad + [v_1\ v_2\ \cdots\ v_q] \begin{bmatrix} f'(net_1) & \cdots & 0 \\ \cdots & \cdots & \cdots \\ 0 & \cdots & f'(net_q) \end{bmatrix} \begin{pmatrix} \text{due to } f(net_0) \equiv 1, \\ f'(net_0) = 0 \end{pmatrix} \\
&\quad \times \begin{bmatrix} \frac{dw_{00}}{dt} & \frac{dw_{01}}{dt} & \cdots & \frac{dw_{0p}}{dt} \\ \frac{dw_{10}}{dt} & \frac{dw_{11}}{dt} & \cdots & \frac{dw_{1p}}{dt} \\ \cdots & \cdots & \cdots & \cdots \\ \frac{dw_{q0}}{dt} & \frac{dw_{q1}}{dt} & \cdots & \frac{dw_{qp}}{dt} \end{bmatrix} \begin{bmatrix} x_0 \\ x_1 \\ \cdots \\ x_p \end{bmatrix} \\
&= F_1^T(WX)\frac{dV}{dt} + \bar{V}^T \bar{F'}_1(WX)\frac{dW}{dt}X = \frac{dV^T}{dt}F_1(WX) + \bar{V}^T \bar{F'}_1(WX)\frac{dW}{dt}X.
\end{aligned}$$

□

In the following, we start to prove Equation (10). The above Lemma together with Equations (6) and (7) gives

$$\Delta\hat{y}(t+1) \approx \left(\frac{d\hat{y}(t+1)}{dt}\right)\Delta t = \begin{pmatrix} \frac{d\hat{y}_1(t+1)}{dt} \\ \frac{d\hat{y}_2(t+1)}{dt} \\ \cdots \\ \frac{d\hat{y}_k(t+1)}{dt} \end{pmatrix}\Delta t = \begin{pmatrix} f'_{2(1)} \cdot \left(F_1^T \frac{dv_1}{dt} + v_1^T \bar{F}'_1 \frac{dW}{dt} X\right) \\ f'_{2(2)} \cdot \left(F_1^T \frac{dv_2}{dt} + v_2^T \bar{F}'_1 \frac{dW}{dt} X\right) \\ \cdots \\ f'_{2(k)} \cdot \left(F_1^T \frac{dv_k}{dt} + v_k^T \bar{F}'_1 \frac{dW}{dt} X\right) \end{pmatrix}\Delta t$$

$$\approx \begin{pmatrix} f'_{2(1)} \cdot \left(F_1^T \frac{\Delta v_1}{\Delta t} + v_1^T \bar{F}'_1 \frac{\Delta W}{\Delta t} X\right) \\ f'_{2(2)} \cdot \left(F_1^T \frac{\Delta v_2}{\Delta t} + v_2^T \bar{F}'_1 \frac{\Delta W}{\Delta t} X\right) \\ \cdots \\ f'_{2(k)} \cdot \left(F_1^T \frac{\Delta v_k}{\Delta t} + v_k^T \bar{F}'_1 \frac{\Delta W}{\Delta t} X\right) \end{pmatrix}\Delta t = \begin{bmatrix} f'_{2(1)} \cdot (F_1^T \Delta v_1 + v_1^T \bar{F}'_1 \Delta W X) \\ f'_{2(2)} \cdot (F_1^T \Delta v_2 + v_2^T \bar{F}'_1 \Delta W X) \\ \cdots \\ f'_{2(k)} \cdot (F_1^T \Delta v_k + v_k^T \bar{F}'_1 \Delta W X) \end{bmatrix}$$

$$= \begin{bmatrix} f'_{2(1)} \cdot (F_1^T [-\eta \nabla_{V_1} E(t)] + \bar{v}_1^T \bar{F}'_1 [-\eta \nabla_W E(t)] X) \\ f'_{2(2)} \cdot (F_1^T [-\eta \nabla_{V_2} E(t)] + \bar{v}_2^T \bar{F}'_1 [-\eta \nabla_W E(t)] X) \\ \cdots \\ f'_{2(k)} \cdot (F_1^T [-\eta \nabla_{V_k} E(t)] + \bar{v}_k^T \bar{F}'_1 [-\eta \nabla_W E(t)] X) \end{bmatrix}$$

$$= -\eta \begin{bmatrix} f'_{2(1)} \cdot (F_1^T \nabla_{V_1} E(t) + \bar{v}_1^T \bar{F}'_1 \nabla_W E(t) X) \\ f'_{2(2)} \cdot (F_1^T \nabla_{V_2} E(t) + \bar{v}_2^T \bar{F}'_1 \nabla_W E(t) X) \\ \cdots \\ f'_{2(k)} \cdot (F_1^T \nabla_{V_k} E(t) + \bar{v}_k^T \bar{F}'_1 \nabla_W E(t) X) \end{bmatrix}$$

$$= -\eta \begin{bmatrix} f'_{2(1)} & 0 & \cdots & 0 \\ 0 & f'_{2(2)} & \cdots & 0 \\ \cdots & \cdots & \cdots & \cdots \\ 0 & 0 & \cdots & f'_{2(k)} \end{bmatrix}$$

$$\times \begin{bmatrix} F_1^T [\lambda \nabla E_{V_1}(t-1) - e_1 f'_{2(1)} F_1] + \bar{v}_1^T \bar{F}'_1 \nabla_W E(t) X \\ F_1^T [\lambda \nabla E_{V_2}(t-1) - e_2 f'_{2(2)} F_1] + \bar{v}_2^T \bar{F}'_1 \nabla_W E(t) X \\ \cdots \\ F_1^T [\lambda \nabla E_{V_k}(t-1) - e_k f'_{2(k)} F_1] + \bar{v}_k^T \bar{F}'_1 \nabla_W E(t) X \end{bmatrix}$$

$$= -\eta F'_2 \left[\lambda \nabla_V^T E(t-1) F_1 - F'_2 e F'_1 F_1 + \bar{V}^T \bar{F}' (\lambda \nabla E_W(t-1) - F'_1 V F'_2 e X^T) X\right]$$

$$= -\eta\lambda F'_2 \left[\nabla_V^T E(t-1) F_1 + \bar{V}^T \bar{F}' \nabla E_W(t-1) X\right] + \eta F'_2 (F'_2 e F'_1 F_1$$

$$-\bar{V}^T \bar{F}' F'_1 V F'_2 e X^T X)$$

$$= -\eta\lambda F'_2 \left[\nabla_V^T E(t-1) F_1 + \bar{V}^T \bar{F}' \nabla E_W(t-1) X\right] + \eta F'_2 (F'_1 F_1 I_{k^2}$$

$$-\bar{V}^T \bar{F}' F'_1 V X^T X) F'_2 e$$

$$= -\eta\lambda\zeta(t-1) + \eta\xi(t) e(t).$$

□

Substituting (10) into (9), we obtain

$$e(t+1) \approx e(t) + \eta\lambda\zeta(t-1) - \eta\xi(t) e(t). \tag{11}$$

The objective here is to derive an optimal learning rate $\eta$. That is, at iteration $t$, an optimal value of the learning rate, $\eta^*(t)$, which minimizes $E(t+1)$, is obtained. Define

the cost function:

$$E(t+1) = 0.5e^T(t+1)e(t+1). \tag{12}$$

Using Equation (11), Equation (12) may be written as

$$E(t+1) = 0.5\left[e(t) + \eta\lambda\zeta(t-1) - \eta\xi(t)e(t)\right]^T\left[e(t) + \eta\lambda\zeta(t-1) - \eta\xi(t)e(t)\right]. \tag{13}$$

In Equation (13), the first and second order conditions are as

$$\begin{aligned}\left.\frac{dE(t+1)}{d\eta}\right|_{\eta=\eta^*(t)} &= -0.5\left[\xi(t)e(t) - \lambda\zeta(t-1)\right]^T\left[e(t) - \eta^*(t)\xi(t)e(t) + \eta^*(t)\lambda\zeta(t-1)\right] \\ &\quad - 0.5[e(t) - \eta^*(t)\xi(t)e(t) + \eta^*(t)\lambda\zeta(t-1)]^T[\xi(t)e(t) - \lambda\zeta(t-1)] = 0,\end{aligned}$$

$$\left.\frac{d^2E(t+1)}{d\eta^2}\right|_{\eta=\eta^*(t)} = [\xi(t)e(t) - \lambda\zeta(t-1)]^T[\xi(t)e(t) - \lambda\zeta(t-1)] > 0.$$

Since $\xi(t)$ and $\zeta(t-1)$ is positively defined, the second condition is met, the optimum learning rate can be obtained from the first order condition, as illustrated in Equation (14). Interestedly, the optimized learning rate that we obtained is distinctly different from the result produced by the work [11]

$$\eta^*(t) = \frac{[\xi(t)e(t) - \lambda\zeta(t-1)]^T e(t)}{[\xi(t)e(t) - \lambda\zeta(t-1)]^T[\xi(t)e(t) - \lambda\zeta(t-1)]}. \tag{14}$$

Finally, the increments of the neural network parameters, found using the optimal learning rate, are obtained by replacing the $\eta^*$ given by Equation (14) to Equations (6) and (7), which yield

$$\begin{aligned}\Delta W(t) = &-\left(\frac{[\xi(t)e(t) - \lambda\zeta(t-1)]^T e(t)}{[\xi(t)e(t) - \lambda\zeta(t-1)]^T[\xi(t)e(t) - \lambda\zeta(t-1)]}\right) \\ &\times\left(\lambda\nabla_W E(t-1) - \bar{F}_1'(t)\bar{V}(t)F_2'(t)e(t)x^T(t)\right),\end{aligned} \tag{15}$$

$$\begin{aligned}\Delta V(t) = &-\left(\frac{[\xi(t)e(t) - \lambda\zeta(t-1)]^T e(t)}{[\xi(t)e(t) - \lambda\zeta(t-1)]^T[\xi(t)e(t) - \lambda\zeta(t-1)]}\right) \\ &\times\left(\lambda\nabla_V E(t-1) - F_1(t)e^T(t)F_2'(t)\right).\end{aligned} \tag{16}$$

It is worth noting that the forgetting factor $\lambda$ is adaptive. During the neural network learning process, if the prediction error $e(t)$ grows, this may mean that the neural network parameters have changed. This implies that the network model is incorrect and needs adjustment. So we should reduce the forgetting factor and allow the neural network model to adapt. An adaptive forgetting factor which allows this is

$$\lambda(t) = s(t-1)/s(t), \tag{17}$$

where $s(t)$ is a weighted average of the past values of $e^Te$ and is calculated by

$$s(t) = [(\tau-1)/\tau]s(t-1) + (e^Te/\tau), \tag{18}$$

$\tau$ is the time constant of the forgetting factor determining how fast $\lambda(t)$ changes.

Using the updated weight formula with optimal learning rates and adaptive forgetting factors, a new online recursive learning algorithm is generated. For convenience, the proposed online learning algorithm is summarized as follows, as shown in Figure 2.1.

To verify the effectiveness of the proposed online learning algorithm, two typical financial time series: S&P 500, a famous stock index, and one foreign exchange rate, euros against US dollars (EUR/USD), are used as testing targets. The simulation experiments are presented in the following section.

```
Set input nodes to the number of input vectors
Set target value for a specific pattern
Initialize weight vectors
While i < Epoch_num
    For j = 1 to N_records
        Compute net_i (i = 1,..., q), y_i (i = 1,..., k) using Equation (1);
        Compute error gradients ∇_w E(t) and ∇_v E(t) using Equations (4)-(5),
        and optimal learning rate η using Equation (14);
        Update the weight vectors with Equations (15)-(16).
    Endfor
Wend
```

**Figure 2.1:** Outline of the proposed online learning algorithm.

## 3 Experimental Analysis

In this section, there are two main motivations: (1) to evaluate the performance of the proposed online learning algorithm, and (2) to compare the efficiency of the proposed online learning algorithm with other similar algorithms. To perform the two motivations, two real-world data experiments are carried out. In this section, we first describe the research data and experiment design and then report the experimental results.

### 3.1 Research data and experiment design

In the experiments, one stock index, S&P 500, and one foreign exchange rate, euros against US dollars (EUR/USD), are used for testing purpose. The historical data are daily and are obtained from Wharton Research Data Service (WRDS), provided by Wharton School of the University of Pennsylvania. The entire data set covers the period from January 1, 2000 to December 31, 2004 with a total of 1256 observations. The data sets are divided into two periods: the first period covers January 1, 2000 to December 31, 2003 with 1004 observations, while the second period is from January 1, 2004 to December 31, 2004 with 252 observations. The first period, which is assigned to in-sample estimation, is used for network learning, i.e., training set. The second period, which is reserved for out-of-sample evaluation, is used for validation, i.e., testing set. For space limitation, the original data are not listed in this paper, and detailed data can be obtained from the WRDS.

For comparison, four related algorithms, standard FNN algorithm [7, 16], batch learning algorithm, Levenberg-Marquart (LM) based learning algorithm [15-16], and extended Kalman filter (EKF) based learning algorithm [12, 17], are employed in this study. For standard FNN learning algorithm, the learning rate is fixed at 0.3, more details about standard FNN learning algorithm can be referred to [7]. In the batch learning algorithm, the weights are updated only at the end of each epoch. Similar to the online learning algorithm, the batch learning algorithm can also be summarized as follows, as illustrated in Figure 3.1.

The Levenberg-Marquart (LM) based algorithm [15-16] is a kind of quick convergence

algorithm which has the little computation time for per iteration. Basically, the link weights of the neural network are updated based on the Jacobian matrix, $J$, collecting the partial derivatives of the neural network error $e$ with respect to the weights. In other words, the update increment $\Delta W$ collecting the corrections of the weights in matrix $W$ is computed by

$$\Delta W = -[J^T J + \mu I]^{-1} J^T e, \tag{19}$$

$$J = \begin{bmatrix} \frac{\partial e}{\partial w_{11}} & \frac{\partial e}{\partial w_{12}} & \cdots & \frac{\partial e}{\partial w_{1n}} \\ \frac{\partial e}{\partial w_{21}} & \frac{\partial e}{\partial w_{22}} & \cdots & \frac{\partial e}{\partial w_{2n}} \\ \cdots & \cdots & \cdots & \cdots \\ \frac{\partial e}{\partial w_{m1}} & \frac{\partial e}{\partial w_{m2}} & \cdots & \frac{\partial e}{\partial w_{mn}} \end{bmatrix}. \tag{20}$$

Set input nodes to the number of input vectors
Set target value for a specific pattern
Initialize weight vectors
While $i <$ Epoch_num
  For $j$ = 1 to $N_{records}$
    Compute $net_i (i = 1, \ldots, q)$, $y_i (j = 1, \ldots, k)$ using Equation (1)
    Compute error gradients $\nabla_w E(t)$ and $\nabla_v E(t)$ using Equations (4)-(5), and optimal learning rate $\eta$ using Equation (14)
  Endfor
  Update the weight vectors with Equations (15)-(16)
Wend

**Figure 3.1:** Outline of the batch learning algorithm.

It is worth noting that the LM-based algorithm is rather flexible. If $\mu$ is sufficiently large, the above weight update algorithm is similar to the gradient descent algorithm. If $\mu$ is equal to zero, the above algorithm will be a Gaussian-Newton algorithm. In this sense, the LM-based algorithm has the characteristics of both the gradient descent algorithm and the Gaussian-Newton algorithm.

The extended Kalman filter (EKF) based algorithm [12, 17] is a novel weight adjustment algorithm for FNN. In this algorithm, the Kalman filter is used to update the weight vector of FNN. The generic principle of EKF-based algorithm is that the EKF can modify the weight parameters to maximize the posterior probability of current instance with respect to its predicted probability distribution of weight parameters. Recent work proposed by Ruck [17] has revealed that the FNN algorithm is actually a degenerated form of the EKF. Due to its excellent convergence properties, a lot of successful applications have been reported. Basically, the EKF-based weight adjustment formulae are illustrated as follows.

$$W(t) = W(t-1) + K(t)[y(t) - \hat{y}(t)], \tag{21}$$

$$K(t) = P(t-1)H^T(t)[H(t)P(t-1)H^T(t) + R(t)]^{-1}, \tag{22}$$

$$P(t) = P(t-1) - K(t)H(t)P(t-1), \tag{23}$$

where $W(t)$ is the connect weight of FNN, $K(t)$ is called the Kalman gain, $y(t)$ is the actual value, $\hat{y}(t)$ is the predicted value produced by neural networks, $P(t)$ is the error covariance matrix, defined by $P(t) = E\{[y(t) - \hat{y}(t)]^T[y(t) - \hat{y}(t)]\}$ and $H(t)$ is the gradient, defined by $H(t) = \frac{\partial \hat{y}(t)}{\partial W}$. Usually, the system actual output$y(t) = \hat{y}(t) + \varepsilon(t)$, $\varepsilon(t)$ is assumed to be white noise vector with covariance $R(t)$ regarded as a modeling error. For more details, please refer to [12, 17].

In all the neural network predictors, five input nodes are determined by auto-regression testing. The appropriate number of hidden nodes is set to 12 in terms of trial and error. The training epochs are set to 3000 due to trial and error and the problem complexity.

To examine the forecasting performance, the root mean square error ($RMSE$) and directional change statistics ($D_{stat}$) [16] of financial time series are employed as the performance measurement of the testing set. In addition, training time and training mean square error ($TMSE$) are used as the efficiency measurement of different algorithms.

### 3.2 Experiment Results

When the data are prepared, we begin to perform experiments according to the previous experiment design. First of all, the prediction results with five algorithms are reported. Figures 3.2 and 3.3 give graphical representations of the forecasting results for two typical financial time series using different FNN learning algorithms. Table 3.1 shows a detailed prediction performance of the different algorithms in terms of both the level measurement ($RMSE$) and direction measurement ($D_{stat}$). From the figures and table, we can generally find that the prediction results of the proposed online learning algorithm are very promising for two typical financial time series under study either where the measurement of forecasting performance is the goodness-of-fit such as $RMSE$ or where the forecasting performance criterion is the $D_{stat}$.

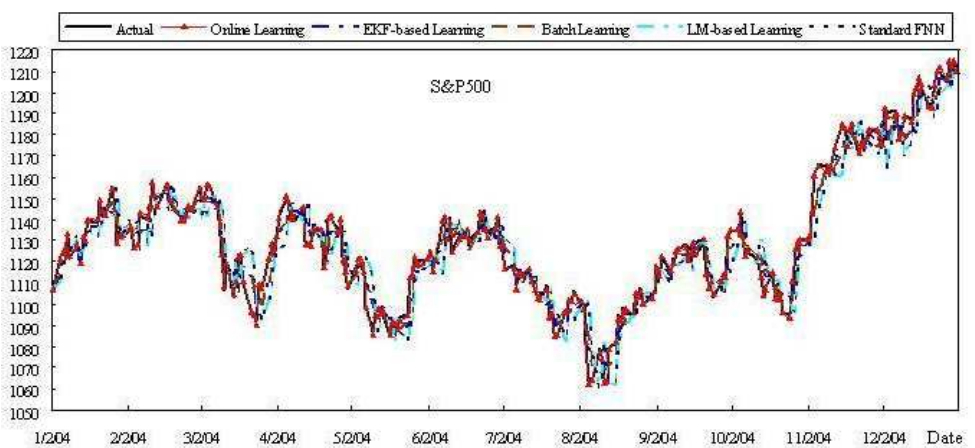


**Figure 3.2:** The forecasting results with different learning algorithm for S&P 500.

In detail, Figure 3.2 reveals that the comparison for the S&P 500 of the proposed

online learning algorithm versus the other four learning algorithm. Similarly, it can be seen from Figure 3.3 that the forecasting performance for ERU/USD has significantly improved using the proposed online learning algorithm. The graphical results indicate that the proposed online learning algorithm performs than the other algorithms presented here.

Subsequently, the concrete prediction performance comparison of various algorithms for two different financial time series via *RMSE* and $D_{stat}$ are given in Table 3.1.

For the S&P 500, the proposed online learning algorithm outperforms the other four learning algorithms in terms of both *RMSE* and $D_{stat}$. Focusing on the *RMSE* indicator, the proposed online learning algorithm performs the best, followed by batch learning, EKF-based learning, LM-based learning and Standard FNN learning algorithm. Comparing with standard FNN learning algorithm, the RMSE of the proposed online learning algorithm is much smaller. From the viewpoint of $D_{stat}$, the performance of the proposed online learning algorithm is the best of the all. Relative to the standard FNN learning algorithm, the performance improvement arrives at 26.82% (80.31%-53.41%) While the performance of the proposed online learning algorithm is slightly improved relative to batch learning algorithm, EKF-based learning algorithm and LM-based algorithm.

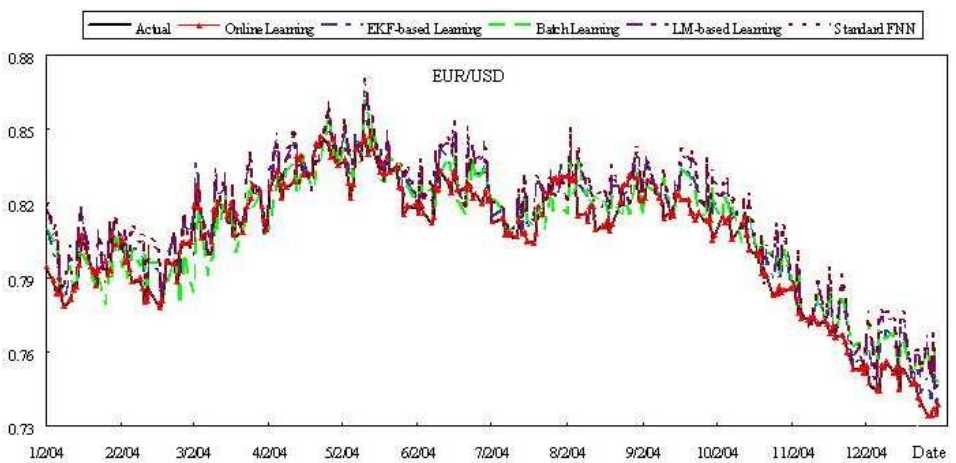


**Figure 3.3:** The forecasting results with different learning algorithm for EUR/USD.

| Algorithms | S&P 500 | | EUR/USD | |
|---|---|---|---|---|
| | *RMSE* | $D_{stat}(\%)$ | *RMSE* | $D_{stat}(\%)$ |
| Online learning | 1.2859 | 80.31 | 0.0799 | 79.87 |
| Batch learning | 2.1467 | 71.42 | 0.0943 | 69.75 |
| EKF-based learning | 2.1538 | 70.35 | 0.1051 | 72.29 |
| LM-based learning | 4.3531 | 71.69 | 0.1544 | 69.34 |
| Standard FNN | 7.8553 | 53.49 | 0.3362 | 55.64 |

**Table 3.1:** Performance comparison of four neural network learning algorithms.

| Algorithms | S&P 500 | | EUR/USD | |
|---|---|---|---|---|
| | *Time (seconds)* | *TMSE* | *Time (seconds)* | *TMSE* |
| Online learning | 197 | 3.41 | 192 | $1.17\times10^{-3}$ |
| Batch learning | 186 | 7.96 | 177 | $5.04\times10^{-3}$ |
| EKF-based learning | 173 | 8.42 | 154 | $4.85\times10^{-3}$ |
| LM-based learning | 535 | 8.77 | 573 | $3.56\times10^{-3}$ |
| Standard FNN | 249 | 12.55 | 269 | $6.09\times10^{-3}$ |

**Table 3.2:** The comparisons of the computational efficiency and training performance.

For the exchange rate of EUR/USD, the performance of the proposed online algorithm is the best, similar to the results of the S&P 500. Likewise, the proposed online algorithm has gained much improvement relative to the standard FNN learning algorithm. Interestedly, the *RMSE* of the batch learning algorithm is slightly better than that of the EKF-based learning algorithm, but the directional performance (i.e., $D_{stat}$) of the batch learning is somewhat worse than that of the EKF-based learning algorithm. The possible reasons are needed to be further addressed later.

In summary, we can conclude that (1) the proposed online learning algorithm with adaptive forgetting factors performs consistently better than other comparable learning algorithm for both the stock index and foreign exchange rate; (2) the evaluation value of the two criteria of the proposed online learning is much better than that of the standard FNN learning algorithm, indicating that the proposed online learning algorithm can effectively reflect error changes and significantly improve network learning performance. One possible reason for this is that the optimal learning rate and adaptive forgetting factors are used in the online learning algorithm.

In addition, the computation speed of the proposed online algorithm is very fast during the experiments when using a personal computer (PC) and the training performance is also well in predicting time series, indicating that the proposed learning algorithm is an efficient online algorithm. For comparison purpose, Table 3.2 reports the comparison of the computation time and training performance between the proposed online learning algorithm and the other four learning algorithm presented here.

From Table 3.2, we can find the following conclusions. First of all, for both S&P 500 and EUR/USD series, the computational time of the EKF-based learning algorithm is the smallest and the LM-based learning algorithm is the largest. The results reported here are basically consistent with the work of Iiguni et al. [12]. The main reason is that the number of iterations of LM-based learning algorithm is much larger than that of EKF-based learning algorithm, although the computation time per iteration of the EKF-based learning algorithm is larger than that of the LM-based learning algorithm [12]. Secondly, the computation time of the batch learning algorithm is smaller than that of the online learning algorithm due to the batch processing of the data. However, relative to the standard FNN learning and LM-based learning algorithms, the computation time of the online learning algorithm is much smaller. The main reason may be that the proposed online learning algorithm adopts optimal learning rate, resulting in the increase of convergence speed. Thirdly, although the computation time of the proposed online learning algorithm is not the best, the training performance (refer to *TMSE* presented by Table 3.2) and the generalized performance (refer to *RMSE* and $D_{stat}$ reported by

Table 3.1) is the best among the entire learning algorithms presented in this study. The possible reason is that the adaptive forgetting factor helps improve the performance of this proposed algorithm. Finally, since the difference of the computation time between the proposed online learning algorithm and EKF-based and batch learning algorithm is marginal, and the difference of the performance between the proposed online learning algorithm and EKF-based and batch learning is significant, in this sense, the computational efficiency of the proposed online learning algorithm is satisfactory when forecasting financial time series. In general, the experimental results reveal that the proposed online learning algorithm provide a feasible solutions to financial time series online prediction.

## 4 Conclusions

In this study, an online learning algorithm with optimized learning rates and adaptive forgetting factors is first proposed. This exploratory research examines the potential of using the proposed online learning algorithm to predict two main financial time series – S&P 500 and the exchange rate for euros against US dollars. Our empirical results suggest that the online learning algorithm may provide much better forecasts than the other four learning algorithms. Furthermore, the learning efficiency is also satisfactory relative to the learning performance. This implies that the proposed online learning algorithm with adaptive forgetting factors is very suitable for online prediction of financial time series.

## Acknowledgements

The authors would like to thanks the guest editors and two anonymous referees for their valuable comments and suggestions. Their comments helped to improve the quality of the paper immensely. The work described in this paper was partially support by National Natural Science Foundation of China (NSFC No. 70221001, 70601029); Key Laboratory of Management, Decision and Information Systems of Chinese Academy of Sciences (CAS) and Strategic Research Grant of City University of Hong Kong (SRG No. 7001677, 7001806).

## References

[1] Hall, J.W. Adaptive selection of US stocks with neural nets. In:*Trading On the Edge: Neural, Genetic, and Fuzzy Systems for Chaotic Financial Markets* (Deboeck, G.J., ed.). Wiley, New York, 1994, 45–65.

[2] Yaser, S.A.M., Atiya, A.F. Introduction to financial forecasting. *Applied. Intelligence* **6** (1996) 205–213.

[3] Hutchinson, J., Lo, A., Poggio, T. A non-parametric approach to pricing and hedging derivative securities via learning networks. *Journal of Finance* **49** (1994) 851–889.

[4] Moody, J., Utans, J. Architecture selection strategies for neural networks: Application to corporate bond rating prediction. In: *Neural Networks in the Capital Markets* (Refenes, A.P., ed.). Wiley, New York, 1994, 277–300.

[5] Kimoto, T., Asakawa, K., Yoda, M., Takeoka, M. Stock market prediction system with modular neural networks. In: *Neural Networks Finance Investing: Using Artificial Intelligence to Improve Real-World Performance* (Trippi, R.R., Turban, E., eds.). Irwin Publishers, Chicago, 1996, 497–510.

[6] Zhang, G.Q., Michael, Y.H. Neural network forecasting of the British Pound/US Dollar exchange rate. *Omega* **26** (1998) 495–506.

[7] Haykin, S. *Neural Networks: A Comprehensive Foundation*. Prentice-Hall Inc., Englewood Cliffs, New-Jersey, 1999.

[8] Kaastra, I., Boyd, M.S. Forecasting futures trading volume using neural networks. *Journal of Futures Markets* **15** (1995) 953–970.

[9] Tollenaere, T. SuperSAB: Fast adaptive back propagation with good scaling properties. *Neural Networks* **3** (1990) 561–573.

[10] Park, D.C., El-Sharkawi, M.A., Marks II, R.J. An adaptive training neural network. *IEEE Transactions on Neural Networks* **2** (1991) 334–345.

[11] Sha, D., Bajic, V.B. An online hybrid learning algorithm for multilayer perceptron in identification problems. *Computers and Electrical Engineering* **28** (2002) 587–598.

[12] Iiguni, Y., Sakai, H., Tokumaru, H. A real-time learning algorithm for a multilayered neural network based on the extended Kalman filter. *IEEE Transactions on Signal Processing* **40** (1992) 959–966.

[13] Jacobs, R.A. Increase rates of convergence through learning rate adaptation. *Neural Networks* **1** (1988) 295–307.

[14] Brent, R.P. Fast training algorithms for multilayer neural nets. *IEEE Transactions on Neural Networks* **2** (1991) 346–35.

[15] Hagan, M.T., Menhaj, M. Training feedforward networks with Marquart algorithm. *IEEE Transactions on Neural Networks* **5** (1994) 989–993.

[16] Yu, L., Wang, S.Y., Lai, K.K. A novel nonlinear ensemble forecasting model incorporating GLAR and ANN for foreign exchange rates. *Computers & Operations Research* **32** (2005) 2523–2541.

[17] Ruck, D.W., Rogers, S.K., Kabrisky, M., Maybeck, P.S., Oxley, M.E. Comparative analysis of backpropagation and the extended Kalman filter for training multilayer perceptrons. *IEEE Transactions on Pattern Analysis and Machine Intelligence* **14** (1992) 686–691.